CYTOTOXICITY AND GENOTOXICITY STUDIES OF SILVER IONS AND VARIOUS SILVER NANOPARTICLES ON MULTIPLE CELL TYPES *IN VITRO* ON THE BASIS OF WOUND HEALING

by
Fatma Melis USLU

Submitted to the Institute of Graduate Studies in
Science and Engineering in partial fulfillment of
the requirements for the degree of
Master of Science
in
Biotechnology

Yeditepe University
2012

CYTOTOXICITY AND GENOTOXICITY STUDIES OF SILVER IONS AND VARIOUS SILVER NANOPARTICLES ON MULTIPLE CELL TYPES *IN VITRO* ON THE BASIS OF WOUND HEALING

APPROVED BY:

Prof. Mustafa ÇULHA
(Thesis Supervisor) .....

Asst. Prof. Andrew John HARVEY .....

Asst. Prof. Dilek TELCİ .....

DATE OF APPROVAL: ..../..../....

ACKNOWLEDGEMENTS

I would like to express my deep gratitude to my supervisor Prof. Mustafa ÇULHA for his support, guidance, and invaluable advice throughout my research period. I am also extremely thankful to Asst. Prof. Dilek Telci for her support and advice during my studies and Asst. Prof. Andrew John Harvey for his friendly encouragement for my thesis.

I also would like to thank the chair of the Department of Genetics and Bioengineering, Prof. Fikrettin Şahin, for his support, encouragement and love during my studentship.

I would like to express my great appreciation to my lab partners and my friends for their help in the experiments and for their understanding and help during my thesis.

Finally, I would like to express my deepest gratitude to my parents for their endless love, patience, and their confidence in me.

ABSTRACT

IN VITRO CYTOTOXICITY AND GENOTOXICITY STUDIES OF SILVER IONS AND VARIOUS SILVER NANOPARTICLES ON MULTIPLE CELL TYPES ON THE BASIS OF WOUND HEALING

Silver has been used for centuries for its antimicrobial and wound healing properties. Although the mechanism of antibacterial effect was almost clarified, the wound healing effect is still not clearly understood. In this study, the effects of silver ions (Ag^+) and silver nanoparticles (AgNP) on wound healing were comparatively investigated *in vitro*. In order to shed a light on the mechanism, the cytotoxic and genotoxic effects of (Ag^+) and various AgNPs, which were synthesized with different reducing agents; AgNP-C (citrate-reduced silver nanoparticle), AgNP-M (maltose-reduced silver nanoparticle), AgNP-L (lactose-reduced silver nanoparticle), AgNP-G (glucose-reduced silver nanoparticle), on three cell types; human dermal fibroblasts (HDF), mouse macrophages (RAW 264.7), and mouse fibroblasts (L929) were studied. MTS assay was applied to analyze the cytotoxic effects of Ag^+ and AgNPs at different concentrations for variable exposure time. Besides, DNA fragmentation and annexin V-PI staining were carried out to detect DNA damage. It was observed that Ag^+ had the highest toxic effect. Although AgNP-C did not exhibit any toxicity, the AgNP-M were toxic for the cells at certain concentrations. The effective reduction process of Ag^+ and dissolution rate were the reasons of the differences in the toxicity of AgNP suspensions. Based on DNA fragmentation and annexin V-PI staining, it was found that toxic concentrations of both Ag^+ and AgNPs caused a necrotic death. In non-toxic concentrations, an irregular proliferative effect was observed for both Ag^+ and AgNPs. In addition, cell types and different exposure times did not affect the results significantly. This study suggests that the Ag^+ other than the AgNPs are toxic on the living cells and therefore the dissolution of the AgNPs could be an important factor since the AgNPs act as a supplier for Ag^+. As a conclusion, a relationship between the toxic effect of silver and the wound healing was established using Ag^+ and AgNPs. It was observed that, under the same conditions, AgNPs showed similar proliferative effect with Ag^+ and less toxic effect than Ag^+.

ÖZET

GÜMÜŞ İYONLARININ VE GÜMÜŞ NANOPARÇACIKLARIN YARA İYİLEŞMESİ ÜZERİNE ÇEŞİTLİ HÜCRE TİPLERİNDEKİ *IN VITRO* SİTOTOKSİSİTE VE GENOTOKSİSİTE ÇALIŞMALARI

Gümüş, antimikrobiyal ve yara iyileştirici etkilerinden dolayı yüzyıllardır kullanılmaktadır. Gümüşün antibakteriyel etki mekanizması bilinmesine rağmen, yara iyileştirici etkisi hala tam olarak anlaşılmış değil. Bu çalışmada, gümüş iyonlarının (Ag^+) ve gümüş nanaoparçacıkların (AgNP) yara iyileşmesindeki etkisi karşılaştırmalı olarak *in vitro* koşullarda incelendi. Mekanizmayı aydınlatmak için, Ag^+ ve farklı indirgeyici ajanlar kullanılarak sentezlenen çeşitli AgNPların; AgNP-C (sitratla indirgenmiş gümüş nanoparçacık), AgNP-M (maltozla indirgenmiş gümüş nanoparçacık), AgNP-L (laktozla indirgenmiş gümüş nanoparçacık), AgNP-G (glikozla indirgenmiş gümüş nanoparçacık), sitotoksik ve genotoksik ektileri üç hücre tipinde; insan dermal fibroblastları (HDF), fare makrofajları (RAW 264.7) ve fare fibroblastları (L929) araştırıldı. Değişen konsantrasyon miktarlarına ve maruziyet sürelerine karşı oluşan sitotoksik etkiler MTS testi, DNA hasarı ise DNA fragmantasyonu ve anneksin V-PI boyaması uygulanarak tespit edildi. Deney sonuçları Ag^+nun en yüksek toksisiteye sahip olduğunu gösterdi. AgNP-C hiçbir toksik etki göstermezken, AgNP-M belirli konsantrasyonlarında hücreler üzerinde toksik etkiye yol açtı. AgNP süspansiyonlarının toksisitelerindeki değişimlerin nedeni, Ag^+nun verimli indirgenme işlemi ve çözünme hızı. DNA fragmantasyonu ve anneksin V-PI boyama sonuçlarına göre de, Ag^+ and AgNPların toksik konsantrasyonlarının nekrotik hücre ölümüne, toksik olmayan konsantrasyonlarının ise düzenli olmamakla birlikte hücre çoğaltıcı bir etkiye neden olduğu gözlendi. Ayrıca, farklı hücre türleri ve maruziyet süreleri sonuçlar üzerinde önemli bir etki oluşturmadı. Bu çalışma gösteriyor ki, AgNPlardan farklı olarak Ag^+ları hücreler üzerinde toksisiteye yol açıyor, bu yüzden AgNPların çözünürlüğü Ag^+ kaynağı olma yönünden önemli bir faktör olabilir. Sonuç olarak, bu çalışmada, Ag^+ ve AgNPlar kullanılarak, gümüşün toksik etkisi ve yara üzerindeki iyileştirici etkisi arasında bir bağ kurulmuş oldu. Aynı şartlar altında, AgNPların Ag^+ ile benzer hücre çoğaltıcı etkisi göstermesine karşın daha az toksik etki gösterdiği tespit edildi.

TABLE OF CONTENTS

LIST OF FIGURES

LIST OF TABLES

LIST OF SYMBOLS / ABBREVIATIONS

Ag^{+}	Silver ion(s)
AgCl	Silver chloride
AgNP(s)	Silver nanoparticle(s)
AgNP-C	Citrate-reduced silver nanoparticle(s)
AgNP-G	Glucose-reduced silver nanoparticle(s)
AgNP-L	Lactose-reduced silver nanoparticle(s)
AgNP-M	Maltose-reduced silver nanoparticle(s)
bp	Base pairs
$C_6H_5O_7^{3-}$	Free citrate ion
Ca^{2+}	Free calcium ion
DLS	Dynamic light scattering
DMEM	Dulbecco's Modified Eagle Medium
DMSO	Dimethylsulfoxide
DNA	Deoxyribonucleic acid
ECM	Extracellular matrix
EDTA	Ethylenediaminetetraacetic acid
FBS	Fetal bovine serum
FITC	Fluorescein isothiocyanate
h	Hour
HDF	Human dermal fibroblasts
ICP-OES	Inductively coupled plasma-Optic emission spectrometer
l	Liter
µg	Microgram
µl	Microliter
mg	Milligram
ml	Milliliter
min	Minute
MMP	Matrix metalloproteinases
MTS	(3-(4,5-dimethyl-thiazol-2-yl)-5-(3-carboxy-methoxy-phenyl)-2-(4-sulfo-phenyl)-2H-tetrazolium)

Na^+	Free sodium ion
$NaNO_3$	Sodium nitrate
$Na_3C_6H_5O_7$	Trisodium citrate
nm	Nanometer
nM	Nanomolar
NC	Negative control
NP(s)	Nanoparticle(s)
PBS	Phosphate buffered saline
pH	Negative log of hydrogen ion concentration
PI	Propidium iodide
PS	Phosphatidylserine
RNA	Ribonucleic acid
rpm	Revolutions per minute
S.D.	Standard deviation
SDS	Sodium Dodecyl Sulfate
SEM	Scanning electron microscopy
TEM	Transmission electron microscopy
Tris-HCl	Tris (hydroxymethyl) aminomethane-Hydrochloride
UV/Vis	Ultraviolet/Visible

1. INTRODUCTION

1.1. WOUND HEALING

A skin wound is the disruption of the integrity of epithelial layer of the skin; sometimes it includes damages deeper into the dermal layer, subcutaneous fat, muscle, fascia or bone [1]. When dermis layer is damaged, fibrous tissue extends down to repair skin wounds and skin scars, which have weak functional activity. When these serious injuries, which go beyond the epithelial damage, happen, wounds heal with scarring [2].

Wound healing is a multi-phased repairing process of tissue that occurs after an injury [3]. These phases are inflammatory, proliferative, and remodeling sequentially.

The inflammatory phase includes hemostasis (clot formation), phagocytosis of bacteria, debris, and damaged tissue, and synthesizing various factors that initiate migration and division of the cells in proliferative phase. When the injury occurs, hemostatic mechanisms start by the extravasating of blood into the wounds. This process induces shrink in vessels and starts coagulation cascade to stop blood loss. Immediately after the injury, platelets (thrombocytes) begin to aggregate at wound site to control bleeding by forming the clot consisting of fibrin, fibronectin, vitronectin, and thrombospondin. Platelets also initiate the healing cascade by synthesizing many growth factors (e.g. PDGF (Platelet-derived growth factor), IGF-1 (Insulin-like growth factor 1), EGF (Epidermal growth factor), and TGF-β (Transforming growth factor beta)) which activate macrophages, endothelial cells, and fibroblasts [4-6]. After hemostatic part, which occurs within seconds after the injury, remained inflammatory phase, which is described by the migration of polymorphonuclear leucocytes (PMNLs) and granulocytes to the wound, can be divided into two phase: early inflammatory phase (starts within 24-48 hours after the injury) and late inflammatory phase (starts within 48-72 hours after the injury). After the wound occurs and pathogens attack to the wound area, inflammation causes many signals, which activate PMNLs and endothelial cells. PMNLs bind to endothelial cells. This induces the endothelial migration. They also go to the infected area and phagocytose bacteria and other foreign substances.

Besides phagocytosis, PMNLs secrete enzymes to degrade microorganisms in the wound bed and growth factors such as TGF-α (Transforming growth factor alpha), HB-EGF (Heparin-binding EGF-like growth factor), and bFGF (Basic fibroblast growth factor) to trigger the inflammatory response further. After PMNL function comes to an end, dismissed or damaged cells are phagocytosed by macrophages or removed from the wound surface as slough. Macrophage is another important cell type which appears in the late inflammatory phase and regulates the repair by releasing growth factors and cytokines, which attract keratinocytes, fibroblasts, and endothelial cells [7, 8].

The proliferative (reconstruction) phase includes the formation of new blood vessels (angiogenesis) [9], collagen deposition, granulation tissue formation, where fibroblasts proliferate and synthesize fibronectin and collagen to form the new extracellular matrix (ECM) [10], the epithelialization of epidermis to cover the new synthesized tissue by the proliferation of the endothelial cells on the wound [11], and the contraction of the wound by myofibroblasts [10]. The proliferative phase starts from the third day of the injury and continues approximately for two weeks. Fibroblasts accumulate at the wound bed and generate fibronectin, hyaluronan (HA), proteoglycans, and collagen as matrix proteins. Among them, collagen (Type I and Type III) synthesis is important to provide stability and strength to skin. While granulation tissue is being formed, new epithelium is also being generated by the epithelial cell growth and differentiation [12]. Besides inflammatory effect, lymphocytes are also effective on collagen and ECM remodeling. They interact with wounds via IL-1 (Interleukin-1) after 3 days from the injury [13]. On the other hand, new vessel and capillary formation occur not only in the proliferative phase but also in all phases of the wound healing. Growth factors such as TGF-β and PDGF generated by platelets attract macrophages, which produce TNF-α (Tumor necrosis factor-alpha) and bFGF for the angiogenesis. Increased capillary formation within days of the injury starts to decrease due to the diminished necessity when collagen starts to increase and remodels with time [14, 15].

In remodeling phase, collagen is rearranged and realigned along the tension lines [16]. Degradation of type III collagen, which actively functions during the proliferation, also takes place in this phase. Stronger type I collagen replaces it. [17]. When epidermal cell migration completes, the remodeling phase starts. Neutrophils, macrophages, and

fibroblasts produce proteolytic enzymes, which degrade Type III collagen to displace it with Type I collagen. In addition, the infiltration of mast cells, which trigger inflammatory signaling, occurs in this phase too. Mast cells secrete IL-4 (Interleukin-4), which regulates the fibroblast proliferation and down-regulates the generation of chemokines, which limit the inflammatory reaction [18, 19].

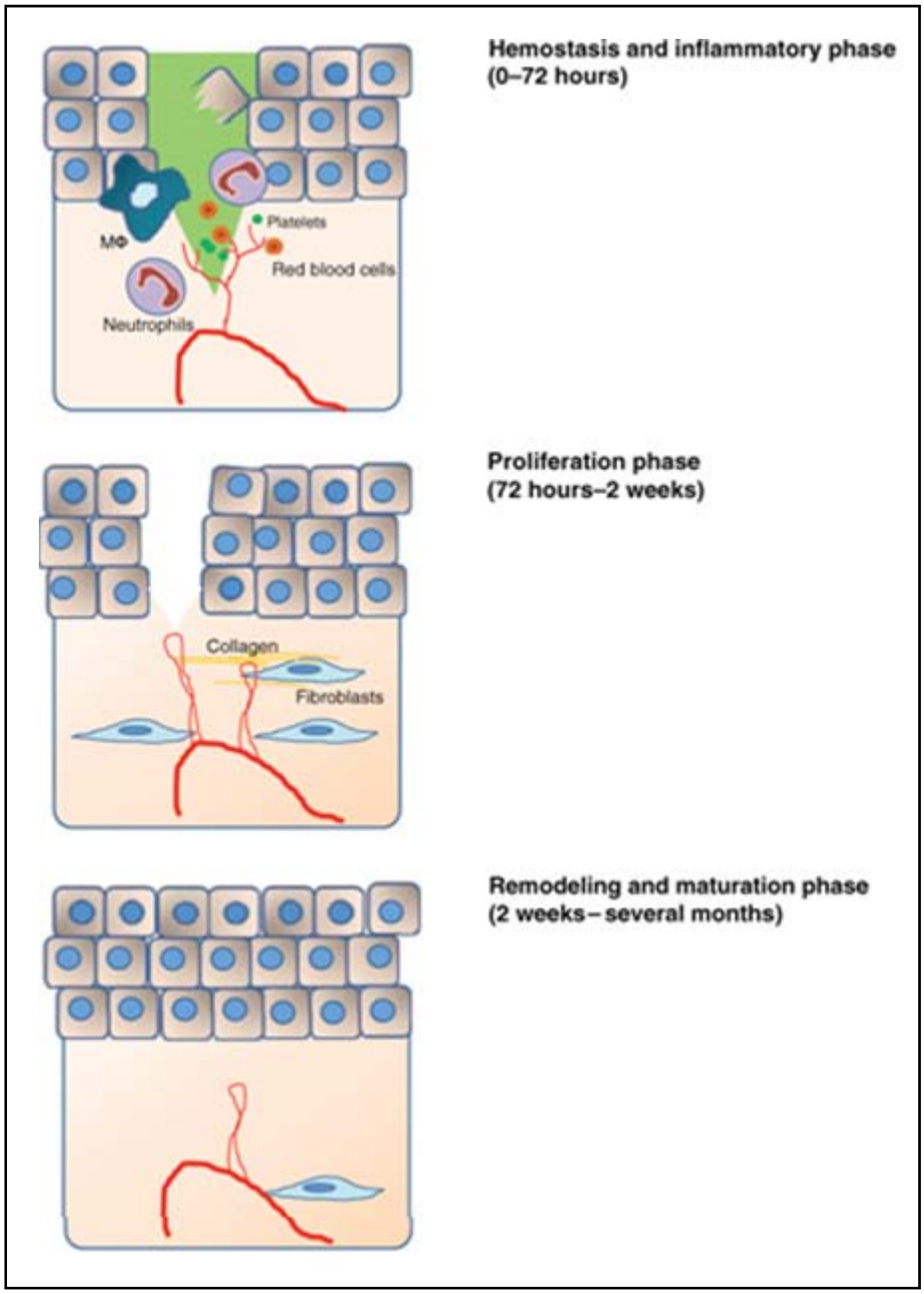

Figure 1.1. Phases of wound healing [20]

1.2. WOUND INFECTION AND SILVER USE

Although antibiotic use is the most widespread and fundamental way to prevent infections on the wounds, today, they are not effective as much as in the past, due to the developing resistance property of pathogens. This condition makes scientists search for new antibacterial agents.

For many years, silver is being used for chronic wounds and burns [21]. Very early, silver nitrate was being used in solid form. While silver nitrate was being used for venereal diseases in the 18th century [22], it was used on wounds with burn origin in the 19th century. Granulation tissues are removed by using various concentrations of silver nitrate, so epithelialization could occur and crust formation becomes fast [22, 23]. In the late 19th century, its application area and usage form extended. Eye drops and skin grafts containing silver nitrate were created [22, 24]. After the discovery of penicillin as an antibiotic in the 20th century, silver lost its importance. Toward the middle of the 20th century, silver was no longer used for the treatment of the bacterial infections as much as in the previous years [25-27]. In the 1960s, a study showed that silver nitrate solution in 0.5% (w/v) concentration did not only prevent epidermal proliferation, but also showed an antibacterial property [28, 29]. Again in the 1960s, the effect of silver nitrate was improved by combining the silver with sulfonamide to form silver sulfadiazine (AgSD). Besides antibacterial effect, it also shows antiviral and antifungal activities [30]. Furthermore, nowadays, silver nanoparticle (AgNP) becomes popular as an antimicrobial agent due to its high surface area [37, 38].

In the present day, silver regains its fame for the treatment of the wounds, after the decrease of antibiotic use due to the emergence of antibiotic-resistant bacteria [27, 31]. These days, silver is still used in clinical studies routinely due to the antibacterial and bactericidal activities. It prevents the colonization of organisms, even antibiotic-resistant bacteria, mold, and yeast, which obstruct the healing, on the wounds [32-35]. In addition to this property, some studies show it also has low toxicity. [36]. Because of these reasons, silver becomes a strong agent that is commonly used in therapeutics and wound dressings.

Silver is not reactive, and poorly absorbed by the cells (bacterial or mammalian) until it ionizes in wound fluids and secretions. When it transforms from metal form into ion form, it gains the ability to bind cell membrane and proteins [36]. Although the exact antimicrobial mechanism of silver is still not known, some studies aim to clarify it.

Many studies show that silver ions cause inhibition by interacting with thiol groups of respiratory enzymes and binding structural proteins and DNA bases to instigate restraint in replication [21, 23, 39-41]. For example, silver ions inhibit the release of glutamine, proline, succinate, mannitol and phosphate, and also inhibit the uptake of phosphate in E-Coli [42-46].

Furthermore, in other possible mechanism it is claimed that the replication ability of DNA changes if DNA molecules are in relaxed or condensed state. If DNA is in the relaxed state, replication occurs without any problem. If DNA is in the condensed state, replication does not occur. Entrance of silver ions into the bacteria causes DNA condensation, that makes replication stopped and bacterial cells begin to die [47, 48].

Therefore, silver is toxic for microorganisms due to interference with the electron transport system of respiration and DNA function [32, 49, 50]. Ion concentration, which induces death, is directly proportional to the number of enzymes in microorganisms. Moreover, not only silver ion but also silver radicals produced by silver releasing agents can cause a lethal effect [36].

On the other hand, although it is not very common, two resistance pathways for silver are characterized in microorganisms. Microorganisms can evacuate silver by using their cellular efflux mechanism or they can work them up into an intracellular complex [51]. According to one study, resistance is triggered by using silver in low concentrations [52]. This means that the use of low concentrations makes bacteria resistant to silver as antibiotics do [51, 53]. However, exhibiting resistance to both antibiotic and noble metals (e.g. silver) at the same time is rare [54, 55].

Another important point is the ability of some substances in wound area (e.g. NaCl) to inhibit free silver activity by precipitating or chelating the ions. In addition to these

substances, which effect silver ion activity negatively, there are some other substances (e.g. EDTA), which enhance antimicrobial effect of the silver by preventing the function of these silver-binding substances [36].

Today, not only metallic but also many forms of the silver are being used for their antimicrobial effects. As it was mentioned before, AgSD is a combination of sulfadiazine and silver, which is used as a 1% (w/v) water-soluble cream. It has a wide range of bacteriocidal effect and provides slow release of silver ions to the wound. Being a kind of metallic silver, AgSD also binds to the cell components and damages the membrane [56]. When it binds to DNA of a bacteria or bacteriophage, transcription becomes inhibited [30, 57, 58].

Besides AgSD, silver zeolite is another silver derivative used as an antibacterial agent. It is generated by complexing the alkaline earth metal with the crystal aluminosilicate, which is partially displaced with silver ions by using an ion exchange method. Two possible inhibition mechanisms are found for silver zeolite. First one depends on the intake of silver ions by bacterial cells, which are in touch with silver zeolite. Second one depends on the generation of the reactive oxygen molecules that effects the respiration negatively [59].

Moreover, nowadays, using AgNPs is the other possible choice. Due to the large surface area, AgNPs contact with microorganisms better than the other salts leading to higher antimicrobial effect. They can penetrate into the bacteria and interact with the phosphorus contained compound, DNA, or attach to the cell membrane by interacting with the sulfur-containing proteins. As silver ions and salts, AgNPs affect the respiratory system to kill the bacteria by releasing the silver ion [37, 48, 60, 61]. Furthermore, shape and size of the nanoparticles are decisive for their antimicrobial efficiency. In many studies, AgNPs with different shapes are investigated to see their effects on the inhibition of the bacteria [37, 62]. According to these studies, AgNPs with different shapes have different influences on the bacteria. While triangular–shaped AgNPs need only 1 μg silver, spherical AgNPs need 12.5 μg and rod-shaped AgNPs need 50 μg to 100 μg silver to inhibit the bacterial growth. In addition to shape, size is also being studied. In one study, it is shown that, in contact with bacteria, AgNPs smaller than 10 nm, leads to an enhancement in their activity by generating electronic properties [37, 63].

1.3. WOUND HEALING AND SILVER USE

Antimicrobial property of the silver is known; however, there are still many concerns about its toxic effect on the healthy cells [64]. The most fundamental reason of this is the incapability of the silver in differentiating bacterial cells and healthy cells in wound beds. In addition, some studies show that lethal concentrations of the silver for the bacteria can also be lethal for the healthy cells such as fibroblasts and keratinocytes on the wounds [65].

Spontaneous wound healing process may be stopped or slowed by many events. Colonization of microorganisms in the wound bed is one of these impeding occasions. This situation causes a prolonged inflammatory response with the help of a great number of protease and toxin generation, sometimes leading damage to the surrounding tissues [66, 67]. Using antimicrobial agents before the development of infection on the wound is important; otherwise healing occurs very late under the infection conditions [66, 68].

Colonization of the bacteria triggers the migration of macrophages, monocytes, and leukocytes as an inflammatory response and this response becomes destructive over the time resulting in delay in the healing. The bacteria colonization also causes a competition between the cells and the bacteria for the nutrients and the oxygen. In addition, leukocytes need oxygen to kill the bacteria in wounds by phagocytosis. Colonization prevents leukocytes to use enough oxygen. Thus, oxygen, which is necessary for the healing, is begun to be consumed and healing is become delayed. Treating infection decreases the chronic inflammatory response and provides a positive effect on dynamics of the oxygen delivery and utilization in the wounds. Therefore, cell growth speeds up. Many silver-based dressings enable this microbe-free environment for wounds [69].

Recent studies claim that silver has not only antimicrobial but also other beneficial effects on wounds. Wound healing is related with both tissue synthesis, which is triggered by growth factors and tissue degradation, which is occurred by matrix metalloproteinases (MMP). Although MMPs, which are the members of collagenases, are necessary for wound healing, excess quantity of them causes the degradation of growth factors for peptide and fibronectin. Silver helps to keep MMPs in a level that is beneficial and necessary to heal the wounds by down-regulation [69].

Furthermore, there are additional studies showing that nanocrystalline form of silver is also effective in facilitating the wound healing by changing the inflammatory events. Increased level of apoptosis, reduced level of matrix metalloproteinases [70], and inhibitory effect on TNF-α, which is a type of proinflammatory cytokine [35], are the proofs of this claim. Besides, nanocrystalline silver prompts apoptosis, which is an anti-inflammatory process, instead of necrosis, which is an inflammatory process [69, 70].

Moreover, there are studies, which show that silver is effective not only in the inflammatory phase but also in the epithelialization phase by up-regulating the zinc metabolism [71, 72]. Silver induces metal-binding metallothioneins. That results the increase of zinc and copper concentrations. These metals are fundamental for epithelial cell proliferation. Increased zinc concentration leads to generation of MMPs, DNA and RNA-synthetases, and some other essential enzymes for a faster healing [36]. In contrast studies, it is observed that silver causes a decrease in surface zinc level leading to a decrease in excess MMP activity, because MMPs need free zinc to be active. In addition to decrease in zinc, silver also oxidizes and binds to sulfur bonds which are other necessary structures for MMPs to be active. Due to the reduced activity of excess MMPs, healing occurs fast.

Another indefinite effect of the silver, besides zinc, is related to calcium. Although mechanism is unknown, calcium levels increase after silver use. This observation is taken into account as a positive effect due to the active role of calcium in hemostasis and wound healing [36].

On the other hand, beneficial effects of the silver on wound healing, as an anti-inflammatory agent, depend on the concentration, duration of release, and sorts of silver [33, 35, 69, 70]. For example; silver nitrate treatment can cause a sudden increase in MMP level resulting in an inflammatory response or silver sulfadiazine can cause an increase in neutrophil level and protease activity on wounds. Although it is a good thing to decompose surface dead tissue, it is lethal for the healing wound bed [69]. Some additional studies about the silver sulfadiazine, again, prove the delay in burn wound healing based on the silver sulfadiazine itself not the re-epithelialization process [65, 73]. Silver sulfadiazine prevents the colonization of the microorganisms on wounds. It results in delay of eschar separation and slowing of the healing [74] with hypertrophic and atrophic scars [22, 75].

As it is seen, silver does not always show beneficial effects on wound healing. Many antimicrobial agents, which contain silver, lead to delay in the wound healing [65, 76]. Eventually, although silver is being used for its antimicrobial property, it also shows cellular toxicity [77]. Many *in vitro* studies indicate that silver ion has negative effect on lymphocytes, hepatocytes [78], and fibroblasts [79]. As to silver nanoparticles, there are variable studies. First *in vitro* studies could not detect any toxicity [80], and then some studies show that, in higher concentrations, AgNPs are also toxic for the cells [77]. Based on another study, at high concentrations between 5–50 mg/ml, AgNPs exhibit toxic effect on the cells. On the other hand, a different study claims that AgNPs at 25 mg/ml and lower concentrations do not have any cytotoxic effects [81]. This negative effect is based on its oxidative stress that decreases glutathione (GSH), reduces mitochondrial membrane potential, and increases reactive oxygen species (ROS), for AgNPs 15 nm and 100 nm in size [82]. Another study shows that concentration is deterministic for cytotoxic effects of silver zeolite like AgNPs [83]. All of these studies show that, whatever the source of the silver, its toxic effect is dependent on the concentration.

Absorption of the silver is another reason of the toxicity. Ionic silver interacts with the wound debris, some proteins, and cell surface receptors and it is accumulated in liver and kidney by passing through the wound area [36]. This case differentiates depending on the wound size. Although in small wounds, silver absorption is relatively low [84, 85], in large sized-wounds absorption amount is significant [86-88]. The fundamental disorder caused by silver is argyria, which indicates silver toxicity [89, 90]. Some recent studies claim that nano crystalline silver may also cause toxicity as transient skin discoloration and abnormalities in liver function [64].

As seen above, there is still a chaotic environment about the use of silver on wound healing because of the toxicity problem, although it shows an antimicrobial effect. Different properties of silver (such as size, surface chemistry, source, concentration) exhibit different effects on cells. This study was carried out to establish a relation between the effects of ion (Ag^+) and nanoparticle (AgNP) forms of silver on wound healing by taking account of the changing concentrations, surface chemistries, exposure times, and using different cell types.

2. MATERIALS

The materials, which were used in this study, were purchased from different suppliers as shown in Table 2.1-2.4.

2.1. CHEMICALS

All chemicals were used as received as demonstrated in Table 2.1 and H_2O was obtained from Ultrapure Water System.

Table 2.1. Overview of used chemicals

Name	**Supplier**
DMSO (Dimethylsulfoxide)	Amresco, UK
EDTA (Ethylenediaminetetraacetic acid)	Sigma, Germany
High Melting Agarose	Sigma, Germany
DNA Ladder (250bp-10000bp)	Fermentas, UK
DNA Ladder (50bp-1000bp)	Biobasic, CANADA
PBS (phosphate buffered saline)	Sigma, Germany
Penicillin/Streptomycin	Gibco, UK
L-Glutamine	Gibco, UK
Silver nitrate ($AgNO_3$)	Fluka, Germany
Sodium nitrate ($NaNO_3$)	Merck, Germany
Trisodium citrate ($Na_3C_6H_5O_7$)	Merck, Germany
0.25% Trypsin-EDTA Solution	Sigma, Germany
Lactose monohydrate	Merck, Germany
Maltose monohydrate	Merck, Germany
Glucose monohydrate	Merck, Germany
SDS (Sodium Dodecyl Sulfate)	Sigma, Germany
DMEM (Dulbecco's modified Eagle's medium)-High Glucose (4500 mg/l)	Sigma, Germany

Table 2.1. Overview of used chemicals (continue)

Name	**Supplier**
FBS (Fetal Bovine Serum)	Sigma, Germany
Proteinase K	Thermo (Finnzymes), USA
Ribonuclease A (RNase A)	Invitrogen, USA

2.2. MATERIALS

Table 2.2. Overview of used materials

Name	**Supplier**
6-96 well plates	TPP, Switzerland
Falcon Tubes (15 ml, 50 ml)	TPP, Switzerland
Micro Pipettes (1000, 200, 100, 10, 2.5 µl)	Eppendorf, Germany
Tissue Culture Flasks (25 cm^2, 75 cm^2)	TPP, Switzerland
Centrifugal Filter Devices	Millipore Amicon Ultra-15 Centrifugal Filter Units, USA
Serological Pipettes (25, 10, 5, 2 ml)	Axygen, USA
Cell Scraper	BD (Becton, Dickinson and Company), USA
Gel Loading Buffer	Sigma, Germany
Microscope Slides	Menzel, Germany
Coverslips (24x60)	Sail Brand, China

2.3. DEVICES

Table 2.3. Overview of used devices

Name	**Supplier**
Fluorescence Microscopy	Nikon Eclipse TE200, USA

Table 2.3. Overview of used devices (continue)

Name	**Supplier**
ICP-OES Spectrometer	Thermo iCAP 6000 Series ICP Spectrometer, USA
Gel Doc XR	BioRed, Germany
Laminar Flow Cabinet	ESCO Labculture Class II Biohazard Safety Cabinet Type 2A, Singapore
UV/Visible Spectrophotometer	Thermo Multiskan Spectrum Microplate Spectrophotometer, USA
Dynamic Light Scattering (DLS) Measurement	Malvern Zetasizer Nano ZS, USA
Water Purification System	Millipore Direct-Q 3 UV Water Purification System, USA
Scanning Electron Microscopy (SEM)	Carl Zeiss EVO 40, Germany
Vortex	Stuart SA8, UK
Transmission Electron Microscopy (TEM)	Oxford Instruments, USA
CO_2 Incubator	Nuaire NU5510/E/G, Germany
Inverted Light Microscope	Nikon Eclipse TS100, USA
Gel Electrophoresis Device	BioRad, Germany
ELISA Microplate Reader	Biotek ELx800 Absorbance Microplate Reader, USA
Centrifuges	Sigma 2-5 Centrifuge, Germany and Hettich Mikro 22R, Germany
Ultrasonic Bath	Bandelin Sonorex Sonorex Super, Germany
pH Meter	Mettler-Toledo, Germany

2.4. KITS

Table 2.4. Overview of used kits

Name	**Supplier**
Dead Cell Apoptosis Kit with Annexin V FITC and PI	Invitrogen, USA
CellTiter96 Aqueous One Solution Cell Proliferation Assay (MTS)	Promega, UK

3. METHODS

3.1. SYNTHESIS OF SILVER NANOPARTICLES (AgNPs)

3.1.1. Synthesis of 50 nm AgNPs with Sodium Citrate

The 50 nm AgNPs were synthesized by using Lee-Meisel method [91]. 90 mg $AgNO_3$ was dissolved in 500 ml distilled water. The solution was heated by stirring until boiling. When it boiled, 1% and 10 ml $Na_3C_6H_5O_7$ (trisodium citrate) solution was added drop by drop. After addition, solution was left to continue boiling until the total volume decreased to 250 ml. At last, the solution acquired a grayish-green color.

3.1.2. Synthesis of 50 nm AgNPs with Lactose Monohydrate, Maltose Monohydrate, and Glucose Monohydrate

In this part 50 nm AgNPs were prepared by using lactose monohydrate, maltose monohydrate, and glucose monohydrate respectively as reducing agents instead of sodium citrate [92]. 50 g maltose and glucose were dissolved in 100 ml dH_2O separately to obtain 500 µg/ml maltose-reduced AgNP (AgNP-M) and glucose-reduced AgNP (AgNP-G). They were left to boil. When they were boiled, 5 ml $AgNO_3$ solution, which was prepared by dissolving 85 mg $AgNO_3$ in 5 ml dH_2O for each AgNPs, was added drop by drop. For lactose-reduced AgNP (AgNP-L), stock solution was prepared as 50 µg/ml, because, in higher concentrations precipitation becomes a problem for AgNP-L. Thus, 5 g lactose was dissolved in 100 ml dH_2O. When it boiled, 5 ml $AgNO_3$ solution, which was prepared by dissolving 17 mg $AgNO_3$ in 10 ml dH_2O, was added drop by drop. After $AgNO_3$ addition, AgNPs were continued to boil for 20 min.

All AgNPs were characterized by using scanning electron microscopy (SEM), transmission electron microscopy (TEM), ultraviolet (UV)-visible spectroscopy, and dynamic light scattering (DLS) after the sonication to get rid of clusters and obtain more homogenous AgNPs suspensions. After these characterization analyses, a solubility test was done additionally for the most reliable AgNPs: AgNP-C and AgNP-M.

3.2. SILVER NANOPARTICLE (AgNP) CHARACTERIZATION

3.2.1. UV-Visible Spectroscopy Analysis

AgNPs were monitored using UV-Visible absorption spectroscopy, which exhibits the formation of AgNPs by showing the typical surface plasmon absorption maxima at 418-420 nm in UV-Vis range.

3.2.2. Dynamic Light Scattering (DLS) Analysis

DLS (Zetasizer, Malvern) was used to measure the size distribution of AgNPs in a colloidal suspension. All measurements were performed at 25 $^{\circ}$C at 173° scattering angle with a 4 mW He–Ne laser in polystyrene cuvettes.

3.2.3. Transmission Electron Microscopy (TEM) Analysis

TEM characterization was accomplished by using JEOL-2100 HRTEM operating at 200 kV (LaB_6 filament) and equipped with an Oxford Instruments 6498 EDS system.

3.2.4. Scanning Electron Microscopy (SEM) Analysis

SEM images of AgNPs were obtained in 156 kV accelerating voltage by using Karl Zeiss EVO 40 model SEM instrument.

3.2.5. Dissolution Analysis

Dissolution of AgNP-C and AgNP-M were analyzed by using a centrifugal filter having 3000 nominal molecular weight limit (NMWL), which allows Ag^+ pass, while keeping AgNPs up onto the filter device reservoir. Therefore, the concentration of Ag^+ released from AgNPs during washing can be determined. As seen on Figure 3.1, the container part of the filter was separately filled with freshly synthesized AgNPs (AgNP-C and AgNP-M) and centrifuged at 5500 rpm for 45 min. Then, the transparent liquids, which were collected in centrifuge tube part, were transferred into a new 50 mL falcon tube as ultrafiltrates of the

first day. The filtrate AgNPs remained on the filter was resuspended into 15 mL of distilled water. The AgNP suspensions were left for 24 h at room temperature. Then, the same centrifuge procedure was repeated for the third and fourth days. The collected samples were analyzed with Inductively Coupled Plasma-Optic Emission Spectrometer (ICP-OES).

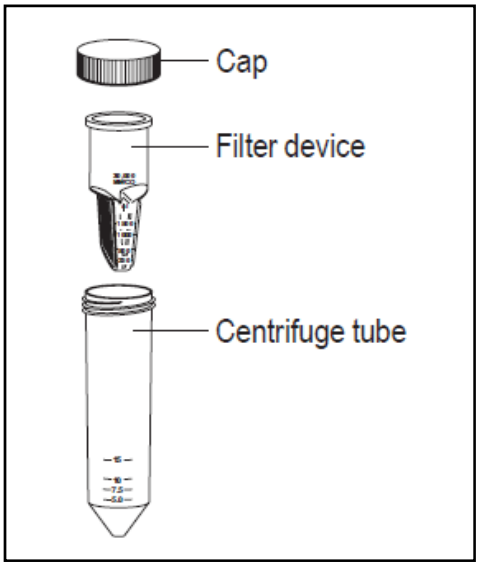

Figure 3.1. Basic parts of Amicon Ultra-15 Centrifugal Device [94]

3.3. CELL CULTURE AND CELL PROLIFERATION ASSAY

3.3.1. Cell Culture

Three cell types: HDF (human dermal fibroblast), L929 (mouse fibroblast), and RAW (mouse macrophage) cells were used during all the experiment. All cells were grown in Dulbecco's Modified Eagle's Medium (DMEM) with high glucose concentration (4500 mg/l) containing 10% fetal bovine serum (FBS) (v/v), 1% penicillin-streptomycin solution and 1% L-Glutamine at 37°C with 5% CO_2.

3.3.2. Preparation of Stock Solutions and MTS Assay

In first part, HDF, L929, and RAW 264.7 cells were treated with ions at different concentrations to see the effect of silver ion (Ag^+) individually and compare its effect with

other ions. For this aim, silver nitrate ($AgNO_3$), sodium nitrate ($NaNO_3$), and trisodium citrate ($Na_3C_6H_5O_7$) were used as ion sources. Stock concentrations were prepared as 500 µg/ml, 250 µg/ml, 100 µg/ml, 50 µg/ml, 25 µg/ml, 10 µg/ml, 5 µg/ml, 0,5 µg/ml, and 0,05 µg/ml for each compounds.

In the second part, AgNP-C was synthesized in the same concentrations as in first part, which was applied for ions.

In the third part, effects of carbohydrate-reduced silver nanoparticles were investigated. Lactose and maltose were chosen as disaccharides; glucose was chosen as monosaccharide among carbohydrates. Same stock concentrations used in first and second parts were prepared for these silver nanoparticles except lactose. AgNP-L exhibit low solubility, therefore stock solutions were prepared as 50 µg/ml, 25 µg/ml, 10 µg/ml, 5 µg/ml, 0,5 µg/ml, and 0,05 µg/ml for this AgNP.

The cytotoxicity caused by AgNPs and ions was detected by using MTS-assay. MTS (3-(4,5-dimethyl-thiazol-2-yl)-5-(3-carboxy-methoxy-phenyl)-2-(4-sulfo-phenyl)-2H-tetrazolium) is a colorimetric assay. In living cells, MTS is reduced to formazan, which is a kind of tetrazolium-salt, in mitochondria of the cells by active enzymes. This reduction reaction gives purple color; hence viable cells can be detected. HDF and L929 cells were seeded in 96-well plates at 5 x 10^3 cells per well; RAW 264.7 cells were seeded in 96-well plates at 22.5 x 10^3 cells per well due to their smaller size. Three replicates were prepared for each ion, AgNP, and control cells. The untreated cells were used as a negative (no treated) control. Seeded cells were incubated at 37°C for 24 h. After 24 h, the cells except control cells were treated with 50 µg/ml, 25 µg/ml, 10 µg/ml, 5 µg/ml, 2.5 µg/ml, 1 µg/ml, 0.5 µg/ml, 0,05 µg/ml, and 0,005 µg/ml ions and AgNPs for 24 h, 48 h, and 72 h by mixing DMEM, which contains high glucose concentration (4500 mg/l), 10% (v/v) fetal bovine serum, 1% (v/v) penicillin-streptomycin solution, with stock solutions in 10% (v/v) ratio. After removal of the medium including ions and AgNPs, MTS assay was applied to the cells. Fresh medium containing 10% MTS solution was put on the cells and cells were incubated for 4 h in incubator. After 4 h, cell viability was measured at 490 nm using the ELISA plate reader (KC junior software, Elx80).

3.4. MORPHOLOGICAL ANALYSIS OF THE CELLS AND DNA FRAGMENTATION

The DNA damage was analyzed by DNA fragmentation method. Endonuclease activation is a characteristic property of apoptosis that degrades genomic DNAs at internucleosomal linker regions. Therefore, smaller sized-DNA fragments are produced. When they are run in agarose gel, a ladder appearance occurs. By using DNA fragmentation, apoptosis and toxic cell death can be distinguished. HDF and L929 cells were seeded in 6-well plates at 15 x 10^4 cells per well; RAW 264.7 cells were seeded in 6-well plates at 67.5 x 10^4 cells per well. The untreated cells were used as a negative (no treated) control. Seeded cells were incubated at 37°C for 24 h. Conversely to cytotoxicity part, a narrow concentration range was chosen for this time. After 24 h incubation, the cells except control cells were treated with 5 µg/ml, 2.5 µg/ml, 1 µg/ml, 0.5 µg/ml, and 0,05 µg/ml Ag^+, AgNP-C, and AgNP-M for 24 h by mixing DMEM, which contains high glucose concentration, 10% (v/v) fetal bovine serum, 1% (v/v) penicillin-streptomycin solution, with stock solutions in 10% (v/v) ratio. Before DNA fragmentation analysis, first, morphological changes of the cells after the exposure were monitored by using light microscopy at 10X magnification (Figure 4.27-4.35).

After obtaining cell images, DNA fragmentation was carried out. The old medium, which includes floating death cells and cell waste, belongs to each well was collected into 2 ml eppendorf tube. Wells were washed with 1X PBS solution and it was transferred into the tubes again. All eppendorf tubes were centrifuged at 2500 rpm for 20 min. During centrifuge, living cells at the bottom of the wells were harvested. At the end of the centrifuge, supernatant part was removed. Cell suspensions, which were obtained after harvesting, were transferred into the tubes. Tubes were recentrifuged at 1500 rpm for 5 min to prevent giving damage to the living cells. After the centrifuge, supernatant was removed completely and pellet was resuspended in a solution that contains 10 mM EDTA, 50 mM Tris-HCl (pH 8.0), and 0.5% (w/v) SDS. Proteinase K, which has 20 mg/ml stock concentration, was then added to the tubes reaching 1 mg/ml final concentration. Proteinase K inactivates nucleases such as DNase and RNase to prevent degredation of DNA or RNA. In addition to this, its activity increases with chemicals, which denature proteins, such as SDS at temperatures 50°C-60°C. Hence, after mixing proteinase K with

SDS solution, tubes were incubated at 50^{o}C for 1 h. After 1 h, ribonuclease A (RNase A) was added into the tubes reaching 1 mg/ml final concentration. RNase A is used to cleave single-stranded RNA, while obtaining DNA alone. After addition, again the tubes were incubated at 50^{o}C for 1 h. While samples were incubating, 1% (w/v) agarose gel was prepared. 1 g agarose was weighed and put into 100 ml 1X TBE (Tris Borate EDTA), then mixed. Agarose solution was heated in microwave for approximately 1 min until it boiled and gained transparency. It was cooled at room temperature to make it possible to hold it with bare hands. 3 µl of ethidium bromide (10 mg/ml) was added and mixed. The gel was then poured into the tank and comb was placed. Bubbles were pushed away and gel solution was left to solidify for about 30 min. After the gel was formed, 0.5X TBE buffer was poured into the tank to run the gel. When incubation of the samples completed, 10 µl loading solution (consists of 10 mM EDTA (pH 8.0), 1% (w/v) agarose with low melting point, 40% (w/v) sucrose, and 0.25% (w/v) bromophenol blue) was added to the tubes and mixed with the samples to give color and density to them. Loading solution makes it easy to load the samples into the wells. The samples were heated to 70^{o}C. 3 µl DNA ladder and 10 µl from each sample were loaded to the wells in 1% (w/v) agarose gel. The gel was run at 40V for 4 h. After 4 h, it was visualized using UV transillumination. Gel images on Figure 4.36-4.39 were obtained and results were analyzed with respect to the morphological changes.

3.5. ANNEXIN V-PI STAINING

For a better understanding, the death mechanism of the cells after the exposure of toxic concentrations of the silver compounds was investigated using Annexin V-propidium iodide (PI) staining. With strong efficiency, Annexin-V can bind phosphatidylserine, which is externalized from the inner (cytosolic) surface of the cell membrane to the outer surface at an early phase of apoptosis. Furthermore, PI can enter the cell if and only if membrane integrity is decomposed severely. Thus, early apoptosis can be differentiated from late apoptosis or necrosis. Annexin V and PI staining was performed by using 'Dead Cell Apoptosis Kit with Annexin V-FITC and PI' kit (Invitrogen). Manufacturer's instruction was followed, while performing experiment. First, 1x10^{6} cells from each cell type were seeded in six-well plate and left for 24 h to attach. After they attached on the surface of the wells, they were treated with toxic concentrations of silver compounds: 5 µg/ml, 2.5 µg/ml,

1 µg/ml for $AgNO_3$ and 5 µg/ml, 2.5 µg/ml for AgNP-M for 24 h. After 24 h, both attached (by harvesting) and non-attached cells were collected and washed with PBS. The cells were centrifuged at 1500 rpm for 10 min. The cells were then resuspended in 500 µl of 1X annexin binding buffer. 5 µl annexin V-FITC, and 3 µl of PI were added and incubated for 15 min at 37˚C in the dark. At the end of 15 min, wet-mount technique was applied to the samples. One drop of each sample was put on the slide and one drop of mounting media was dropped on it. It was then covered with a coverslip. Finally, cells were observed under fluorescent microscope with appropriate filters. Images were taken at 520 nm for annexin V-FITC, and 620 nm for PI.

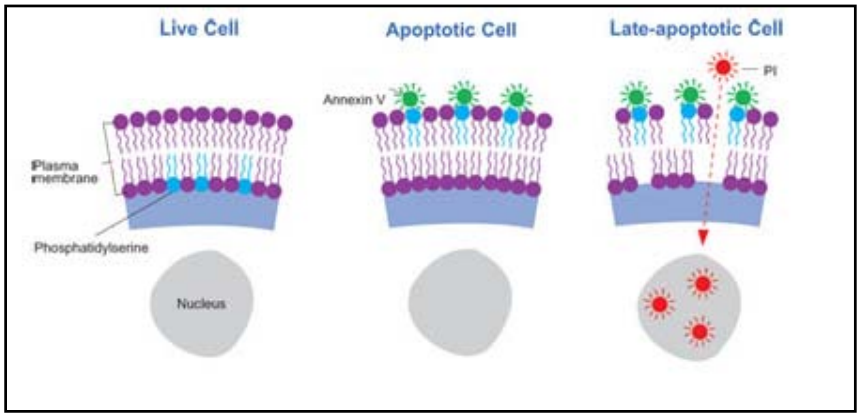

Figure 3.2. Schematic representation of Annexin V-PI function [93]

4. RESULTS AND DISCUSSIONS

4.1. CHARACTERIZATION OF AgNPS

The size and surface chemistry of AgNPs were confirmed by using dynamic light scattering (DLS), UV-Visible spectroscopy, transmission electron microscopy (TEM) and scanning electron microscopy (SEM). The dissolution of AgNP-C and AgNP-M were also analyzed.

The AgNPs both absorb and scatter light. At specific wavelengths, due to the strong interaction between light and AgNPs, electrons on the surface of AgNPs oscillate. This oscillation generates a magnetic field called surface plasmons, which strongly depends on the size and shape of AgNPs. The light scattering property is also influenced by the shape and size of the NPs. For spherical AgNPs as in this study, size of the NPs is deterministic for their optical properties. Thus, UV-Vis spectroscopy can be used to determine the size of AgNPs. The UV-Vis spectra of all synthesized AgNPs are in good agreement with the ones reported in literature [91, 92]. AgNPs prepared with Lee method have a maximum peak at around 420 nm and the size of NPs is in the range of 20-200 nm with an average size of 60 nm [91]. As in Lee method, carbohydrate-reduced AgNPs have a similar absorption spectrum with a maximum at around 420 nm and have the average size of 50 nm. Figure 4.1 shows AgNP-G and AgNP-L have almost same absorptions at about 410 nm on the UV-Vis spectrum. Besides, AgNP-M and AgNP-C have also almost same absorptions at about 420 nm. This means, based on UV-Vis spectra, all AgNPs were synthesized approximately 50 nm in size. AgNP-C and AgNP-M showed broader peaks, which shifted towards longer wavelengths than AgNP-G and AgNP-L did. Although it means that AgNP-C and AgNP-M have larger size than AgNP-G and AgNP-L, size distribution is closer to 50 nm.

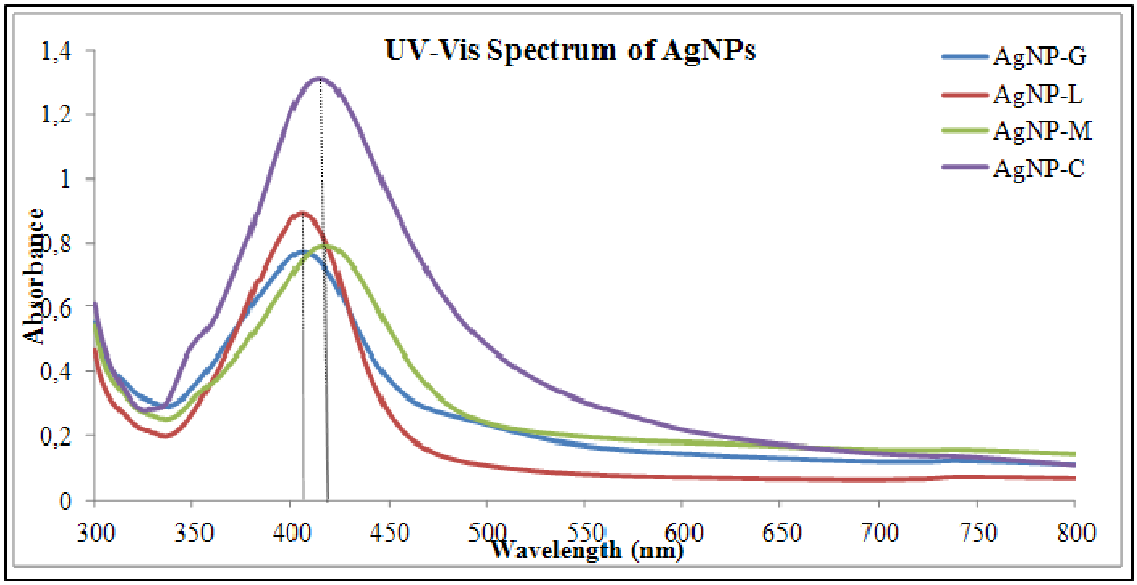

Figure 4.1. UV–Visible absorption spectra of AgNPs containing suspensions

AgNP-C and AgNP-M were also characterized with TEM and SEM. Figure 4.2 shows a. SEM image of 50 nm AgNP-C, b. TEM image of 50 nm AgNP-C, c. TEM image of 50 nm AgNP-M. As seen, the shapes of AgNPs are spherical and the sizes are about 50 nm. In addition, AgNP-M are slightly larger than 50 nm.

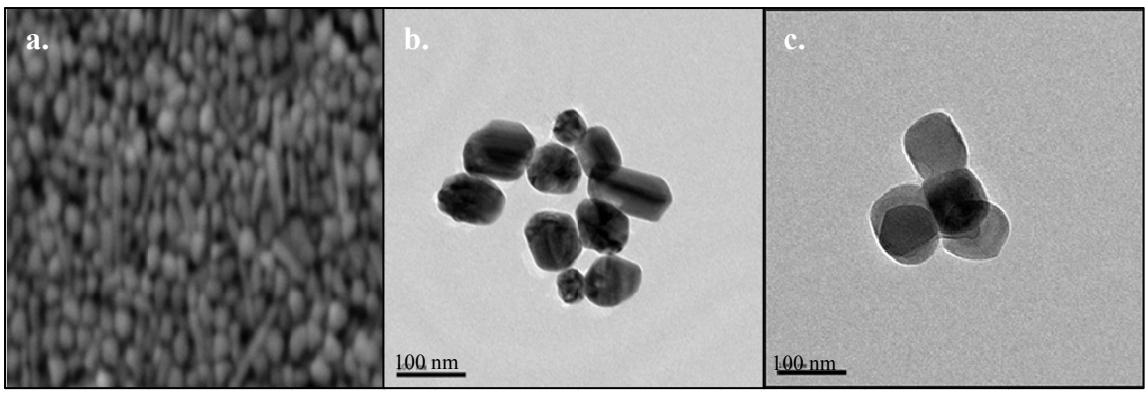

Figure 4.2. a. SEM image of 50 nm AgNP-C, b. TEM image of 50 nm AgNP-C, c. TEM image of 50 nm AgNP-M

Dynamic light scattering (DLS) was used to observe the size distribution of AgNPs in suspensions (Figure 4.3). Even though it is expected to obtain larger size than 50 nm due to the measurement of hydrodynamic diameters in DLS analyses, as seen in Figure 4.3, none

of the AgNPs had a size distribution around 50 nm. While AgNP-M and AgNP-C showed a size distribution around 100 nm, AgNP-L and AgNP-G were synthesized larger than 100 nm in size. On the other hand, although being at lower concentrations than it should be, AgNP-C and AgNP-M suspensions had nanoparticles about 50 nm in size. When all the other characterization analyses (TEM and SEM images, UV-Vis Spectra, dissolution rates) were considered, even though the results belong to DLS analysis do not seem reliable, synthesized AgNPs can be acceptable to use.

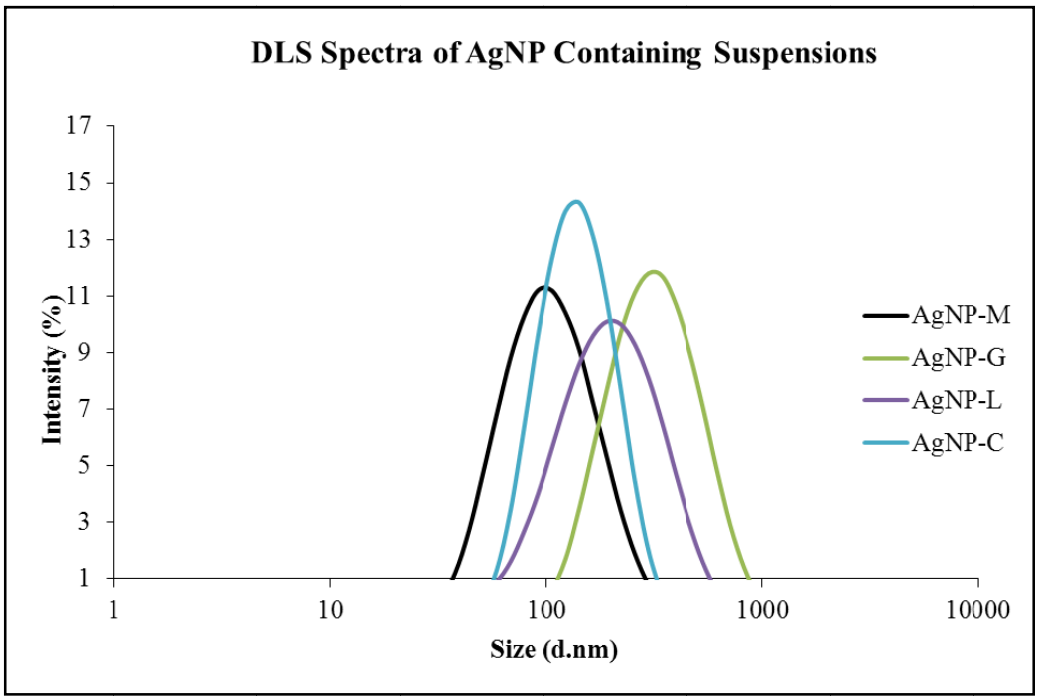

Figure 4.3. DLS Spectra of AgNP containing suspensions

Dissolution of the synthesized NPs is very important to evaluate toxicity and antimicrobial property of AgNPs. Therefore, dissolution of the AgNPs in distilled water used in this study was investigated. The dissolution rate depends on chemical species on the particle surface, particle size, particle crystallinity, and the surface functionalization [104, 105]. In this part, two AgNPs (AgNP-C and AgNP-M), which were synthesized with two different reagents and have better characterization results, were tested for their dissolution in pure water during 4 days. Figure 4.4 and Figure 4.5 show the release of Ag^{+} concentration from AgNP-C and AgNP-M during 4 days respectively. The values represent the mean of three experiments and error bars are not visible due to small deviation for some values. The

reducing agent influences not only the atomic crystal packing but also the surface chemistry of the nanoparticle. Therefore, the dissolution of citrate and carbohydrate-reduced AgNPs were investigated. As seen in Figure 4.4, released Ag concentration is almost zero, and it does not dissolve for the rest of the days. This data show that, within 4 days period, AgNP-C do not release significant amount of Ag^{+} to the environment and keep their integrity.

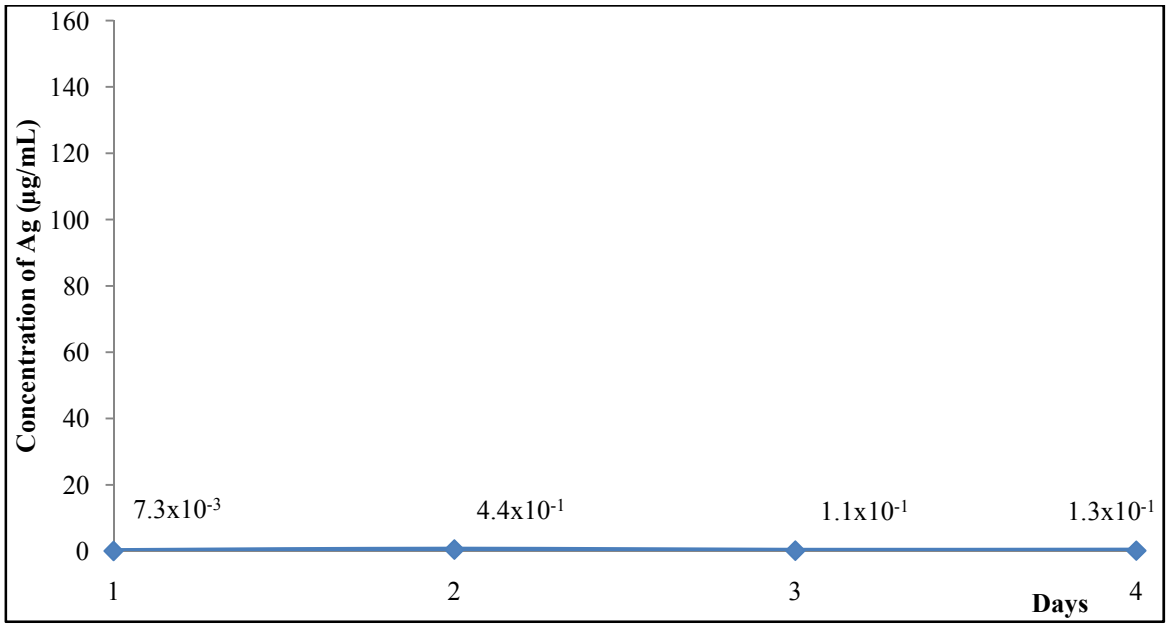

Figure 4.4. Dissolution of AgNP-C in pure water

Figure 4.5 show the dissolved Ag^{+} from the AgNP-M in water with increasing days. As seen, the concentration of Ag^{+} is very high as it is synthesized, which means there is some unreduced Ag^{+} in the reaction mixture. After the first washing step and keeping the AgNPs in water, there is still some Ag^{+} are present in the solution. However, after the third day, there is almost no observed Ag^{+}. Based on the similar toxicity grades, it can be said that the other carbohydrate-reduced AgNPs (AgNP-L and AgNP-G) possibly dissolve in a rate resembles AgNP-M.

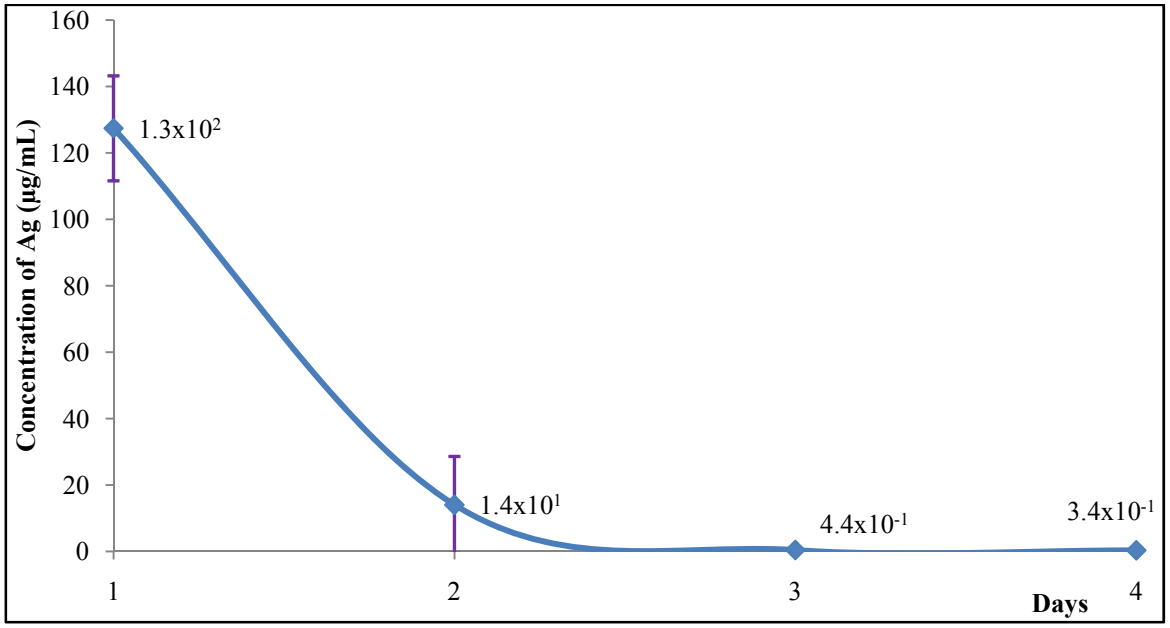

Figure 4.5. Dissolution of AgNP-M in pure water

The high concentration of unreduced Ag^+ is very important for the toxicity explanation of the colloidal suspension used for the cell culture experiments. Although it was chosen to use AgNPs after synthesis without any dialysis process in this experiment, an additional dialysis step to remove uncoupled ions from the suspensions can be carried out for AgNPs to eliminate the toxicity that may be caused by these free ions (such as $C_6H_5O_7^{3-}$ and Ag^+) and to see the difference between the toxic effects of AgNPs and AgNPs after the dialysis. Based on the Figure 4.4 and Figure 4.5, dialysis can be important especially for carbohydrate-reduced AgNPs such as AgNP-M, which shows high solubility after the synthesis.

As seen, the AgNPs prepared both synthesis methods dissolves at a certain level. Therefore, when the toxicity is concerned, these points must be taken into the account. It must be said that dissolution of AgNPs change depending on matrices that they are present. Therefore, when it comes to cell culture, many other supplements, which exist in growth media, can cause different dissolution rates of AgNPs from the dissolution in pure water. For example, many biological solutions contain chloride ions, which form AgCl particles or aqueous $AgCl_2^-$ or $AgCl_3^{2-}$ compounds with dissolved silver ions. Dissolution rates in DMEM are higher than in pure water because of the higher chloride concentration in

DMEM. Chloride generates complexes with silver ions that may cause faster dissolution in high chloride concentrations [106].

Although AgNPs may dissolve higher concentrations in DMEM than in pure water, dissolution rates of AgNPs in pure water shed a light on the toxicity of them in cell growth media. When the dissolution in pure water and the cell toxicity results are compared, it is observed that the toxic effect on the cells was caused by Ag^+ not the nanoparticles. While AgNP-C, which do not release any Ag^+ to the environment in time, show no toxic effect, AgNP-M, which show a high concentration of uncoupled Ag^+ after the synthesis, is observed more toxic than AgNP-C but less toxic than Ag^+ itself.

Based on the analyses, citrate is more favorable and reliable reducing agent than carbohydrates for the synthesis of AgNPs when the toxicity of the AgNPs is considered.

4.2. CYTOTOXICITY STUDIES

Fibroblasts, are the most common cells in connective tissue of animals, which have many functions. Their main function is synthesizing collagen, which is a protein and has an important role in the wound healing [10]. In addition to fibroblasts, macrophages are also another essential cell type for wound healing especially during inflammatory phase [7]. Therefore, these two types of the cells were chosen to study the effects of Ag^+ and AgNPs on their behavior.

In the first part, the effect of Ag^+ on cells was investigated by comparing with Na^+ and $C_6H_5O_7^{3-}$. $AgNO_3$ was used as the source of Ag^+, $NaNO_3$ was used as the source of Na^+ and $Na_3C_6H_5O_7$ was used as the source of $C_6H_5O_7^{3-}$. For this aim, moles of NO_3^- (in $AgNO_3$ and $NaNO_3$ solutions) were made equal to each other and $3Na^+$ (in $Na_3C_6H_5O_7$). After that, concentration NO_3^- of $AgNO_3$ and $NaNO_3$ were calculated approximately 500 μg/ml by dissolving 137 mg of $AgNO_3$ and 68.5 mg of $NaNO_3$ in 100 ml distilled water, respectively, to observe the effect of Ag^+ compared to Na^+. The same concentration was then equalized with $3Na^+$ of $Na_3C_6H_5O_7$ by dissolving 79.1 mg $Na_3C_6H_5O_7$ in 100 ml distilled water to see the effect of $C_6H_5O_7^{3-}$ only. For this, the stock solutions of $AgNO_3$ and $NaNO_3$, which contained 500 μg/ml of NO_3^- (0.806×10^{-3} mole), and stock solution of

$Na_3C_6H_5O_7$, which contained approximately 500 µg/ml of $3Na^+$ ($0.806x10^{-3}$ mole), were prepared.

In this part, an idea about the effects of Ag^+, Na^+, and $C_6H_5O_7^{3-}$ can be individually observed. The test concentrations were determined as 500 µg/ml (stock), 250 µg/ml, 100 µg/ml, 50 µg/ml, 10 µg/ml, 5 µg/ml, 0,5 µg/ml, 0,05 µg/ml. For the cell culture experiment, the first day, cells that were grown in DMEM containing high glucose concentration (4500 mg/l) with 10% (v/v) FBS and 1% (v/v) PS were seeded on 96 well-plates with a 100 µl volume and left for 24 h in an incubator (at 37^oC, 5% CO_2) to provide attachment of the cells. Due to the different morphologies and sizes, the number of the cells, which were seeded in each well, differs for the each cell type. This cell count was 5000 for HDF and L929 cells, 22500 for RAW 246.7 due to their smaller size. The second day, after they regained their original morphologies, the cells were exposed to the compound solutions for 24 h, 48 h, and 72 h incubation periods.

During incubation, the cells need medium to continue for their functions to live, thus the ions and AgNPs cannot be used alone. They were mixed with the medium. In this process, it is important to prepare this mixture in an equal ratio for all the samples not to obtain incorrect results, when the compound solution-medium mixture was prepared in a variable ratio. All prepared concentrations were again diluted with cell medium (DMEM containing high glucose (4500 mg/l) with 10% FBS and 1% PS) in 1/10 (v/v) ratio; 10 µl of ion solution or AgNP suspension and 90 µl of medium having 100 µl total volume for each well. After the dilution with medium, samples were ready to test for the cell viability with final concentrations; 50 µg/ml, 25 µg/ml, 10 µg/ml, 5 µg/ml, 1 µg/ml, 0,5 µg/ml, 0,05 µg/ml, and 0,005 µg/ml. At the end of every exposure time, old medium containing the ion solution or AgNP suspension was removed, and MTS assay was carried out for detection of the cell viability. MTS (3-(4,5-dimethylthiazol-2-yl)-5-(3-carboxymethoxyphenyl)-2-(4-sulfophenyl)-2H-tetrazolium), assay is a colorimetric assay based on the enzyme activity to detect cell viability and growth [95]. Basically, living cells have active enzymes that can be transform MTS to a kind of formazan salt, which has an absorbance in the range of 490-500 nm. This transformation gives purple color that allows the observation with naked eye. To apply MTS assay, first MTS reagent was mixed with fresh medium in 1/10 (v/v) ratio (10 µl of MTS reagent and 90 µl of medium having 100 µl total volume for each well)

avoiding direct light not to lose luminescence property. The cells were incubated for 4 h in incubator (at 37°C, 5% CO_2) at dark. After the incubation, color change (to purple) was observed for living cells and absorbances were measured at 492 nm. Based on the absorbance values, the cell viability percentages were calculated and presented on Figure 4.6-8 for HDF cells, Figure 4.9-11 for L929 cells, and Figure 4.12-14 for RAW 264.7 cells.

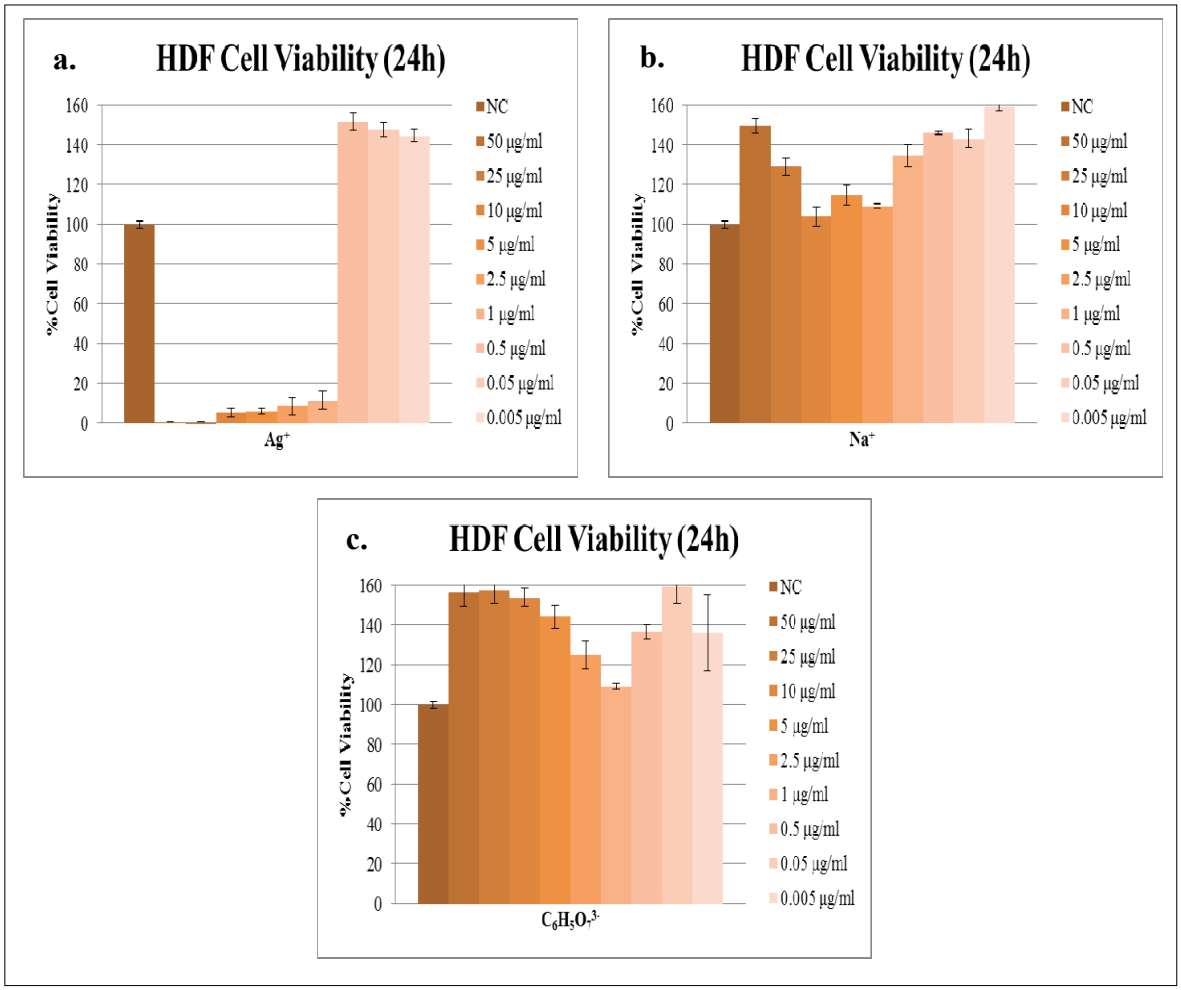

Figure 4.6. Viability of HDF cells, after treatment with a. Ag^+, b. Na^+, and c. $C_6H_5O_7^{3-}$ for 24 hours in the presence of 50, 25, 10, 5, 2.5, 1, 0.5, 0.05, and 0.005 µg/ml concentrations. 'NC' denotes negative control and the values represent the mean of three replicates.

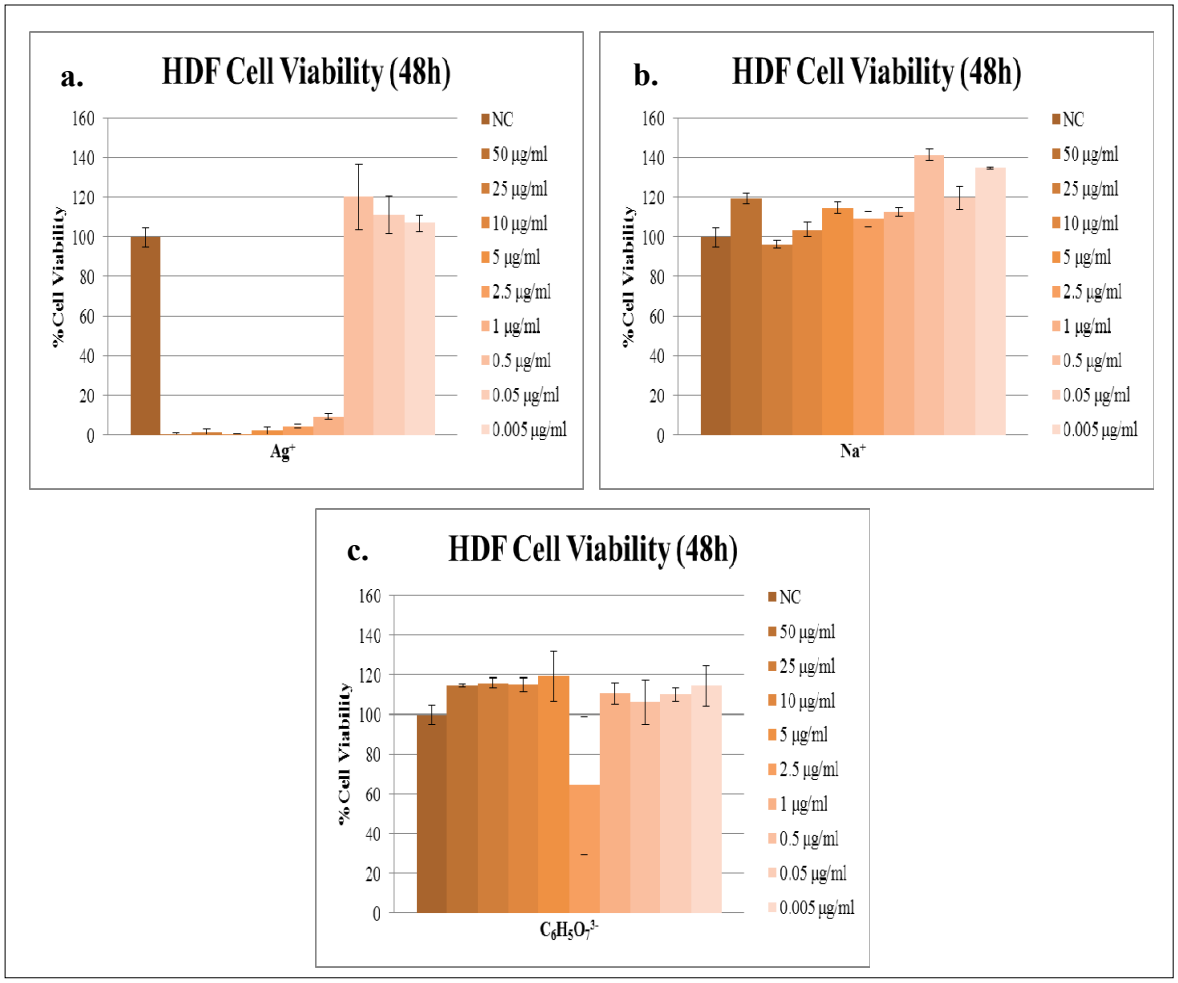

Figure 4.7. Viability of HDF cells, after treatment with a. Ag^{+}, b. Na^{+}, and c. $C_6H_5O_7^{3-}$ for 48 hours in the presence of 50, 25, 10, 5, 2.5, 1, 0.5, 0.05, and 0.005 µg/ml concentrations. 'NC' denotes negative control and the values represent the mean of three replicates

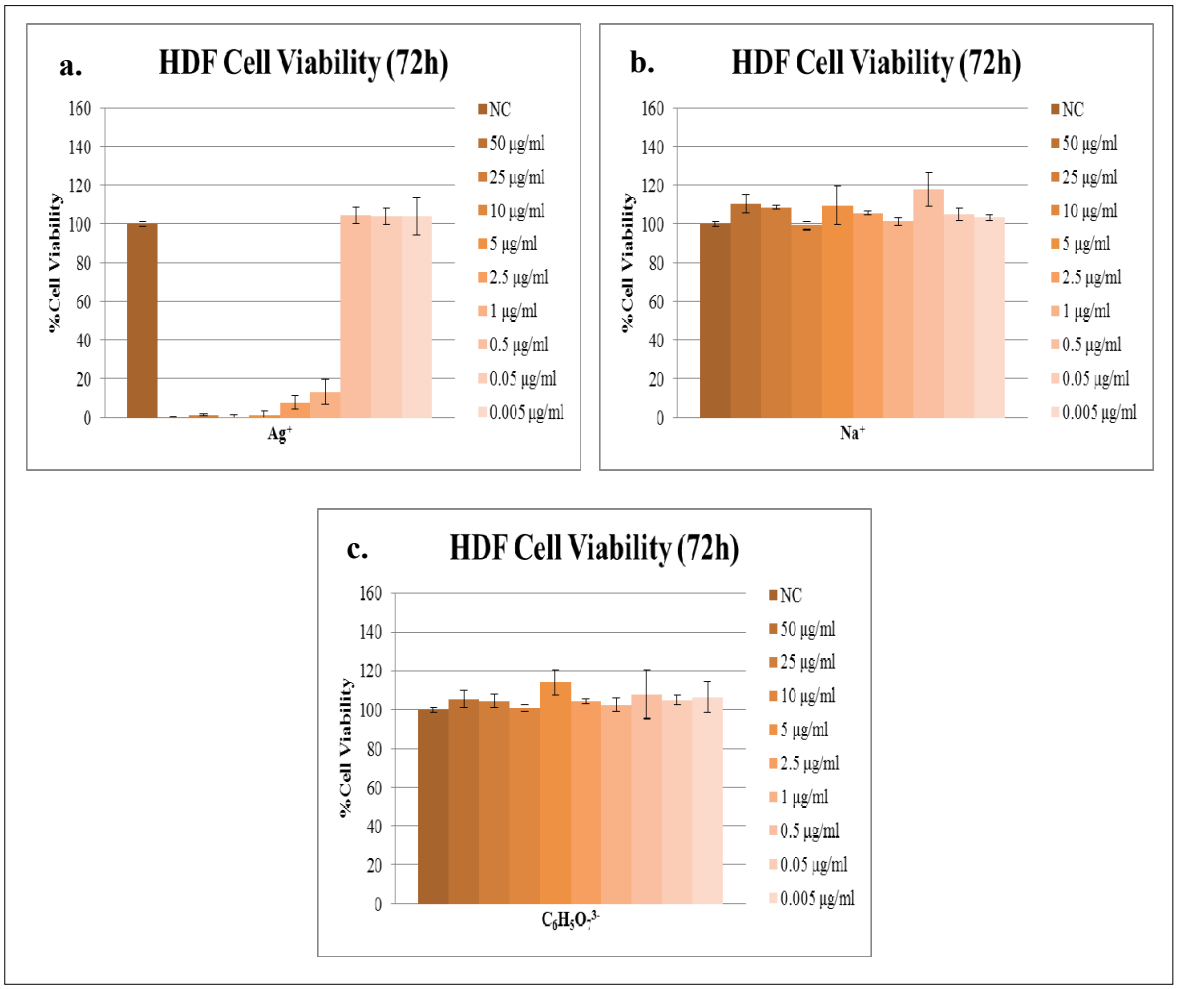

Figure 4.8. Viability of HDF cells, after treatment with a. Ag^{+}, b. Na^{+}, and c. $C_6H_5O_7^{3-}$ for 72 hours in the presence of 50, 25, 10, 5, 2.5, 1, 0.5, 0.05, and 0.005 µg/ml concentrations. 'NC' denotes negative control and the values represent the mean of three replicates

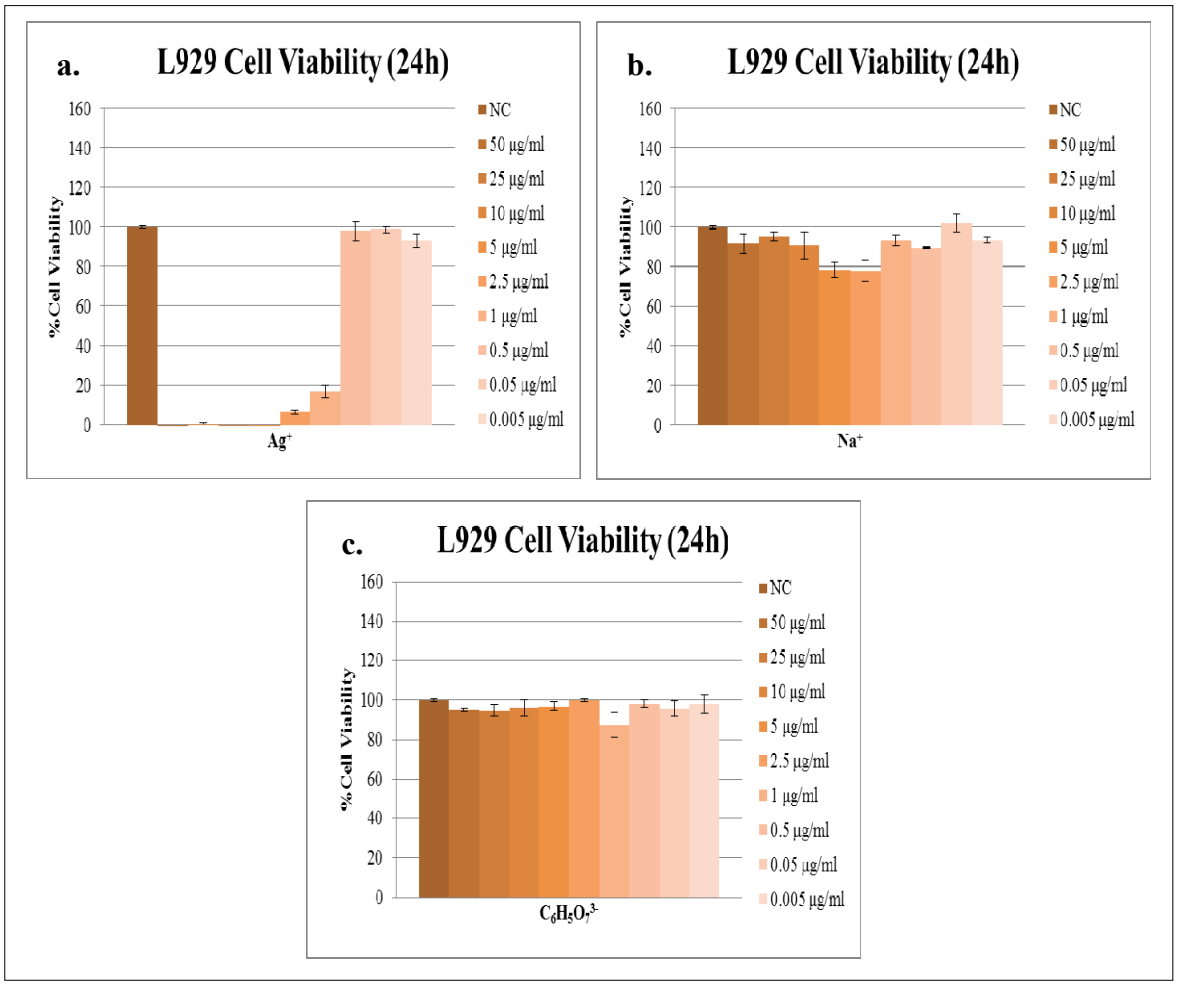

Figure 4.9. Viability of L929 cells, after treatment with a. Ag^{+}, b. Na^{+}, and c. $C_6H_5O_7^{3-}$ for 24 hours in the presence of 50, 25, 10, 5, 2.5, 1, 0.5, 0.05, and 0.005 µg/ml concentrations. 'NC' denotes negative control and the values represent the mean of three replicates

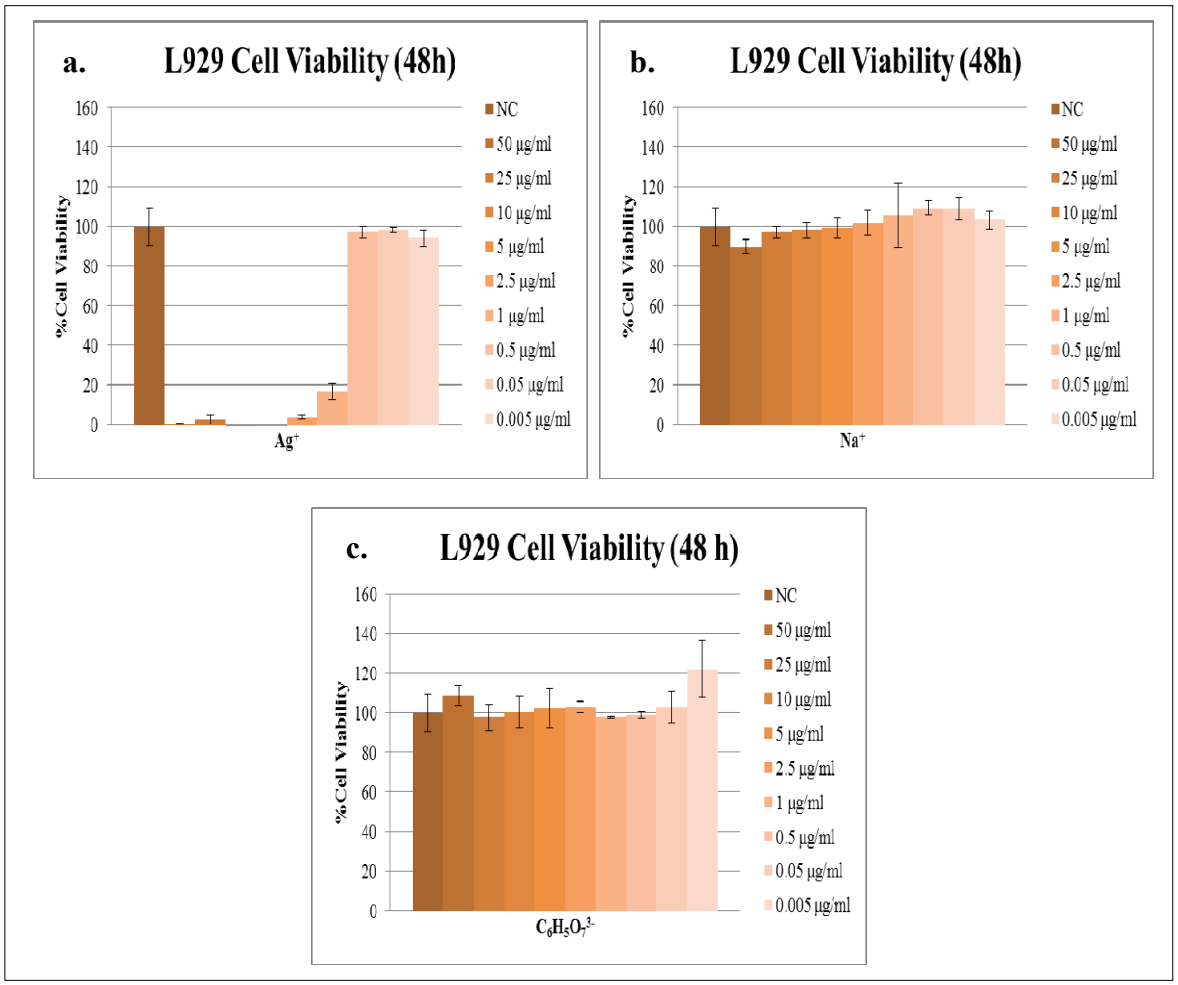

Figure 4.10. Viability of L929 cells, after treatment with a. Ag^{+}, b. Na^{+}, and c. $C_6H_5O_7^{3-}$ for 48 hours in the presence of 50, 25, 10, 5, 2.5, 1, 0.5, 0.05, and 0.005 µg/ml concentrations. 'NC' denotes negative control and the values represent the mean of three replicates

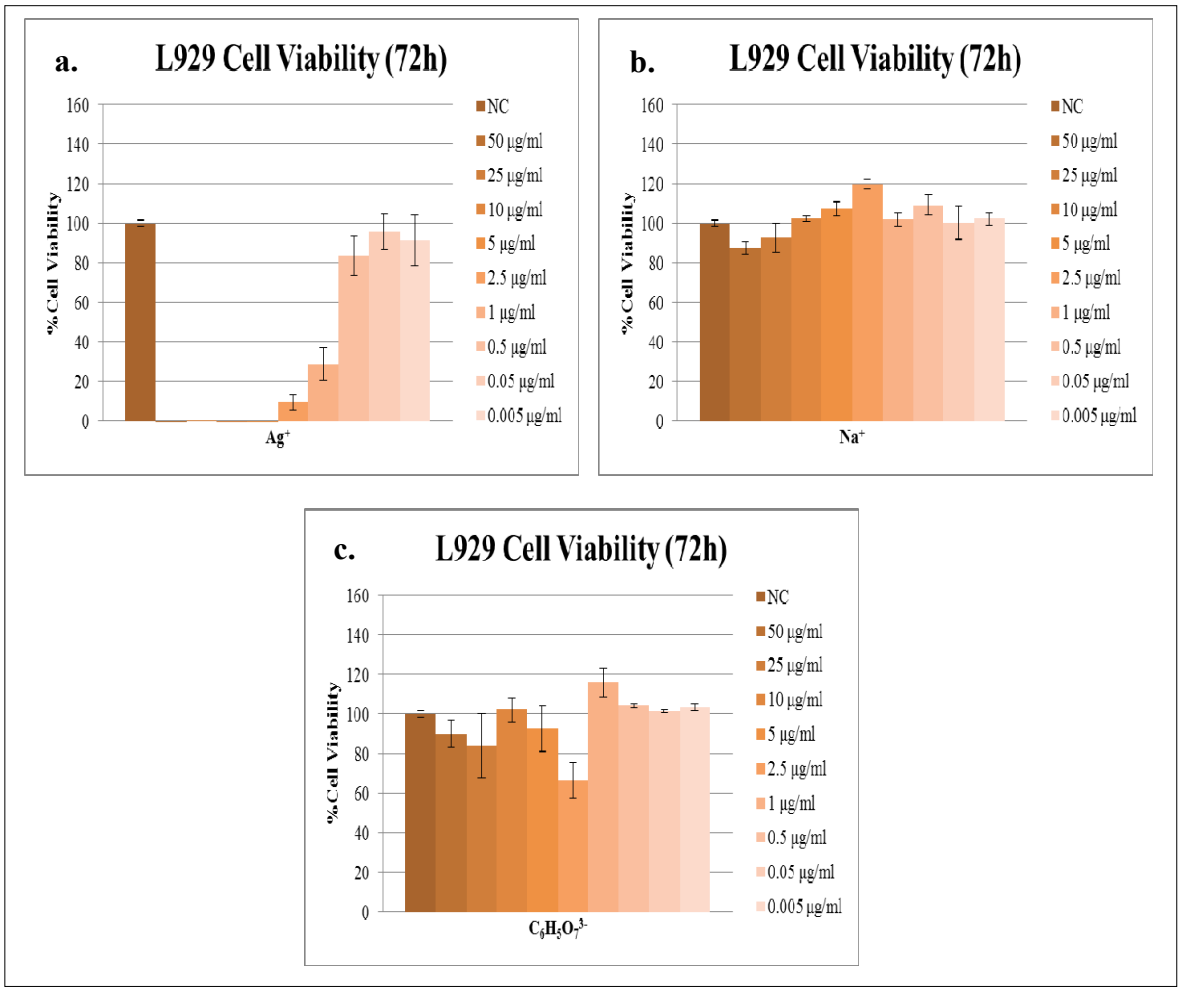

Figure 4.11. Viability of L929 cells, after treatment with a. Ag^{+}, b. Na^{+}, and c. $C_6H_5O_7^{3-}$ for 72 hours in the presence of 50, 25, 10, 5, 2.5, 1, 0.5, 0.05, and 0.005 µg/ml concentrations. 'NC' denotes negative control and the values represent the mean of three replicates

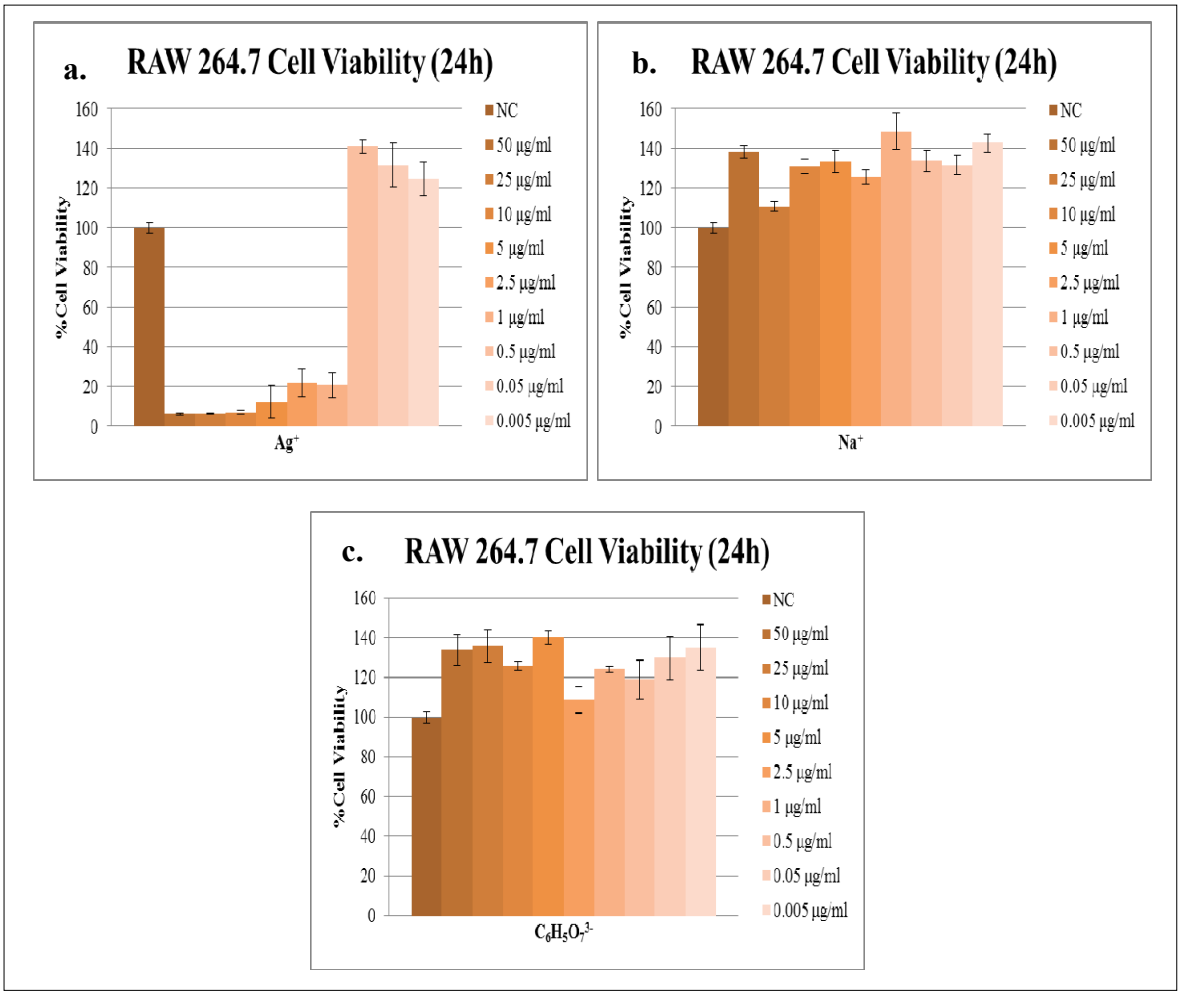

Figure 4.12. Viability of RAW 264.7 cells, after treatment with a. Ag^{+}, b. Na^{+}, and c. $C_6H_5O_7^{3-}$ for 24 hours in the presence of 50, 25, 10, 5, 2.5, 1, 0.5, 0.05, and 0.005 µg/ml concentrations. 'NC' denotes negative control and the values represent the mean of three replicates

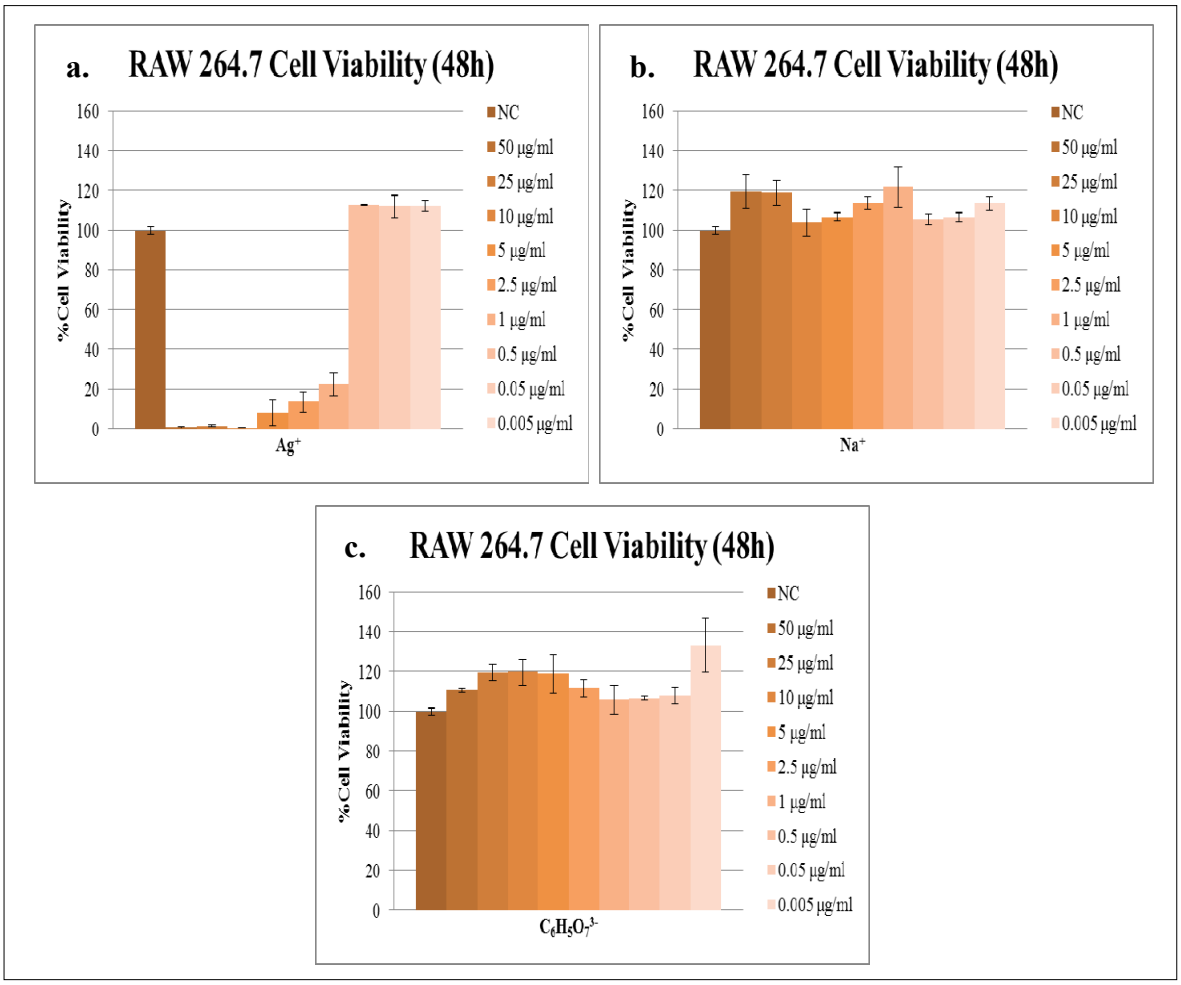

Figure 4.13. Viability of RAW 264.7 cells, after treatment with a. Ag^{+}, b. Na^{+}, and c. $C_6H_5O_7^{3-}$ for 48 hours in the presence of 50, 25, 10, 5, 2.5, 1, 0.5, 0.05, and 0.005 µg/ml concentrations. 'NC' denotes negative control and the values represent the mean of three replicates

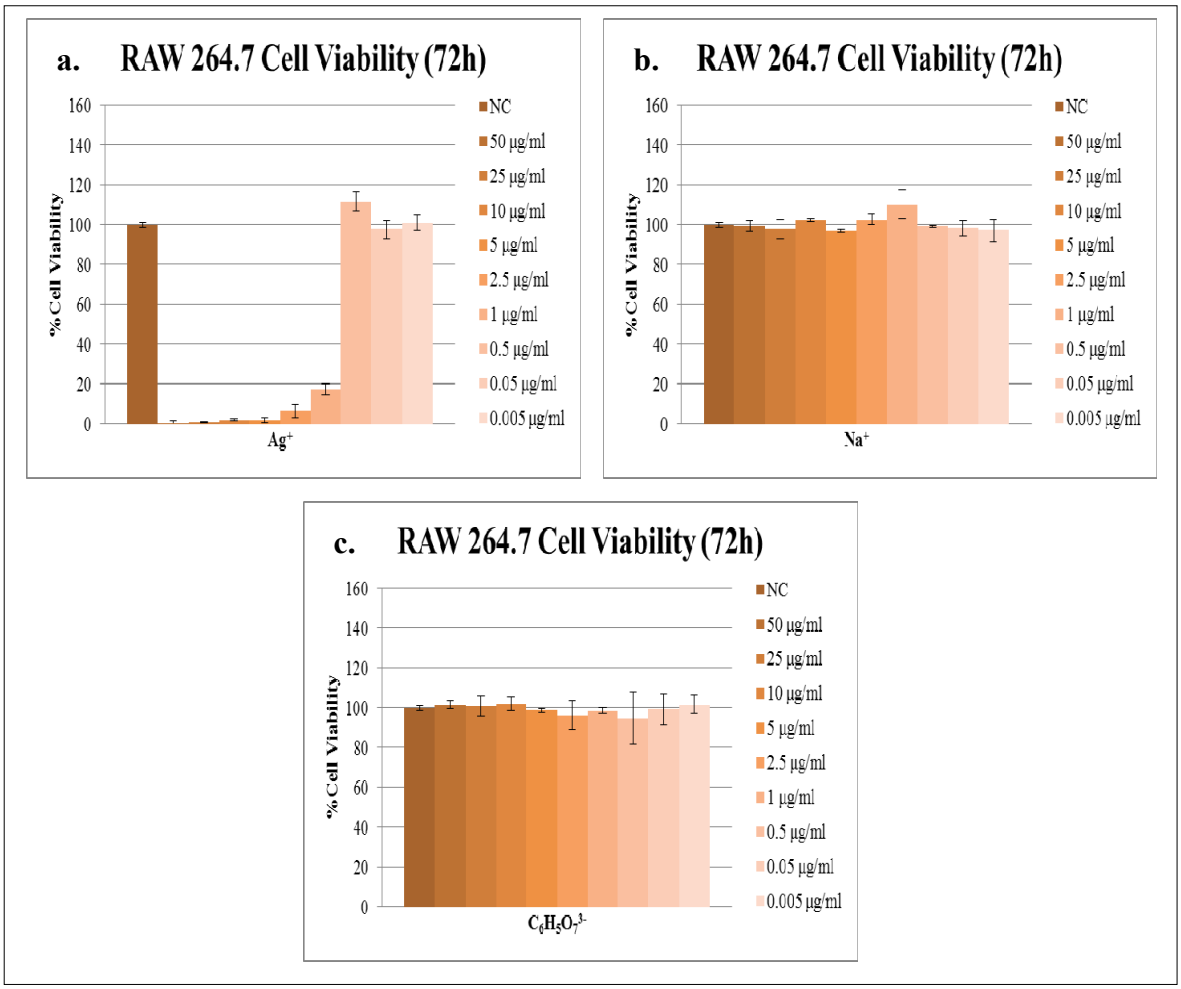

Figure 4.14. Viability of RAW 264.7 cells, after treatment with a. Ag^+, b. Na^+, and c. $C_6H_5O_7^{3-}$ for 72 hours in the presence of 50, 25, 10, 5, 2.5, 1, 0.5, 0.05, and 0.005 µg/ml concentrations. 'NC' denotes negative control and the values represent the mean of three replicates

This part of the study showed that, although Ag^+ has known beneficial effects on wound healing, concentration is one of the deterministic factors to decide if Ag^+ is toxic for the cells or it has a proliferative effect on the cells. Based on the results, Ag^+ was highly toxic for all three studied cell types; HDF, L929, and RAW 264.7, in the concentrations at 50 µg/ml, 25 µg/ml, 10 µg/ml, 5 µg/ml, 2.5 µg/ml, and 1 µg/ml. In concentration 0.5 µg/ml, toxic effect of Ag^+ completely vanished and an irregular proliferative effect seemed to begin. At very low concentrations as 0.05 µg/ml, and 0.005 µg/ml, its proliferative effect was continuing. When Na^+ and $C_6H_5O_7^{3-}$ were analyzed, it was observed that Na^+ and $C_6H_5O_7^{3-}$ had approximately same effect on cell viability for all cell types with no dramatic

difference from each other. They also had no dramatic toxic effect on any cell type at the specified concentration range; moreover they also triggered an irregular proliferation effect on the cells for almost all concentrations. On the other hand, the individual analysis of the all ions suggests that toxic effect of $AgNO_3$ did not originate from NO_3^-. In equal NO_3^- concentration, Ag^+ still caused toxicity. Additionally, exposure time was not deterministic for 24 h, 48 h, and 72 h time intervals for any concentration and any cell type. As time goes by, due to the decreasing activity of the ions, sharp effects of them diminished in time from 24 h to 72h.

In second part, same concentrations; 50 µg/ml, 25 µg/ml, 10 µg/ml, 5 µg/ml, 2.5 µg/ml, 1 µg/ml, 0.5 µg/ml, 0.05 µg/ml, and 0.005 µg/ml were analyzed with the same steps in the cell culture and MTS assay for AgNP-C. Effects of AgNP-C were tested on HDF, L929, and RAW 264.7 cells for 24 h, 48 h, and 72 h time intervals. Percentages of cell viability results based on MTS assay were shown in Figure 4.15 for HDF cells, Figure 4.16 for L929 cells and Figure 4.17 for RAW 264.7 cells.

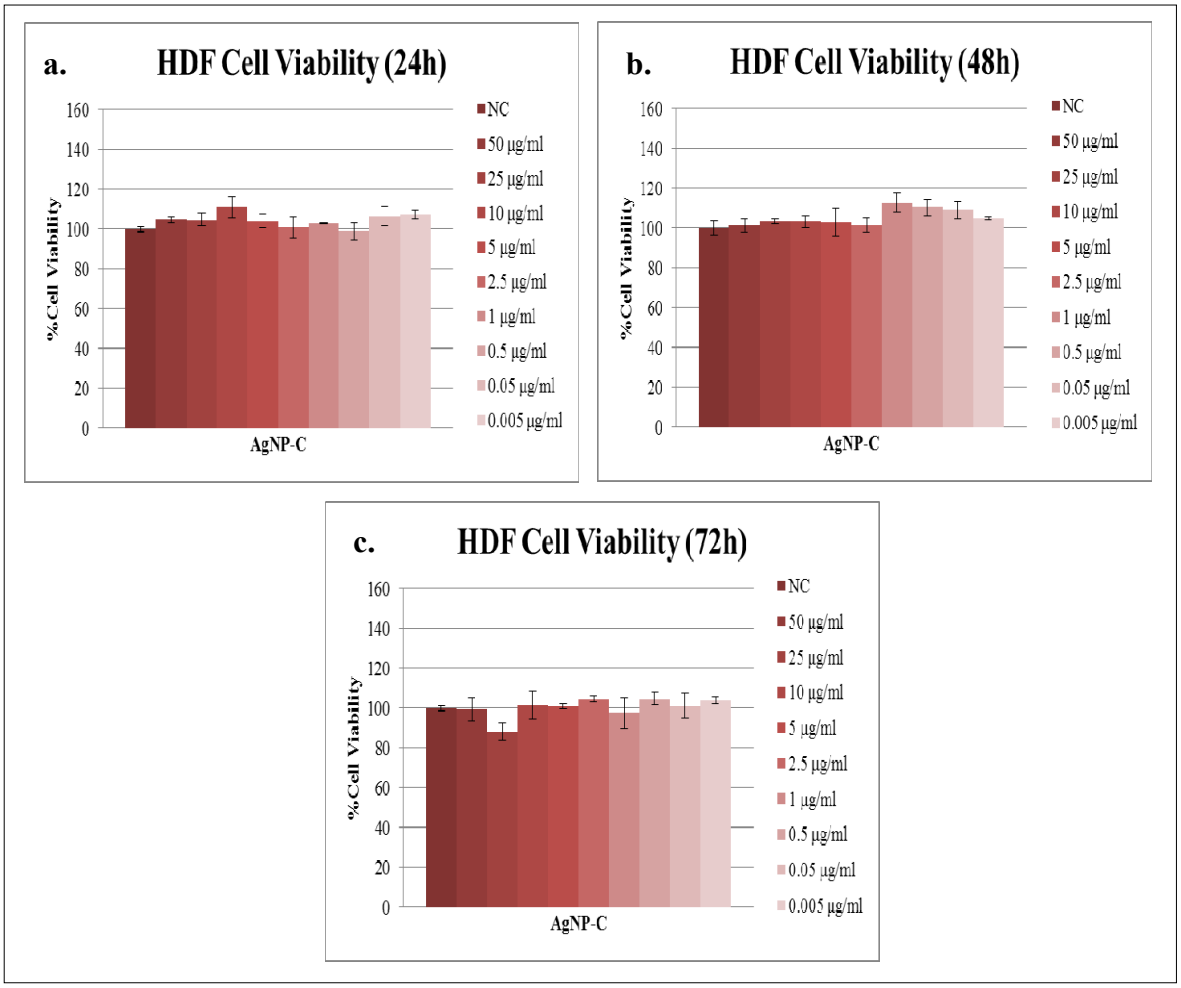

Figure 4.15. Viability of HDF cells, after treatment with AgNP-C for a. 24 hours, b. 48 hours, and c. 72 hours in the presence of 50, 25, 10, 5, 2.5, 1, 0.5, 0.05, and 0.005 µg/ml concentrations. 'NC' denotes negative control and the values represent the mean of three replicates

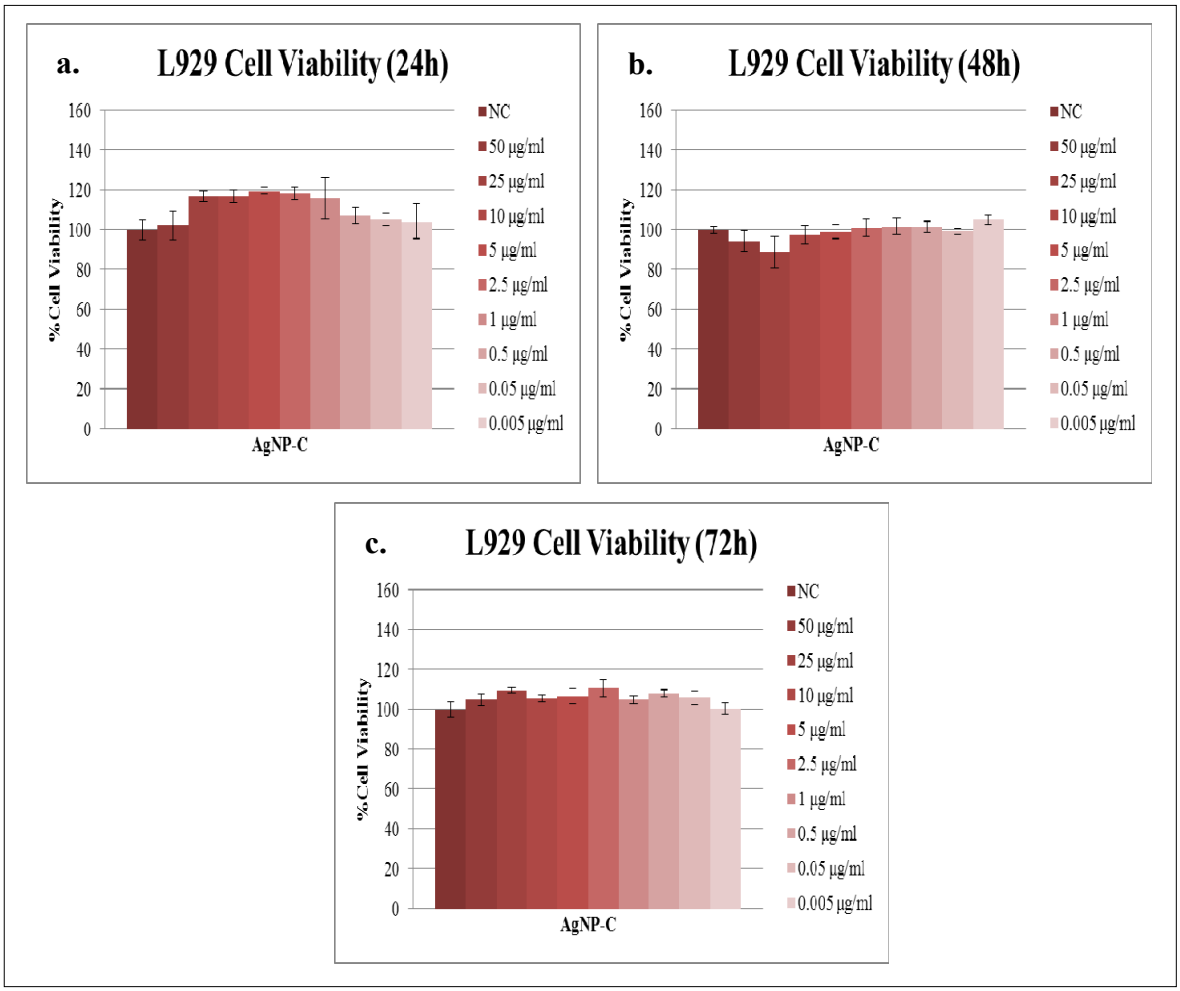

Figure 4.16. Viability of L929 cells, after treatment with AgNP-C for a. 24 hours, b. 48 hours, and c. 72 hours in the presence of 50, 25, 10, 5, 2.5, 1, 0.5, 0.05, and 0.005 µg/ml concentrations. 'NC' denotes negative control and the values represent the mean of three replicates

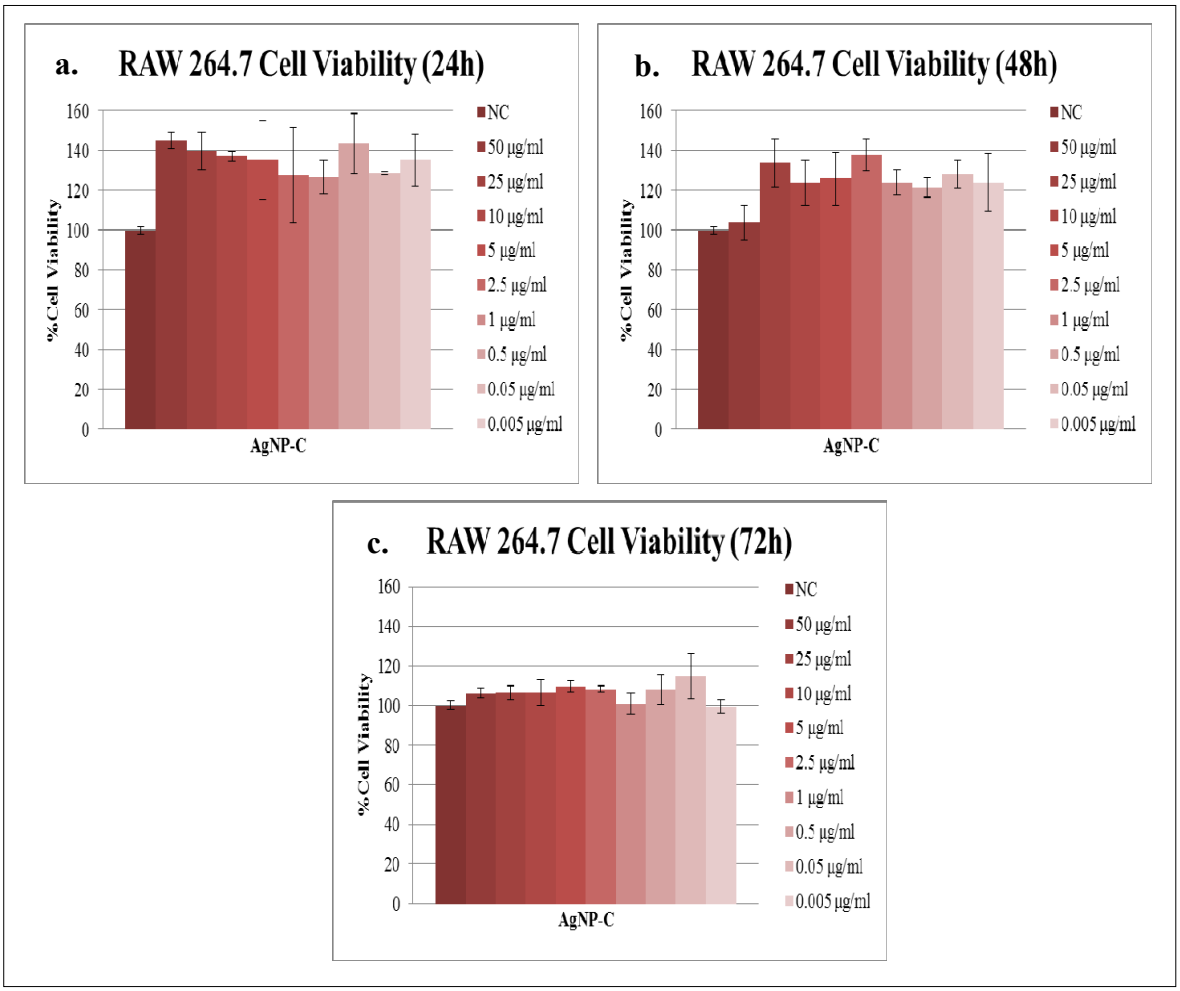

Figure 4.17. Viability of RAW 264.7 cells, after treatment with AgNP-C for a. 24 hours, b. 48 hours, and c. 72 hours in the presence of 50, 25, 10, 5, 2.5, 1, 0.5, 0.05, and 0.005 µg/ml concentrations. 'NC' denotes negative control and the values represent the mean of three replicates

Depending on the cell viability percentages on Figure 4.15-17, the variable exposure time did not cause any dramatic effect on the cell viability. Merely, longer exposure time caused a decrease on proliferation, because of the diminishing effect of the nanoparticles in time. For HDF cells, cell viability did not change with exposure time (Figure 4.15). Compared with 24 h (Figure 4.16.a, Figure 4.17.a) of exposure time, 48 h (Figure 4.16.b, Figure 4.17.b) and 72 h (Figure 4.16.c, Figure 4.17.c) showed a decrease on the cell viability of L929 and RAW 264.7 cells. Different from Ag^{+}, AgNP-C did not give damage to cells, even in very high concentrations as 50 µg/ml and 25 µg/ml. Basically, it can be said that AgNP-C does not have any toxic effect on the cells in this concentration range. Although some variable proliferative effects were also observed, these effects were not explicit and clear as toxic effects in ions. They were low and variable for each cell type and each concentration.

In the third part, lactose, maltose, and glucose were used to obtain the AgNPs by reduction. Different from the second part, the AgNPs were synthesized by using these three carbohydrates as reducing agents instead of the citrate. In this manner, AgNPs, synthesized with different reducing agents, can be compared with each other. The cytotoxic effects on the cells were investigated for the same concentrations (50 µg/ml, 25 µg/ml, 10 µg/ml, 5 µg/ml, 1 µg/ml, 0.5 µg/ml, 0.05 µg/ml, and 0.005 µg/ml) used in Ag^{+}, AgNP-C and its dialysis form using the same exposure time range (24 h, 48 h, 72 h). However, for AgNP-L there was a difference. Three concentrations; 50 µg/ml, 25 µg/ml, and 10 µg/ml could not be tested because in their stock concentrations; 500 µg/ml, 250 µg/ml, and 100 µg/ml, AgNP-L precipitates. Thus, stock concentrations were prepared as 50 µg/ml, 25 µg/ml, 10 µg/ml, 5 µg/ml, 0.5 µg/ml, and 0.05 µg/ml for AgNP-L. Figure 4.18-26 shows the MTS test results using the same cell culture steps for HDF (Figure 4.18-20), L929 (Figure 4.21-23), and RAW 264.7 (Figure 4.24-26),

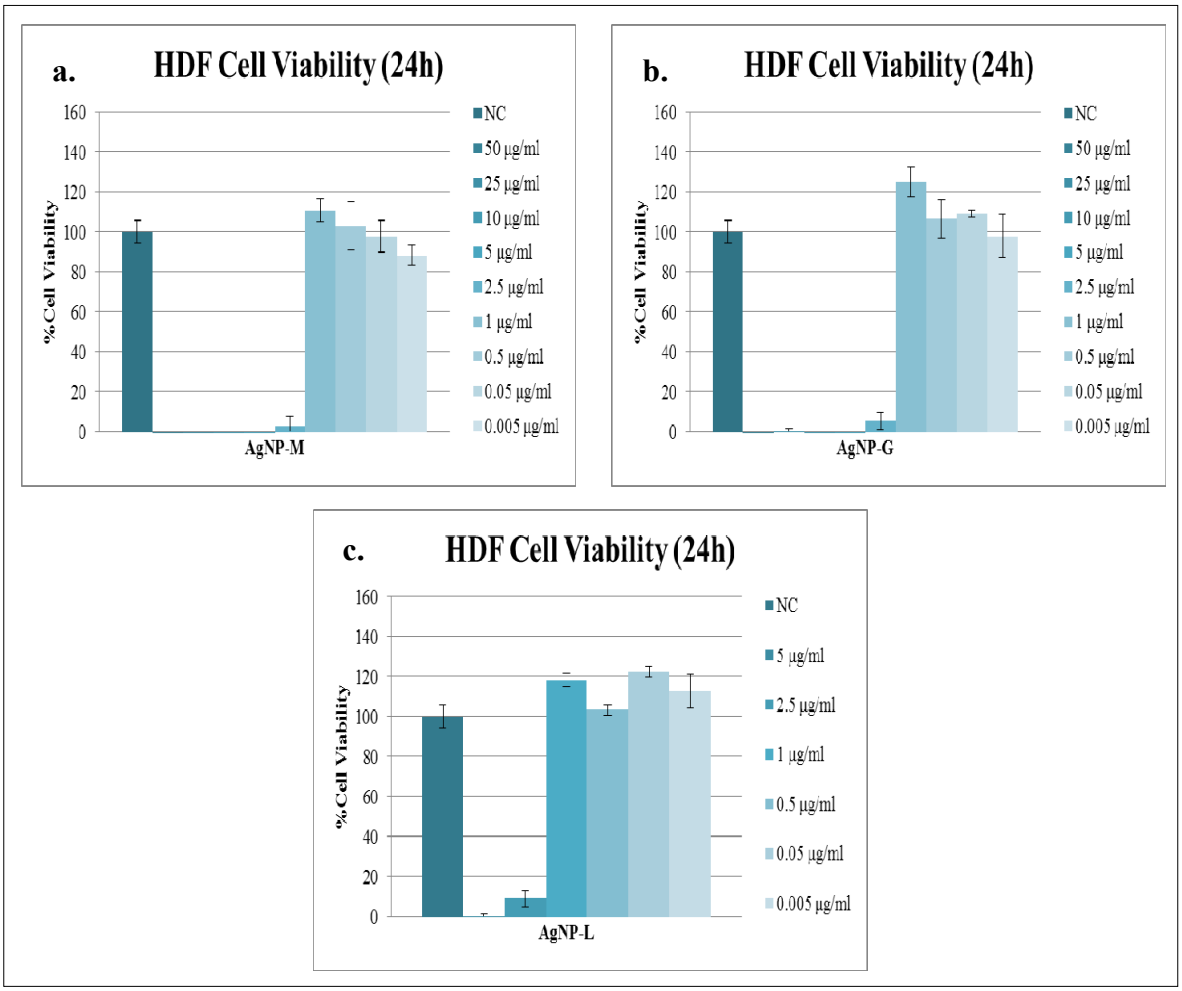

Figure 4.18. Viability of HDF cells, after treatment with a. AgNP-M, b. AgNP-G, and c. AgNP-L for 24 hours in the presence of 50, 25, 10, 5, 2.5, 1, 0.5, 0.05, and 0.005 µg/ml concentrations for AgNP-M and AgNP-G; 5, 2.5, 1, 0.5, 0.05, and 0.005 µg/ml concentrations for AgNP-L. 'NC' denotes negative control and the values represent the mean of three replicates

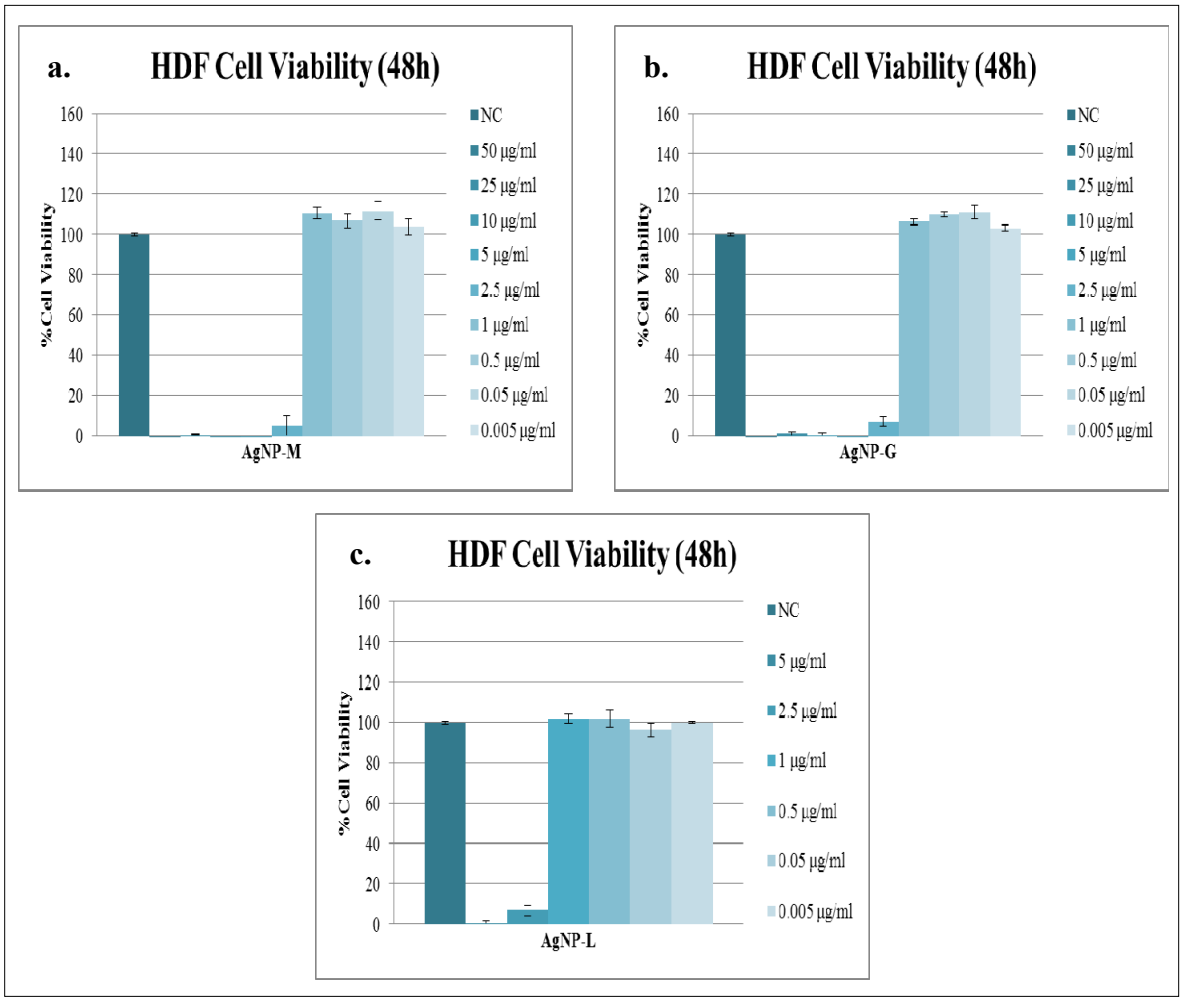

Figure 4.19. Viability of HDF cells, after treatment with a. AgNP-M, b. AgNP-G, and c. AgNP-L for 48 hours in the presence of 50, 25, 10, 5, 2.5, 1, 0.5, 0.05, and 0.005 µg/ml concentrations for AgNP-M and AgNP-G; 5, 2.5, 1, 0.5, 0.05, and 0.005 µg/ml concentrations for AgNP-L. 'NC' denotes negative control and the values represent the mean of three replicates

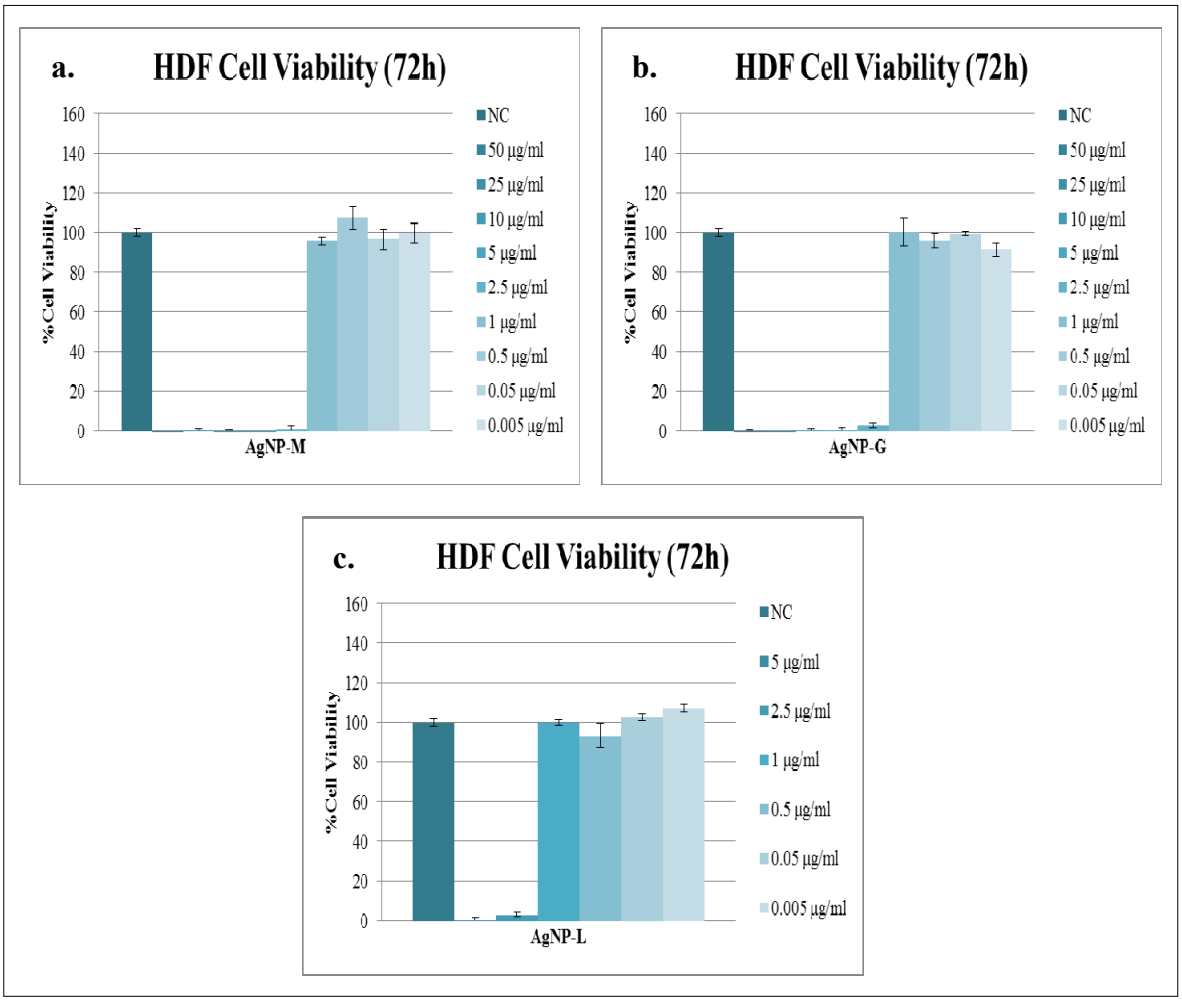

Figure 4.20. Viability of HDF cells, after treatment with a. AgNP-M, b. AgNP-G, and c. AgNP-L for 72 hours in the presence of 50, 25, 10, 5, 2.5, 1, 0.5, 0.05, and 0.005 µg/ml concentrations for AgNP-M and AgNP-G; 5, 2.5, 1, 0.5, 0.05, and 0.005 µg/ml concentrations for AgNP-L. 'NC' denotes negative control and the values represent the mean of three replicates

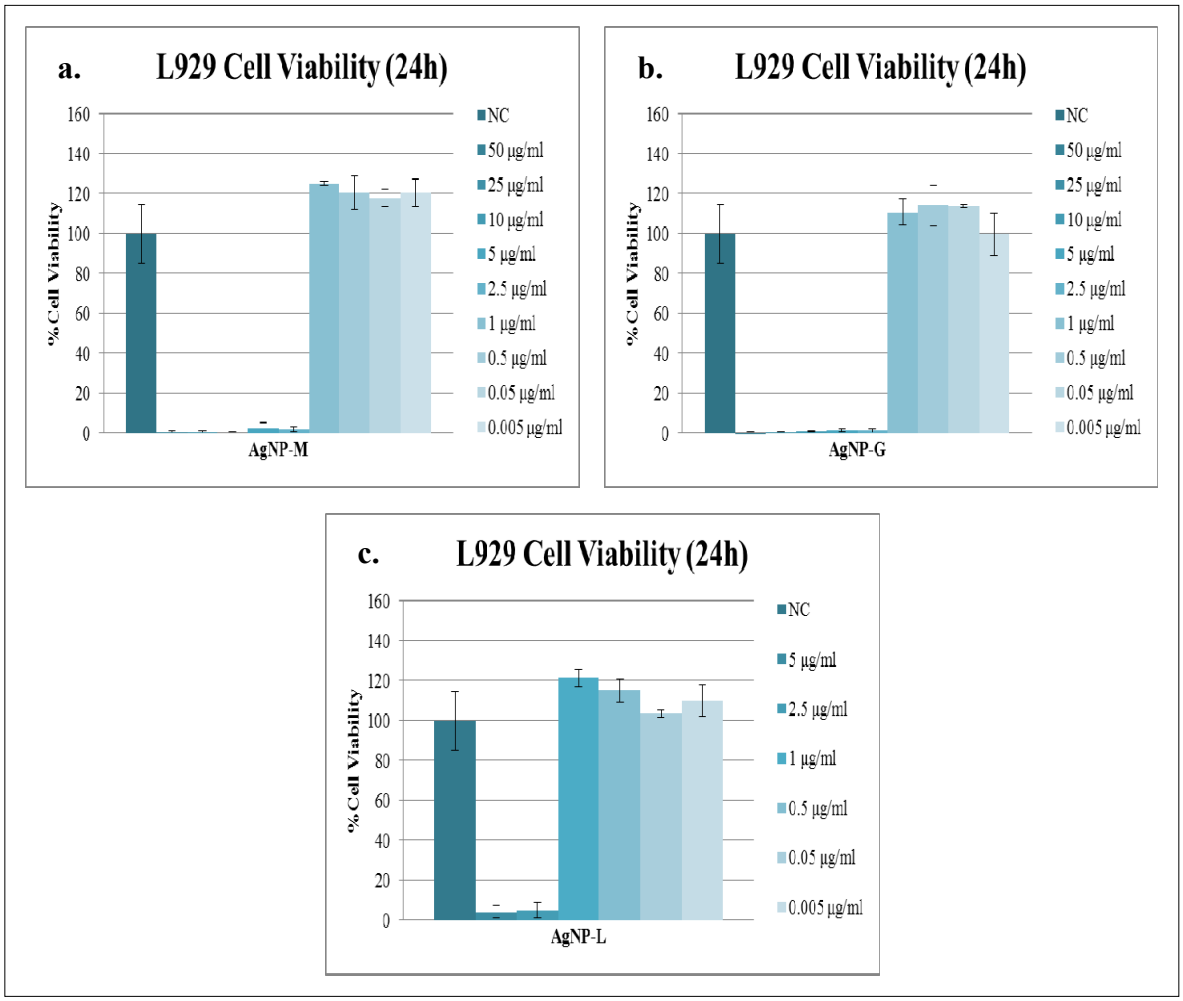

Figure 4.21. Viability of L929 cells, after treatment with a. AgNP-M, b. AgNP-G, and c. AgNP-L for 24 hours in the presence of 50, 25, 10, 5, 2.5, 1, 0.5, 0.05, and 0.005 µg/ml concentrations for AgNP-M and AgNP-G; 5, 2.5, 1, 0.5, 0.05, and 0.005 µg/ml concentrations for AgNP-L. 'NC' denotes negative control and the values represent the mean of three replicates

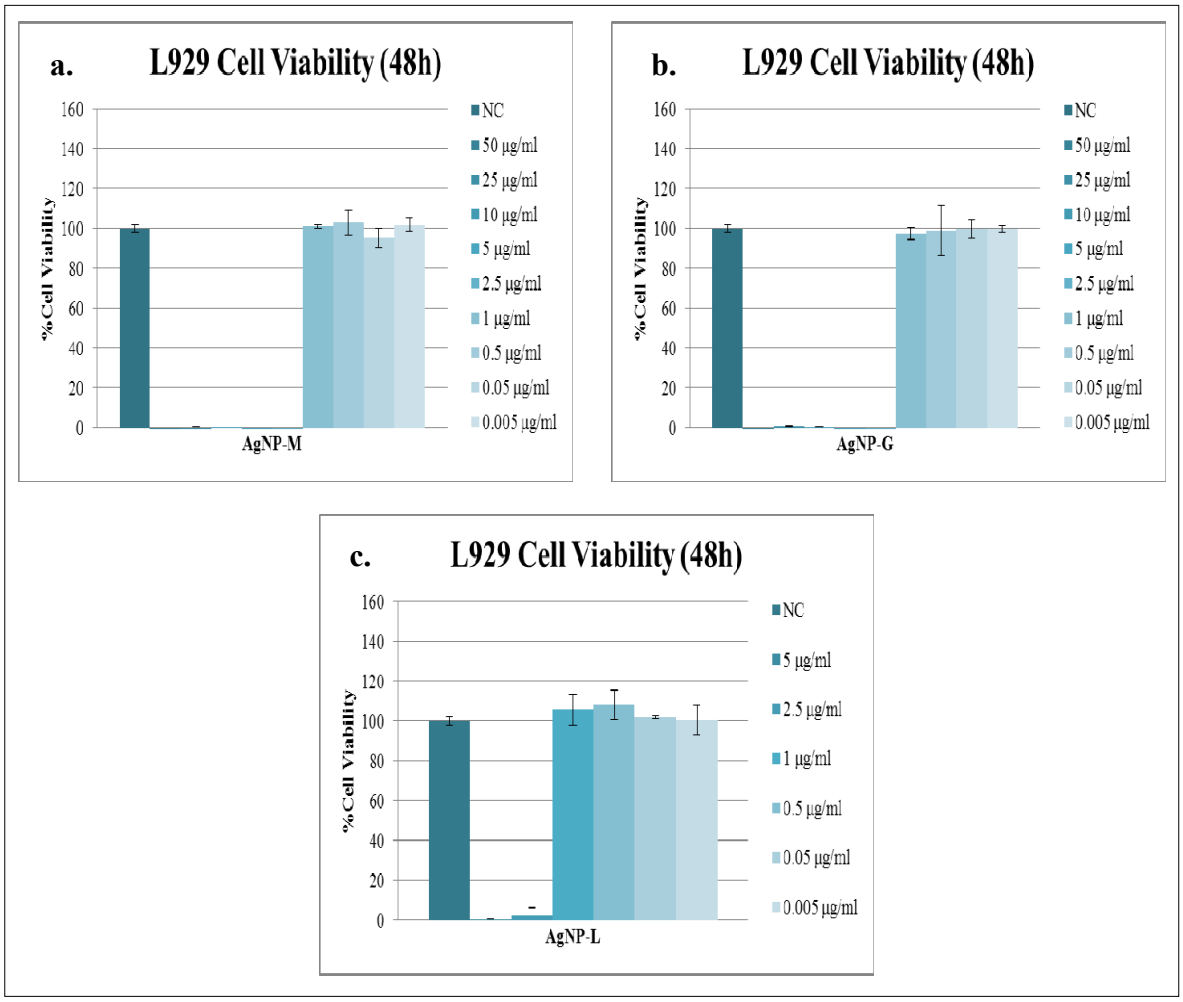

Figure 4.22. Viability of L929 cells, after treatment with a. AgNP-M, b. AgNP-G, and c. AgNP-L for 48 hours in the presence of 50, 25, 10, 5, 2.5, 1, 0.5, 0.05, and 0.005 µg/ml concentrations for AgNP-M and AgNP-G; 5, 2.5, 1, 0.5, 0.05, and 0.005 µg/ml concentrations for AgNP-L. 'NC' denotes negative control and the values represent the mean of three replicates

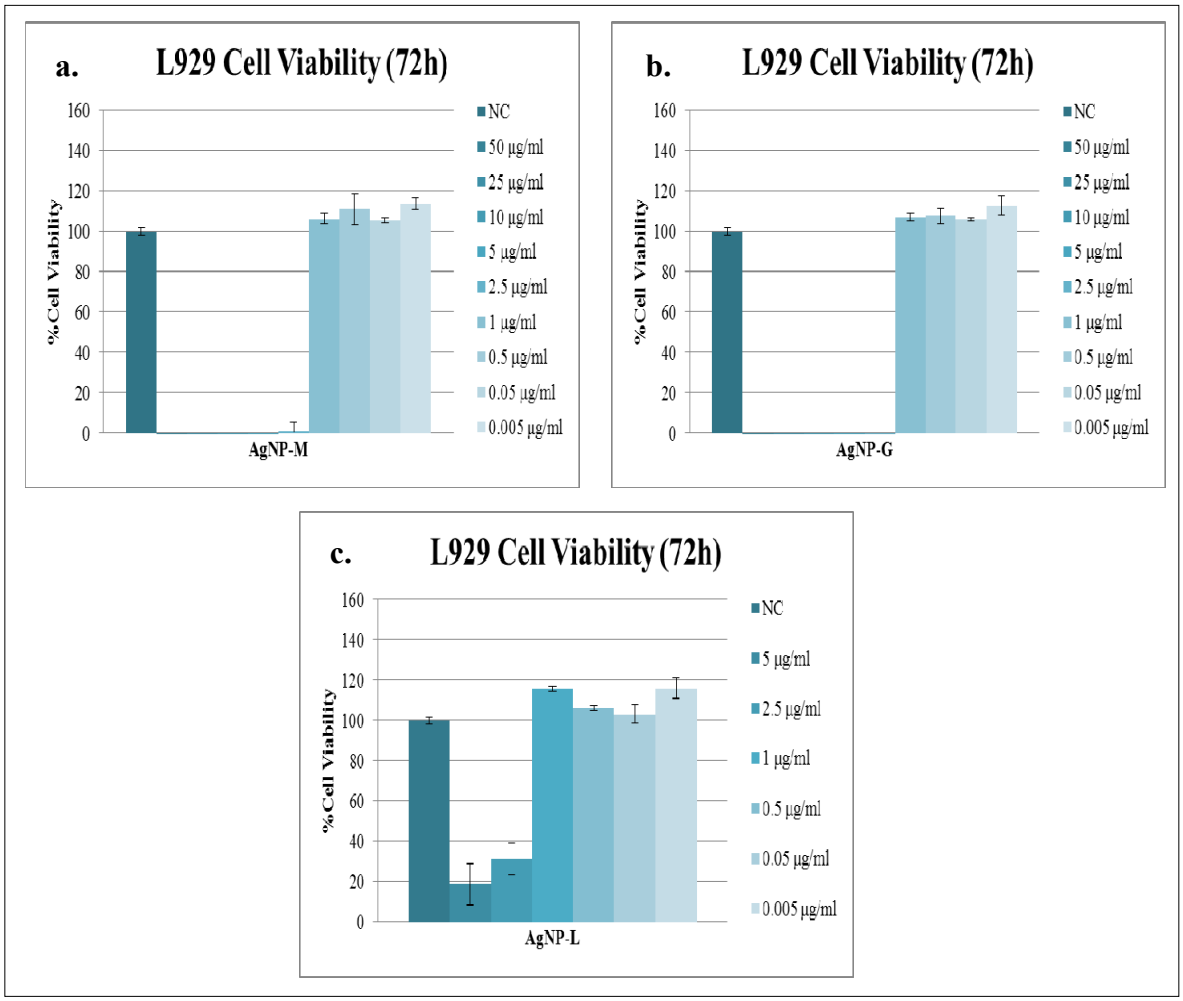

Figure 4.23. Viability of L929 cells, after treatment with a. AgNP-M, b. AgNP-G, and c. AgNP-L for 72 hours in the presence of 50, 25, 10, 5, 2.5, 1, 0.5, 0.05, and 0.005 µg/ml concentrations for AgNP-M and AgNP-G; 5, 2.5, 1, 0.5, 0.05, and 0.005 µg/ml concentrations for AgNP-L. 'NC' denotes negative control and the values represent the mean of three replicates

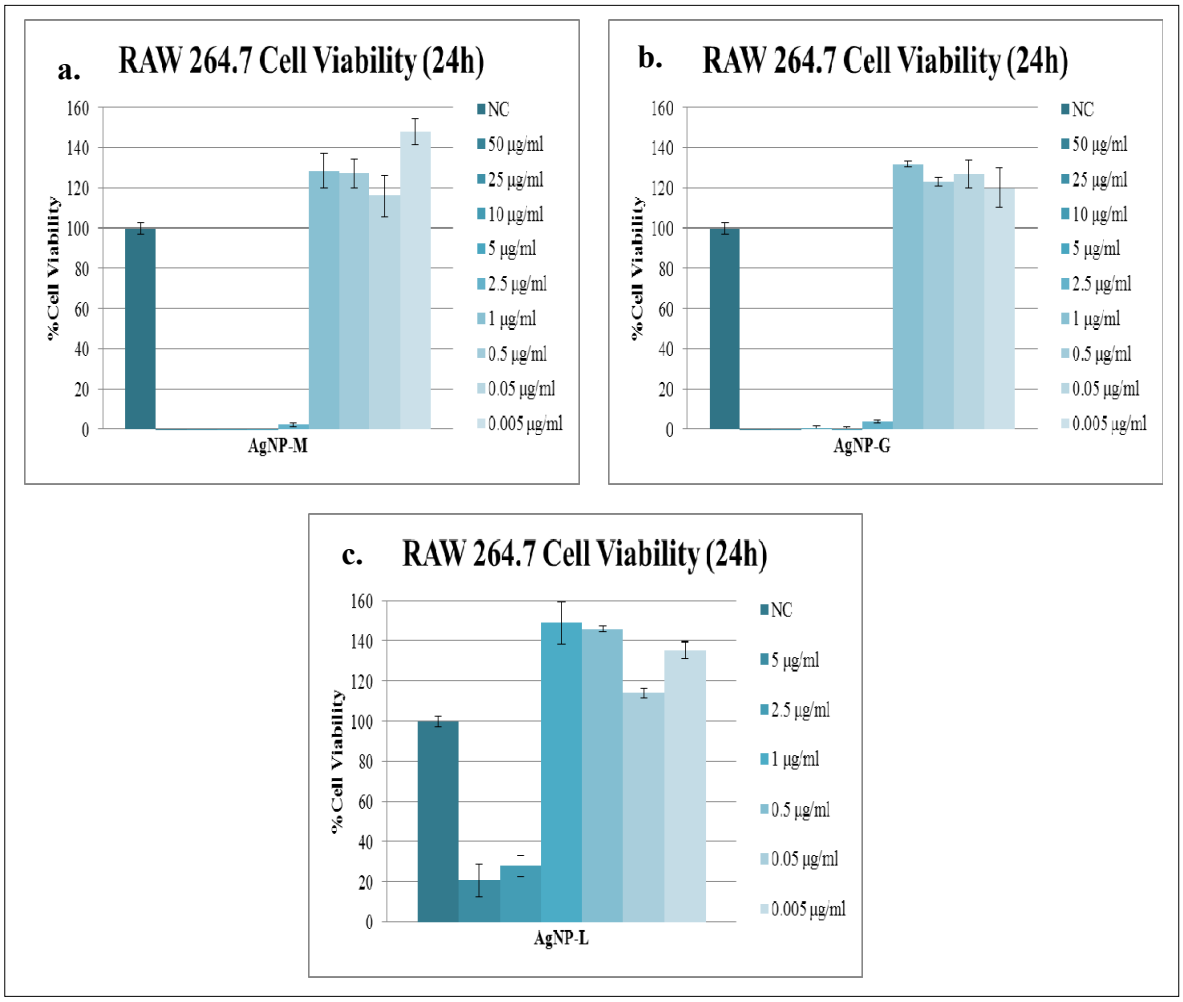

Figure 4.24. Viability of RAW 264.7 cells, after treatment with a. AgNP-M, b. AgNP-G, and c. AgNP-L for 24 hours in the presence of 50, 25, 10, 5, 2.5, 1, 0.5, 0.05, and 0.005 µg/ml concentrations for AgNP-M and AgNP-G; 5, 2.5, 1, 0.5, 0.05, and 0.005 µg/ml concentrations for AgNP-L. 'NC' denotes negative control and the values represent the mean of three replicates

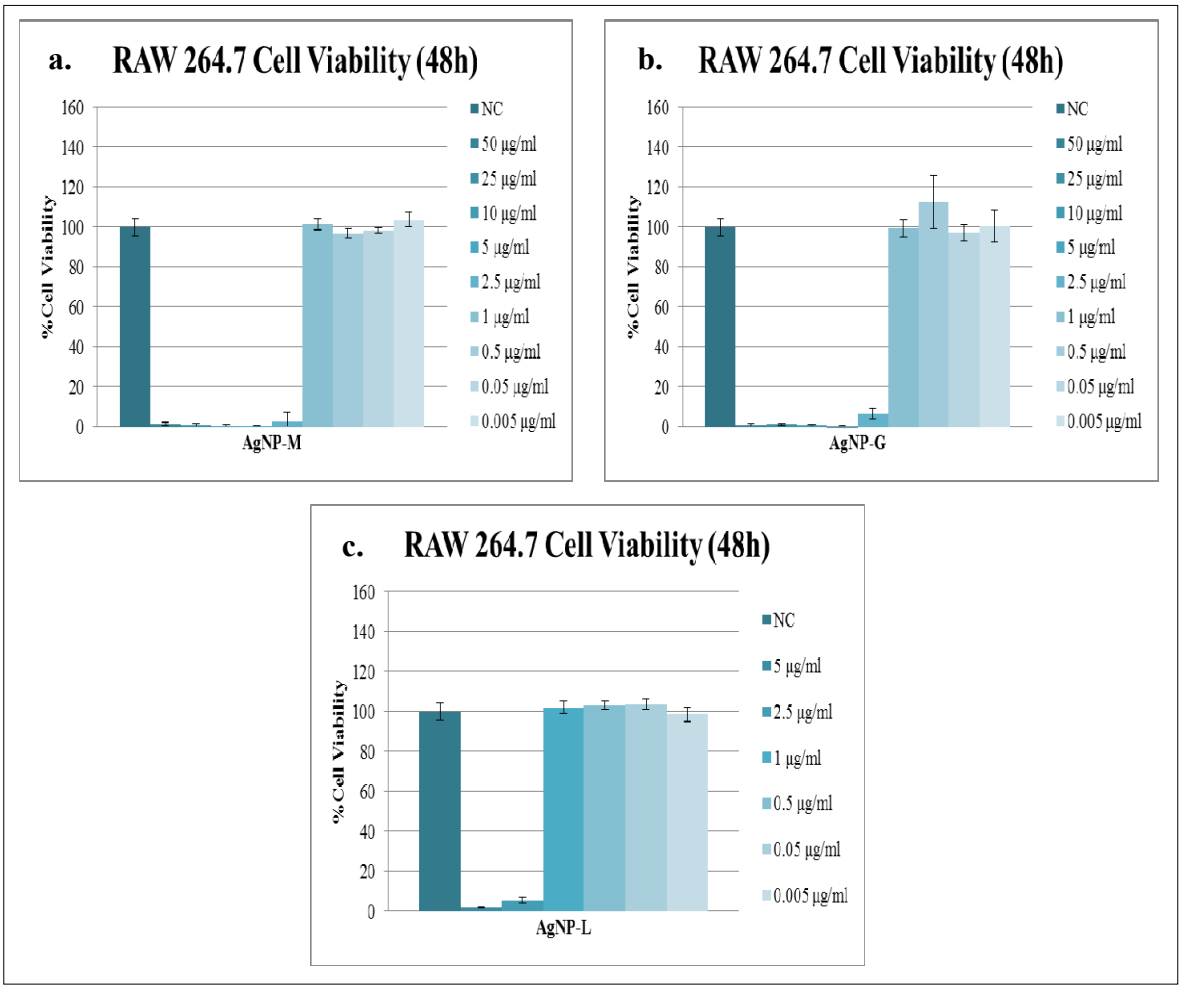

Figure 4.25. Viability of RAW 264.7 cells, after treatment with a. AgNP-M, b. AgNP-G, and c. AgNP-L for 48 hours in the presence of 50, 25, 10, 5, 2.5, 1, 0.5, 0.05, and 0.005 µg/ml concentrations for AgNP-M and AgNP-G; 5, 2.5, 1, 0.5, 0.05, and 0.005 µg/ml concentrations for AgNP-L. 'NC' denotes negative control and the values represent the mean of three replicates

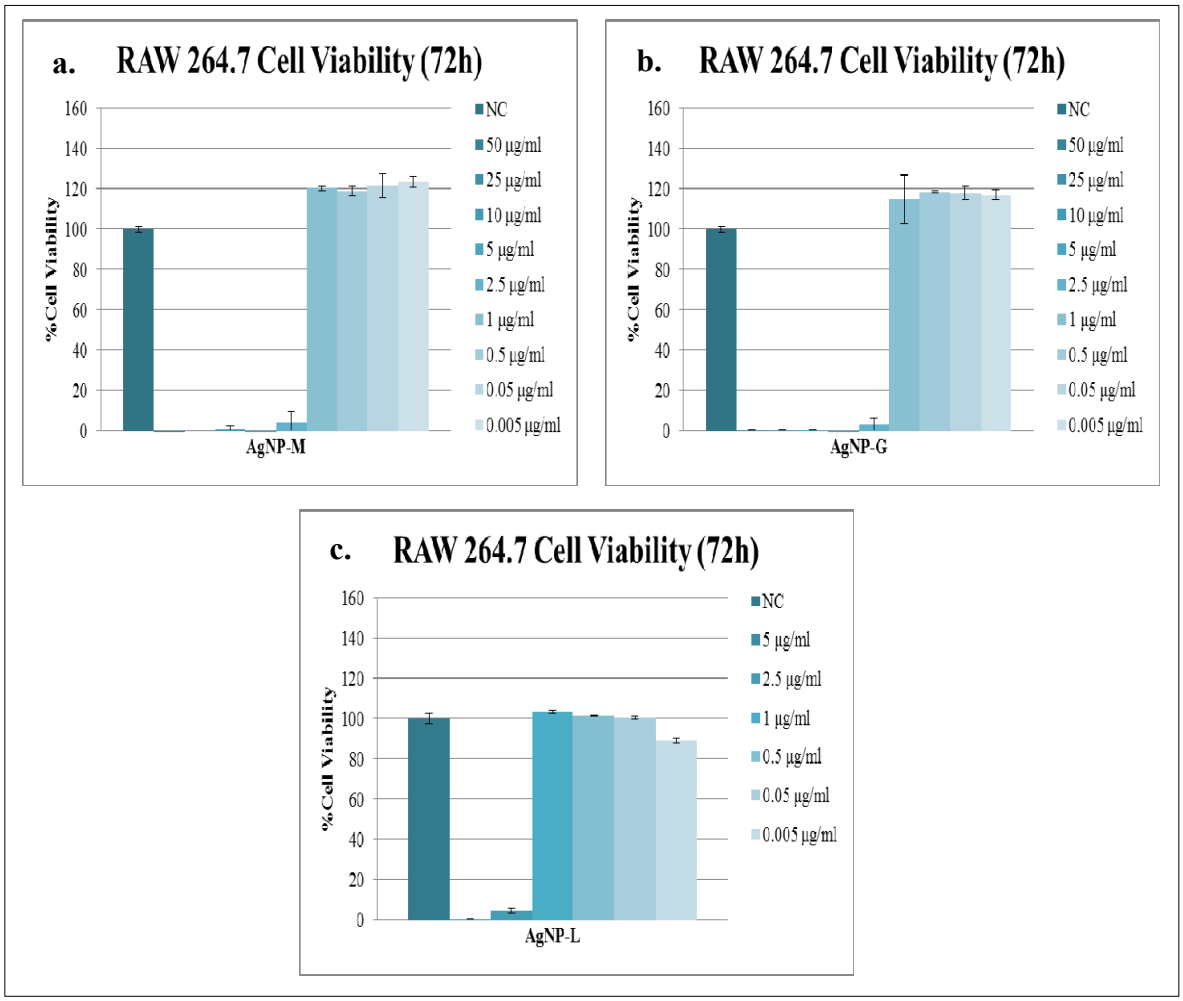

Figure 4.26. Viability of RAW 264.7 cells, after treatment with a. AgNP-M, b. AgNP-G, and c. AgNP-L for 72 hours in the presence of 50, 25, 10, 5, 2.5, 1, 0.5, 0.05, and 0.005 µg/ml concentrations for AgNP-M and AgNP-G; 5, 2.5, 1, 0.5, 0.05, and 0.005 µg/ml concentrations for AgNP-L. 'NC' denotes negative control and the values represent the mean of three replicates

Based on the results, both disaccharide (lactose, maltose)-reduced AgNPs and monosaccharide (glucose)-reduced AgNPs showed similar toxicity for the cells. The AgNP-M and AgNP-G were toxic in 50 µg/ml, 25 µg/ml, 10 µg/ml, 5 µg/ml, and 2.5 µg/ml. Although 50 µg/ml, 25 µg/ml, and 10 µg/ml concentrations could not be analyzed for AgNP-L, for other two concentrations; 5 µg/ml and 2.5 µg/ml, AgNP-L showed similar toxic effect as in AgNP-M and AgNP-G. Lower concentrations; 1 µg/ml, 0.5 µg/ml, 0.05 µg/ml, and 0.005 µg/ml were not toxic for any cells. Furthermore, a slight, irregular proliferative effect, which decreased from 24 h to 72 h, was seen for non-toxic

concentrations. Depending on the results, AgNP-M, AgNP-G, and AgNP-L showed more toxic effect than AgNP-C, lower toxic effect than Ag^+. This part of the study shows that, AgNPs exhibited different effects on the cells based on their synthesis by different reducing agents. Different reductants provide different surface chemistry properties while forming AgNPs. These properties cause different interactions between cells and AgNPs. When the characterization of AgNPs was considered, high concentration of Ag^+ after the synthesis of AgNP-M in the solubility analysis made the cell viability results clear. Similarities of the toxic effects of AgNP-M, which had almost same results with AgNP-L and AgNP-G, and $Ag^{+,}$ were caused by high concentration of Ag^+ after the synthesis of carbohydrate-reduced AgNPs. Thus, AgNP-M, AgNP-L, and AgNP-G showed lower toxicity than Ag^+ itself, and higher toxicity than AgNP-C. To make the results more reliable, an additional dialysis step can be occurred after the synthesis of AgNPs to ensure if the toxicity is caused by the uncoupled ions or not.

In brief, cytotoxicity studies show that, the source of silver is one of the determining factors for the wound healing. Among all AgNPs and $AgNO_3$ (source of Ag^+), $AgNO_3$ was the most toxic for the cells; although known beneficial effect of Ag^+ on the wound healing. Among AgNPs, AgNP-C was not toxic for the cells in any concentration that was tested. Due to the fact that carbohydrates were not good reducing agents as much as citrate based on the characterization part, carbohydrate-reduced AgNPs (AgNP-M, AgNP-L, AgNP-G) were observed more toxic than AgNP-C. To improve the results, different silver sources in different concentrations should be analyzed to obtain the most efficient and beneficial effect of the silver for the wound healing process. In addition to this, use of AgNPs, which have no dramatic toxic effect on the cells, may become more prevalent, and they can be enriched with different modifications as an alternative for silver sources. Different sizes (50 nm in this study), different synthesis procedures, different reducing agents, and different shapes can be tried.

4.3. GENOTOXICITY STUDIES

4.3.1. Morphological Analysis of Cells

After cytotoxicity studies, $AgNO_3$ (as the source of Ag^+), AgNP-C, and AgNP-M were chosen to analyze genotoxic effects of AgNPs, which were synthesized with different reducing agents, and silver ion on cells. Carbohydrate-reduced AgNPs had similar cell viability percentages in cytotoxicity studies, so only one of them (AgNP-M) was used to detect DNA damage. DNA damage was analyzed by DNA fragmentation. Before DNA fragmentation, morphological changes of the cells after the treatment were monitored under the light microscope. Thereby, a connection could be established between morphological changes and DNA fragmentation results. At the end of 24 h of exposure time, all types of cells were monitored for the concentrations (5, 2.5, 1, 0.5, and 0.05 μg/ml), that were specified for the genotoxicity study of $AgNO_3$, AgNP-C, and AgNP-M, using light microscopy. Figure 4.27-Figure 4.35 represented HDF, L-929, and RAW 264.7 cells respectively after the treatment. In a coherent with DNA fragmentation, all cell types showed similar outcome to the same concentrations of $AgNO_3$, AgNP-C, and AgNP-M. $AgNO_3$ was toxic at 5, 2.5, and 1 μg/ml concentrations, although AgNP-M caused cell death at 5 and 2.5 μg/ml concentrations only. In addition to this, AgNP-C did not show any toxicity for the cells.

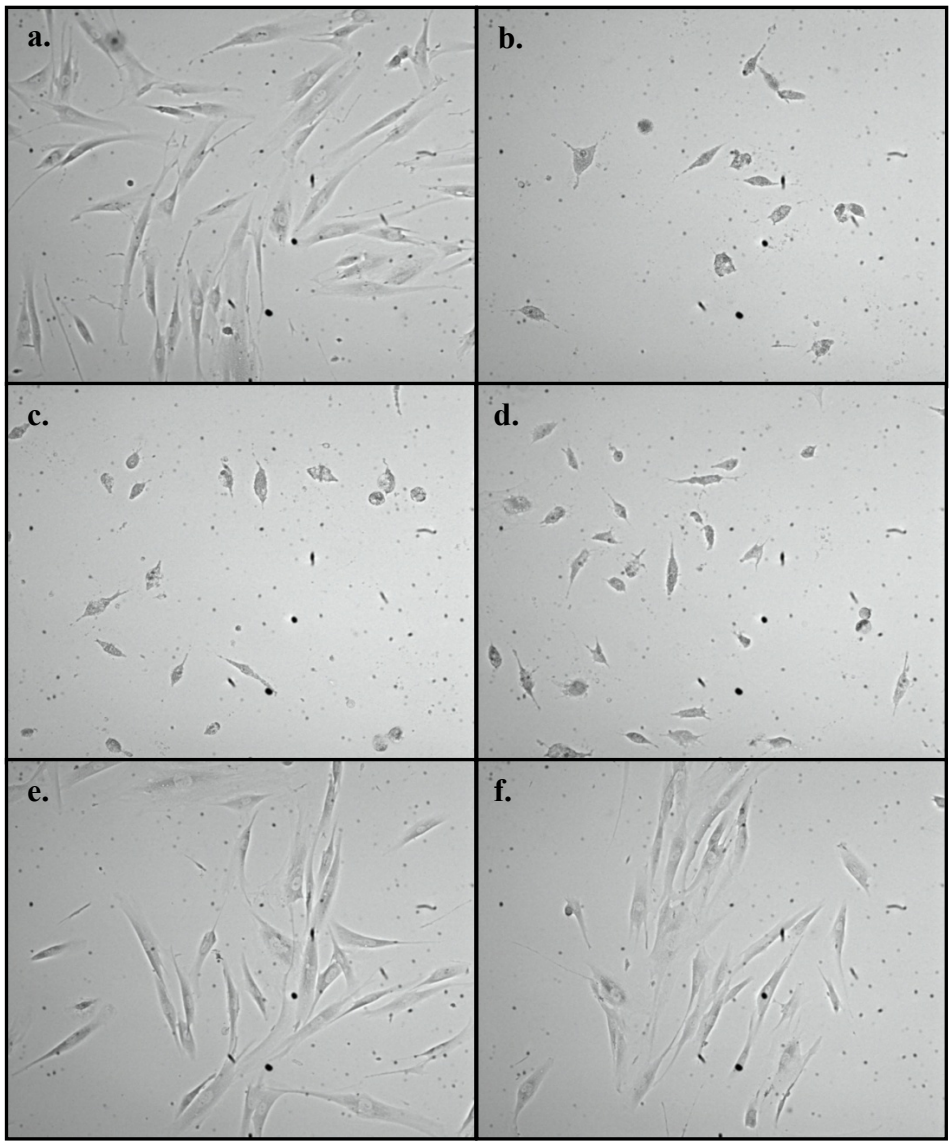

Figure 4.27. Images of HDF cells under light microscope with 10X magnification. a. Negative control with no treatment, b. After 24 hours of exposure with 5 µg/ml $AgNO_3$, c. After 24 hours of exposure with 2.5 µg/ml $AgNO_3$, d. After 24 hours of exposure with 1 µg/ml $AgNO_3$, e. After 24 hours of exposure with 0.5 µg/ml $AgNO_3$, f. After 24 hours of exposure with 0.05 µg/ml $AgNO_3$

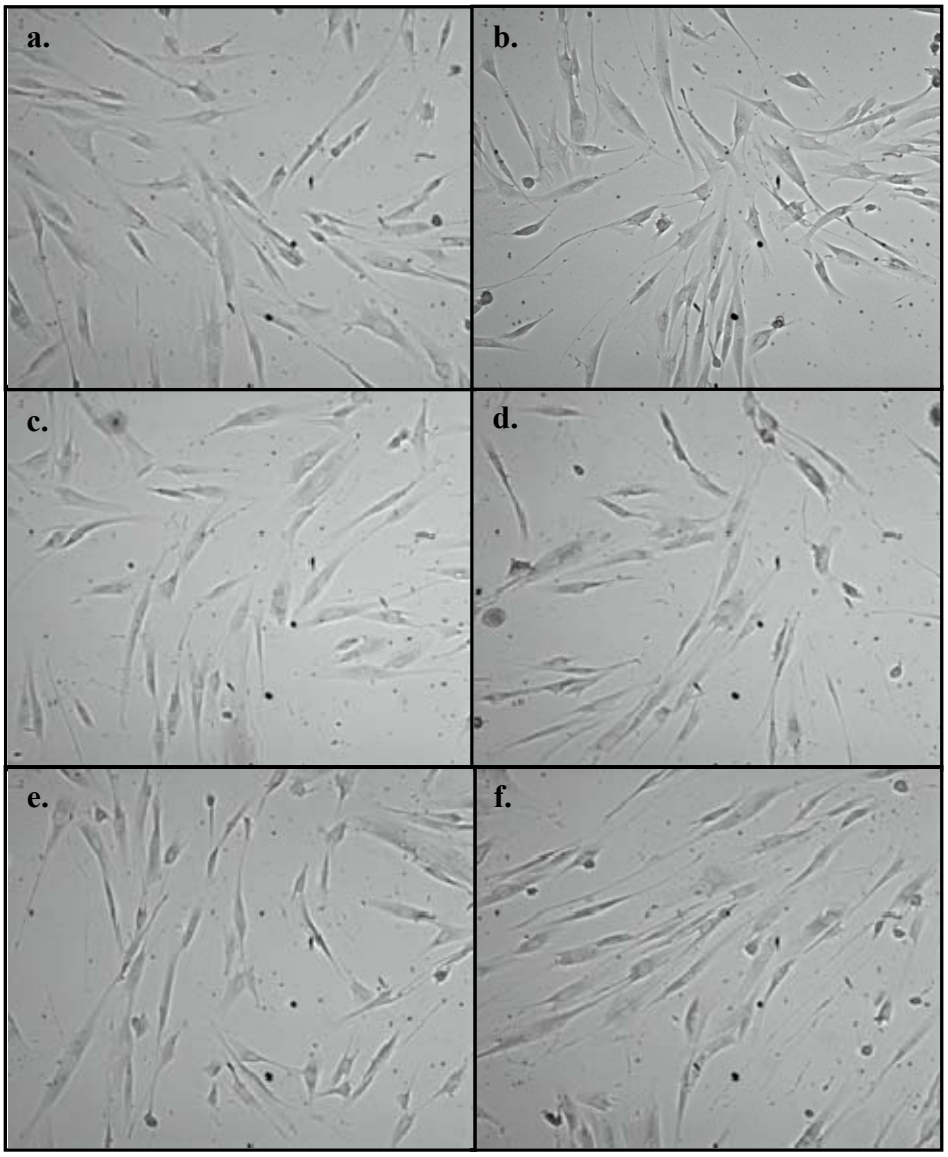

Figure 4.28. Images of HDF cells under light microscope with 10X magnification. a. Negative control with no treatment, b. After 24 hours of exposure with 5 µg/ml AgNP-C, c. After 24 hours of exposure with 2.5 µg/ml AgNP-C, d. After 24 hours of exposure with 1 µg/ml AgNP-C, e. After 24 hours of exposure with 0.5 µg/ml AgNP-C, f. After 24 hours of exposure with 0.05 µg/ml AgNP-C

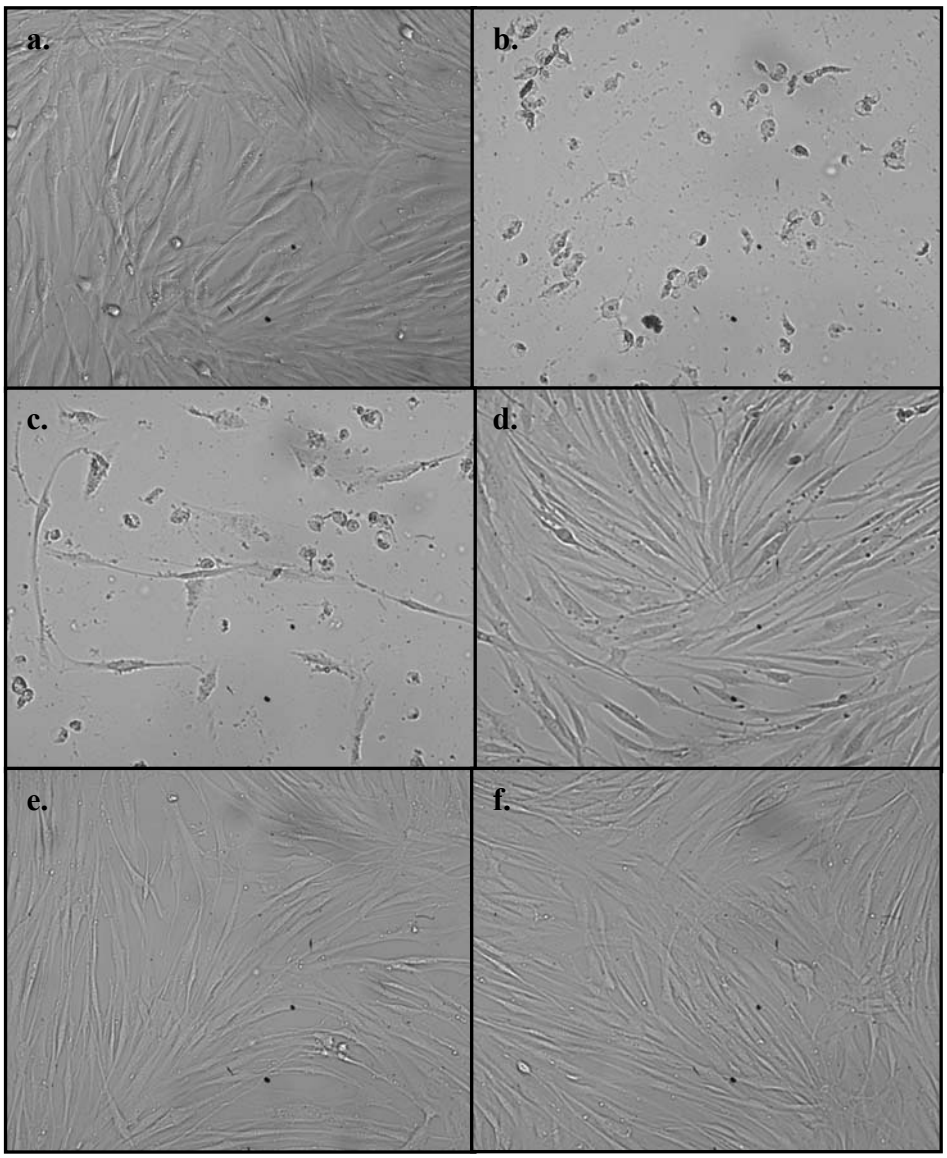

Figure 4.29. Images of HDF cells under light microscope with 10X magnification. a. Negative control with no treatment, b. After 24 hours of exposure with 5 µg/ml AgNP-M, c. After 24 hours of exposure with 2.5 µg/ml AgNP-M, d. After 24 hours of exposure with 1 µg/ml AgNP-M, e. After 24 hours of exposure with 0.5 µg/ml AgNP-M, f. After 24 hours of exposure with 0.05 µg/ml AgNP-M

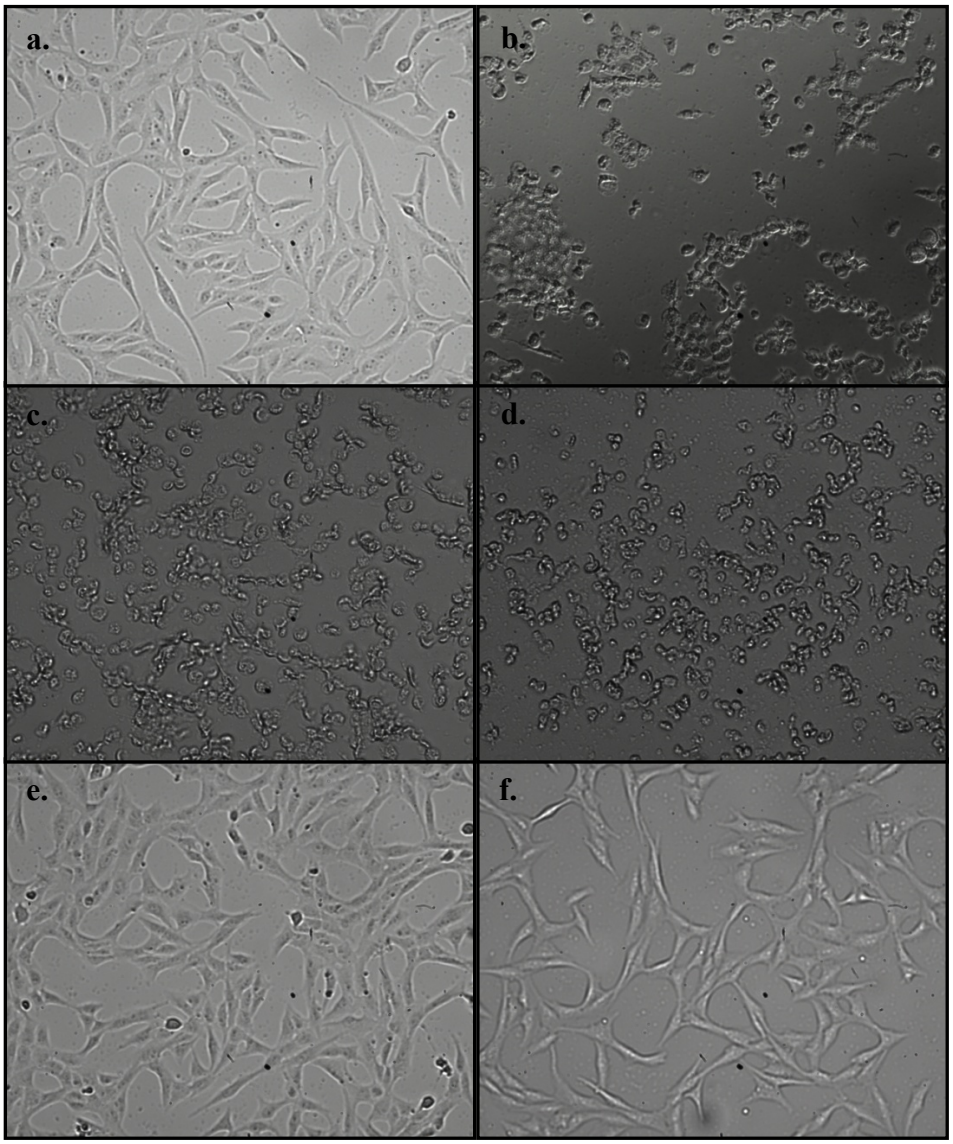

Figure 4.30. Images of L929 cells under light microscope with 10X magnification. a. Negative control with no treatment, b. After 24 hours of exposure with 5 µg/ml $AgNO_3$, c. After 24 hours of exposure with 2.5 µg/ml $AgNO_3$, d. After 24 hours of exposure with 1 µg/ml $AgNO_3$, e. After 24 hours of exposure with 0.5 µg/ml $AgNO_3$, f. After 24 hours of exposure with 0.05 µg/ml $AgNO_3$

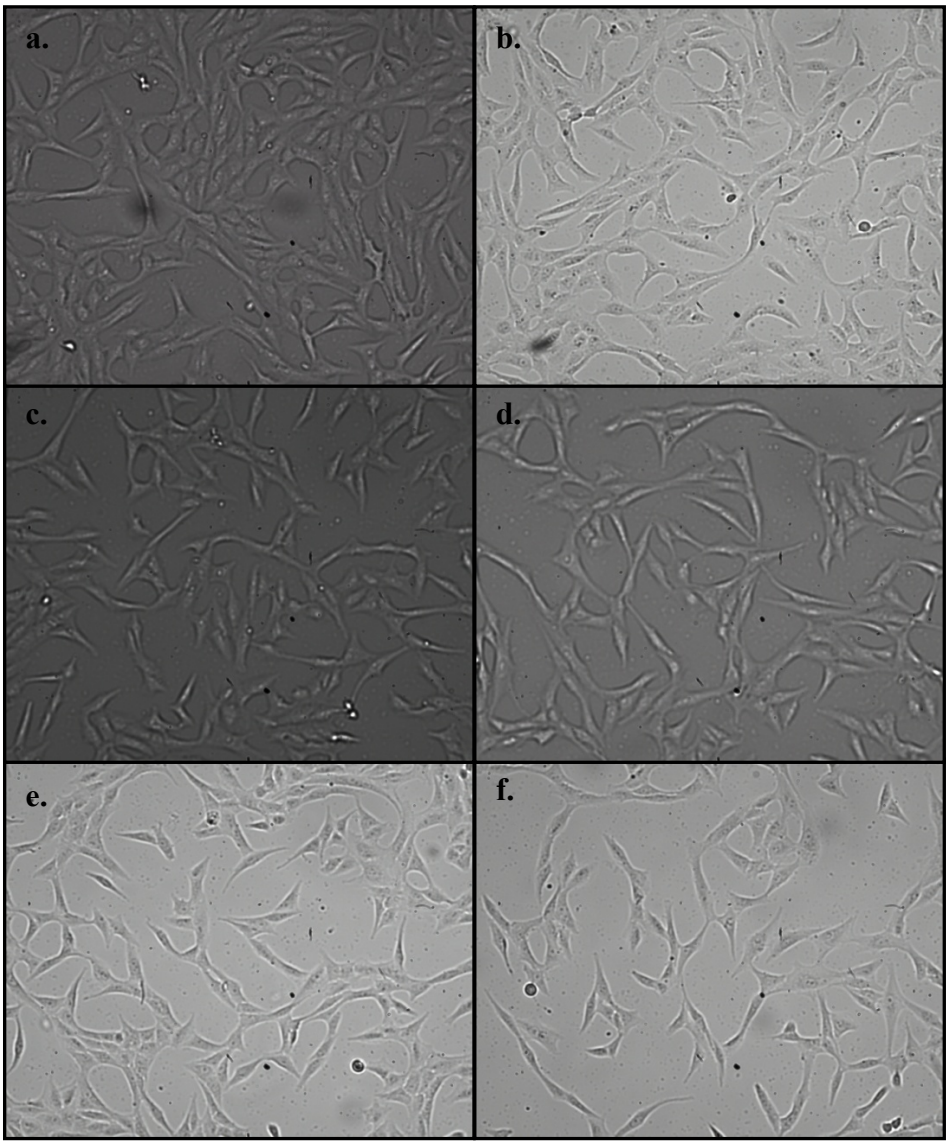

Figure 4.31. Images of L929 cells under light microscope with 10X magnification. a. Negative control with no treatment, b. After 24 hours of exposure with 5 µg/ml AgNP-C, c. After 24 hours of exposure with 2.5 µg/ml AgNP-C, d. After 24 hours of exposure with 1 µg/ml AgNP-C, e. After 24 hours of exposure with 0.5 µg/ml AgNP-C, f. After 24 hours of exposure with 0.05 µg/ml AgNP-C

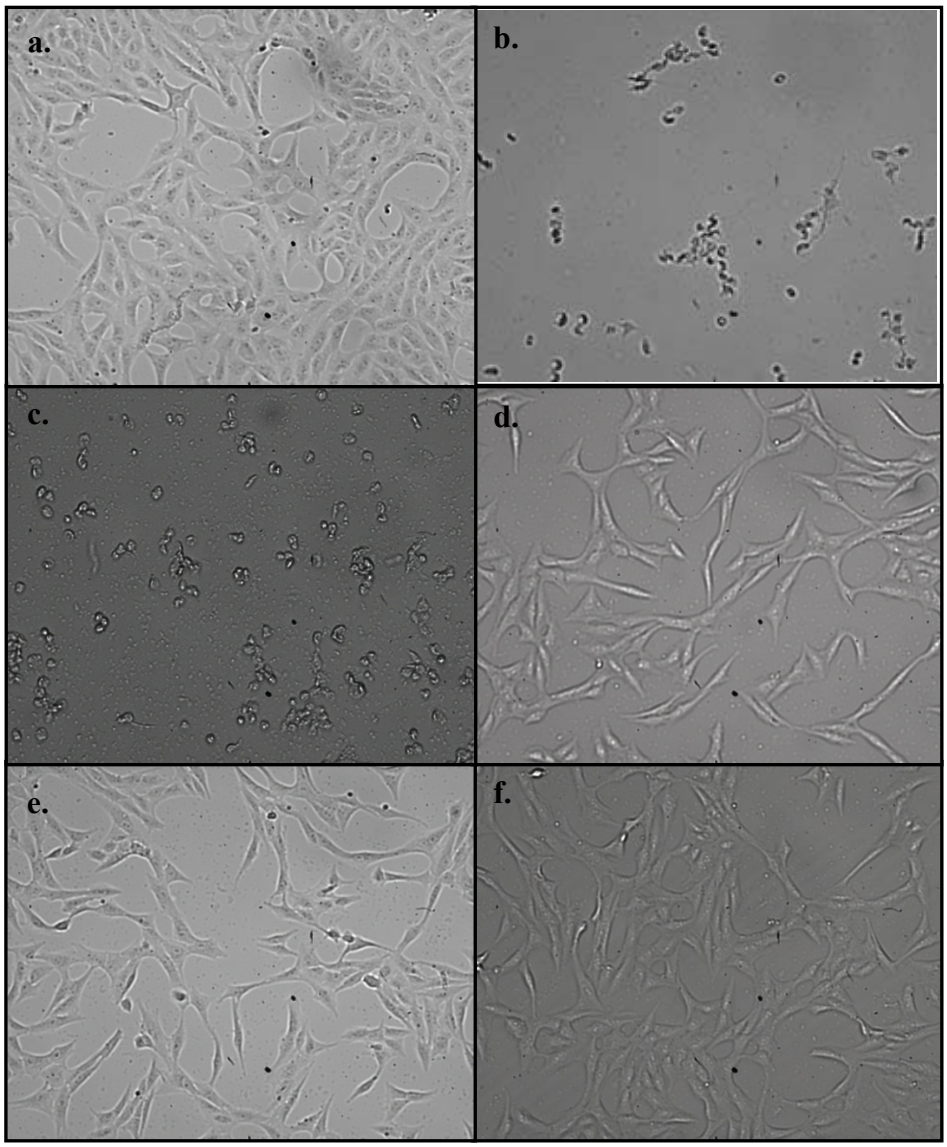

Figure 4.32. Images of L929 cells under light microscope with 10X magnification. a. Negative control with no treatment, b. After 24 hours of exposure with 5 µg/ml AgNP-M, c. After 24 hours of exposure with 2.5 µg/ml AgNP-M, d. After 24 hours of exposure with 1 µg/ml AgNP-M, e. After 24 hours of exposure with 0.5 µg/ml AgNP-M, f. After 24 hours of exposure with 0.05 µg/ml AgNP-M

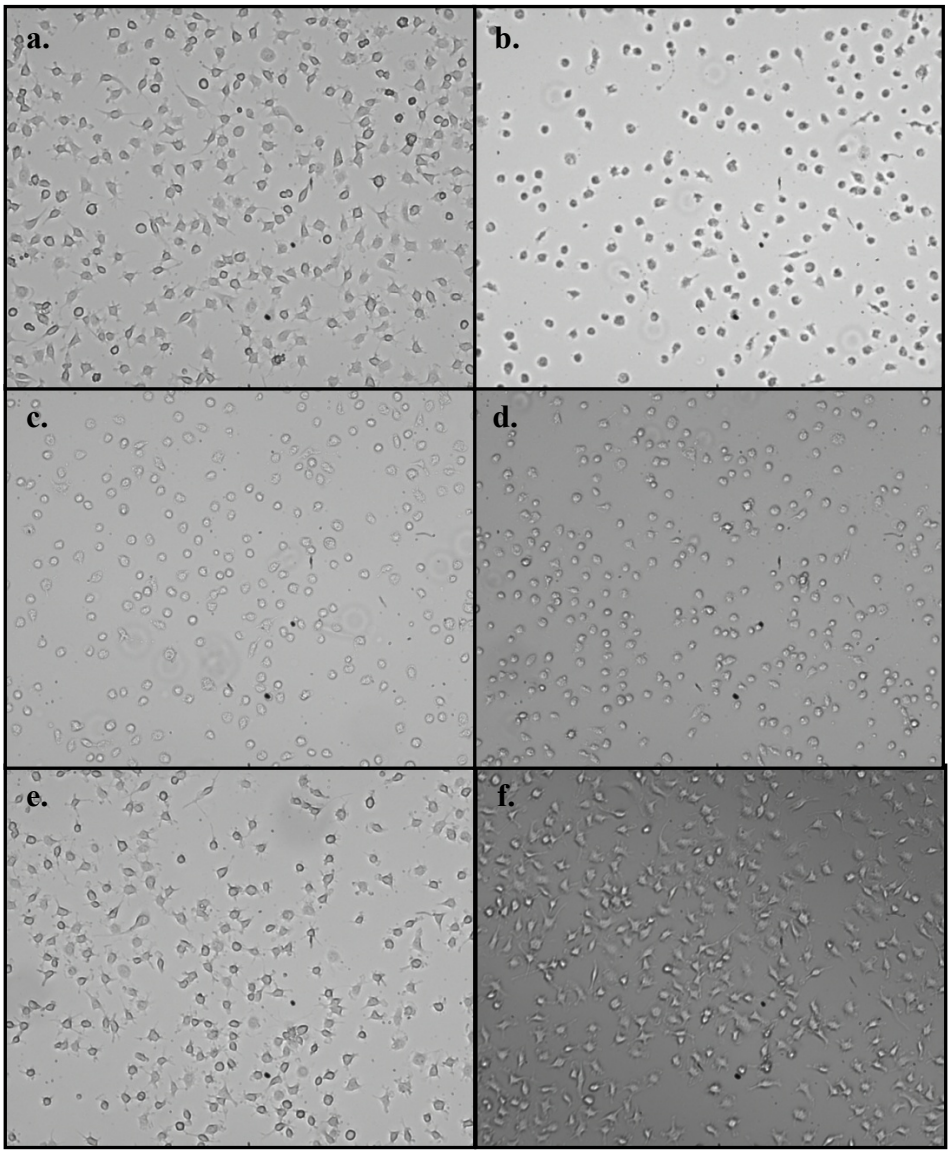

Figure 4.33. Images of RAW 264.7 cells under light microscope with 10X magnification. a. Negative control with no treatment, b. After 24 hours of exposure with 5 µg/ml $AgNO_3$, c. After 24 hours of exposure incubation with 2.5 µg/ml $AgNO_3$, d. After 24 hours of exposure with 1 µg/ml $AgNO_3$, e. After 24 hours of exposure with 0.5 µg/ml $AgNO_3$, f. After 24 hours of exposure with 0.05 µg/ml $AgNO_3$

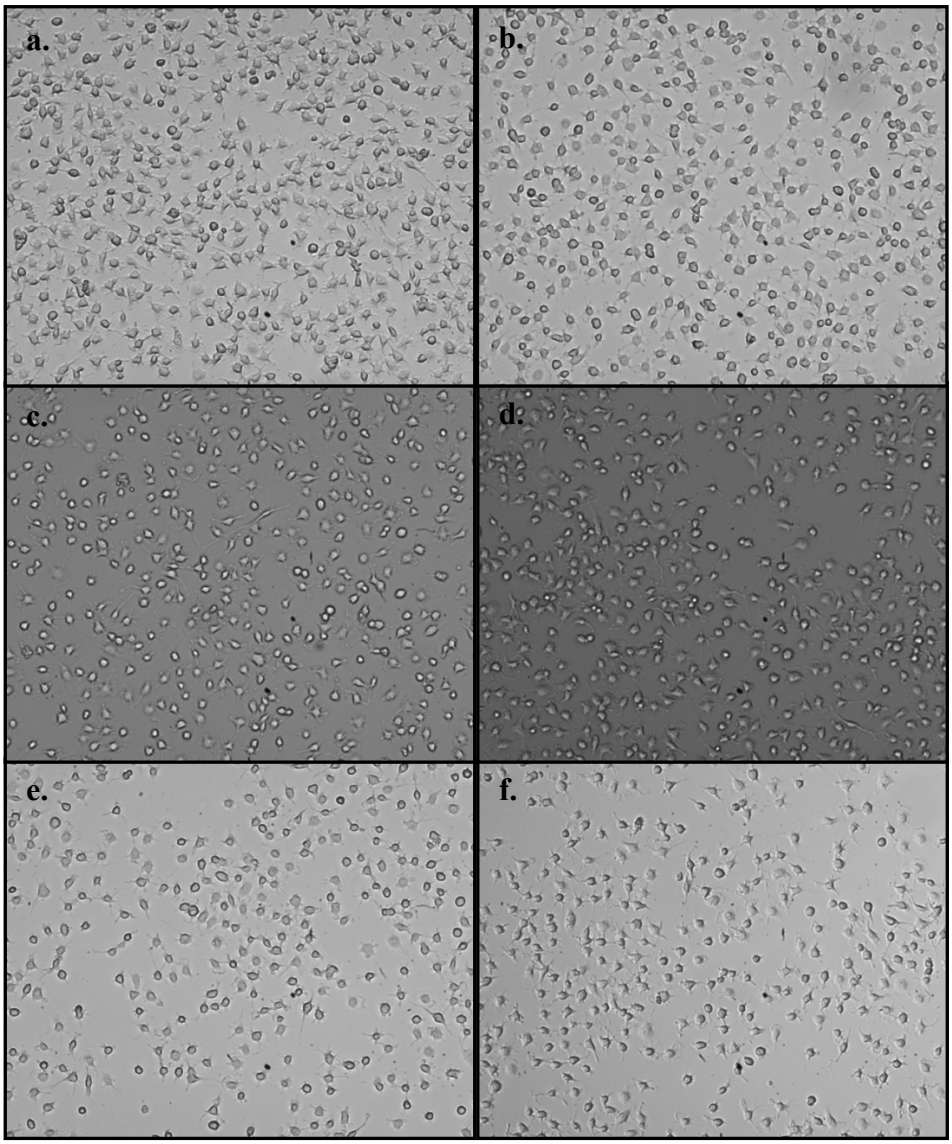

Figure 4.34. Images of RAW 264.7 cells under light microscope with 10X magnification. a. Negative control with no treatment, b. After 24 hours of exposure with 5 µg/ml AgNP-C, c. After 24 hours of exposure with 2.5 µg/ml AgNP-C, d. After 24 hours of exposure with 1 µg/ml AgNP-C, e. After 24 hours of exposure with 0.5 µg/ml AgNP-C, f. After 24 hours of exposure with 0.05 µg/ml AgNP-C

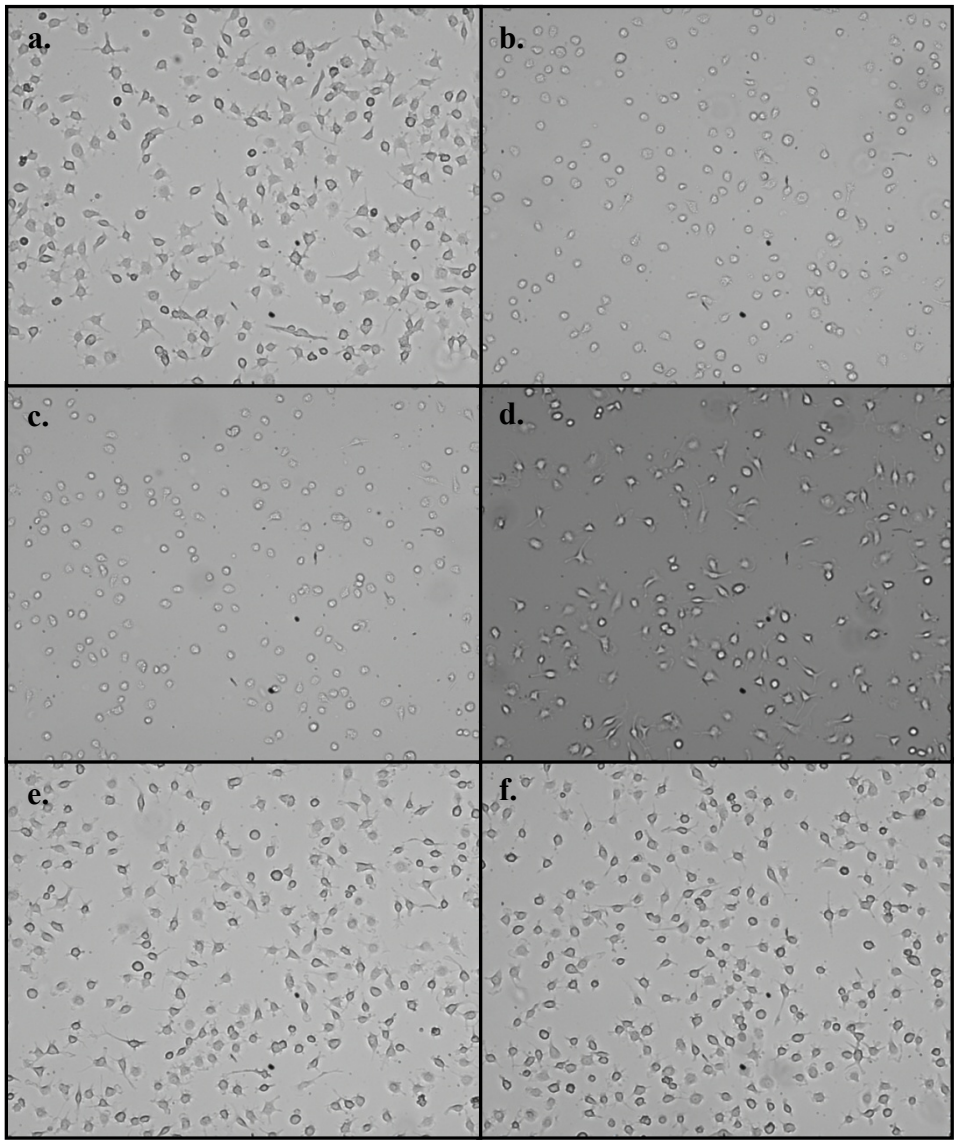

Figure 4.35. Images of RAW 264.7 cells under light microscope with 10X magnification. a. Negative control with no treatment, b. After 24 hours of exposure with 5 µg/ml AgNP-M, c. After 24 hours of exposure with 2.5 µg/ml AgNP-M, d. After 24 hours of exposure with 1 µg/ml AgNP-M, e. After 24 hours of exposure with 0.5 µg/ml AgNP-M, f. After 24 hours of exposure with 0.05 µg/ml AgNP-M

4.3.2. DNA Fragmentation

After morphological observations, DNA fragmentation was carried out. DNA fragmentation is one of the methods that are used to detect DNA damage by the help of gel electrophoresis. In this method, although non-damaged DNAs are observed as genomic

DNAs with intact bands in agarose gel image, DNAs belong to apoptotic cells have fragmented bands on the gel image due to the enzymes that are active during the programmed cell death (apoptosis) mechanism. Besides, non-apoptotic, damaged DNAs cause a smear path in the gel instead of several, certain sized, fragmented bands, that means breaks in DNAs were not occurred by a programmed cell death mechanism.

After the DNA fragmentation experiment, gel images belong to human dermal fibroblasts (HDF), mouse fibroblasts (L929), and mouse macrophages (RAW 264.7) treated with $AgNO_3$, AgNP-C, and AgNP-M were obtained in Figure 4.36, Figure 4.37, Figure 4.38, and Figure 4.39 respectively. All concentrations in the figures were in µg/ml unit. Beside, DNA ladders (250 bp-10000 bp in Figure 4.36-Figure 4.38 and 50 bp-1000 bp in Figure 4.39) were used to observe approximate sizes of genomic DNAs (above 10000 bp based on the images) of the cells and fragments if occurs.

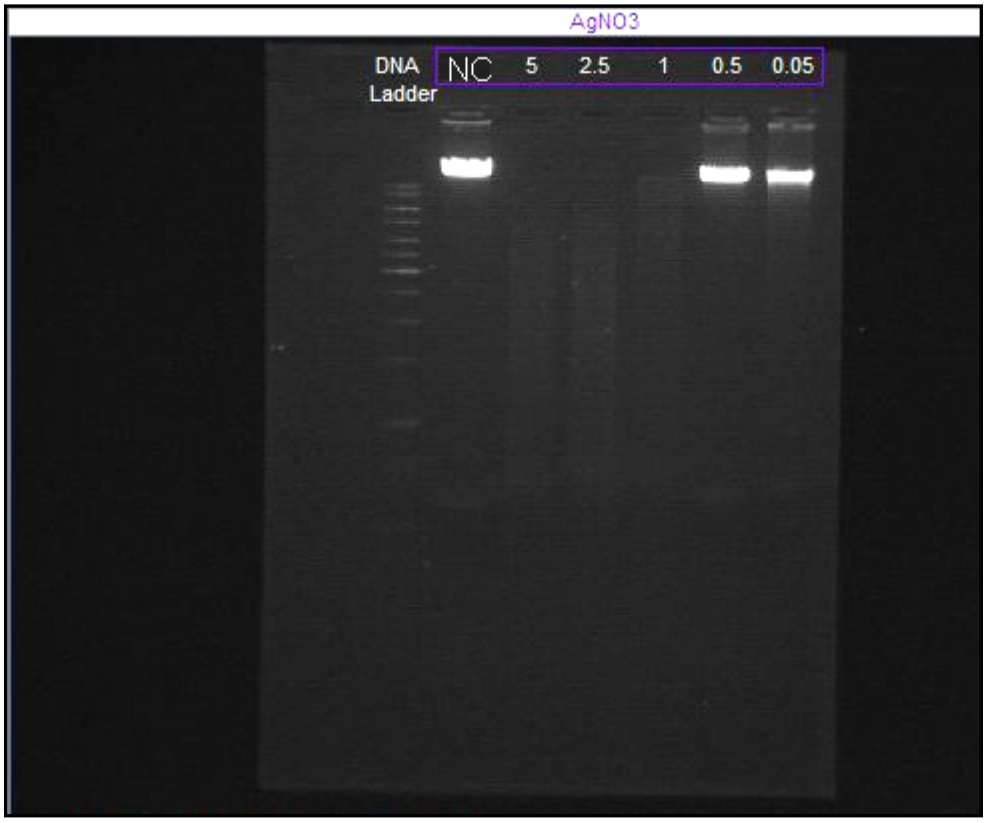

Figure 4.36. Agarose gel image of HDF cells after 24 hours of exposure with $AgNO_3$

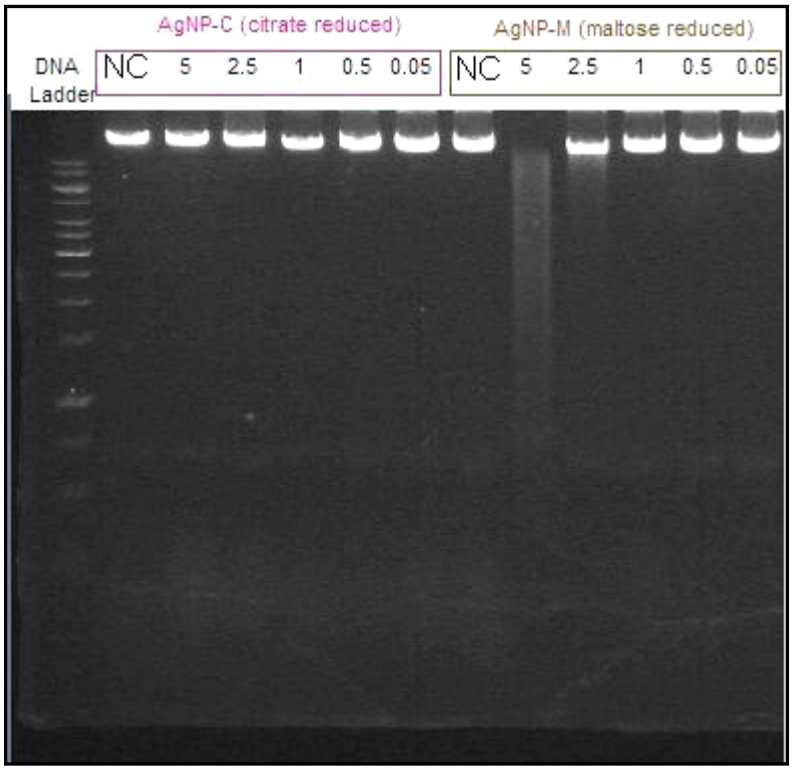

Figure 4.37. Agarose gel image of HDF cells after 24 hours of exposure with AgNP-C and AgNP-M

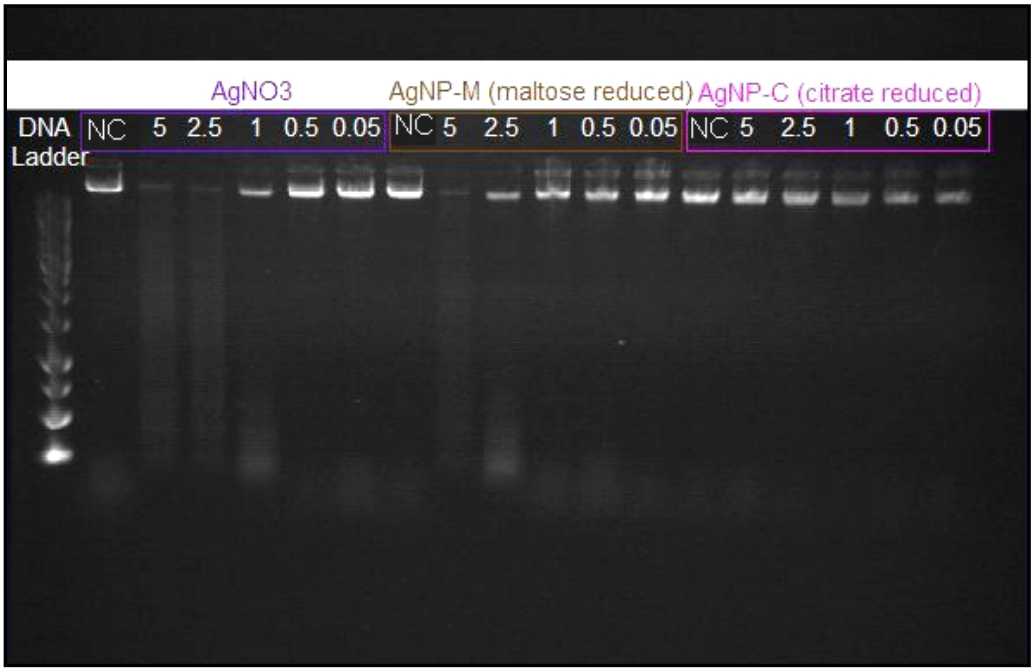

Figure 4.38. Agarose gel image of L929 cells after 24 hours of exposure with $AgNO_3$, AgNP-C, and AgNP-M

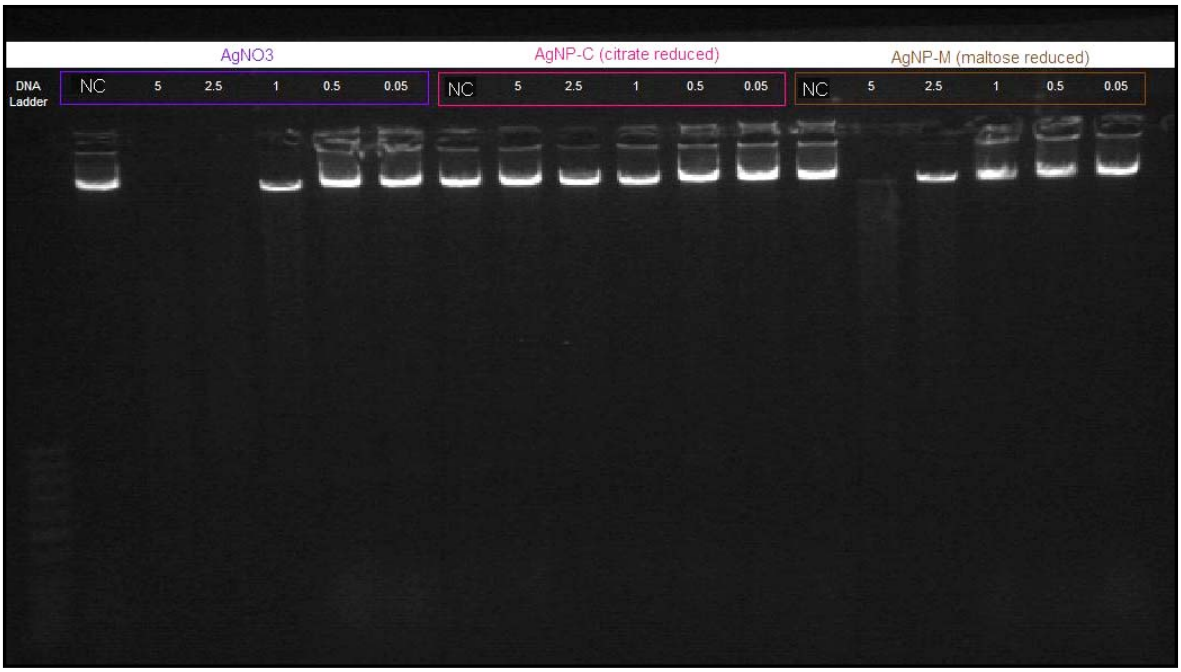

Figure 4.39. Agarose gel image of RAW 264.7 cells after 24 hours of exposure with $AgNO_3$, AgNP-C, and AgNP-M

Based on the DNA fragmentation, $AgNO_3$ had the most toxic effect at 5 µg/ml, 2.5 µg/ml, 1 µg/ml concentrations and AgNP-M showed toxicity for concentrations of 5 µg/ml, and 2.5 µg/ml for all cell types. However, no detectable toxic effect was recorded for AgNP-C. These results were parallel with cytotoxicity studies, which were performed by MTS assay. According to smear paths on the agarose gel images, it can be said that genotoxic concentrations caused necrotic cell death, instead of apoptosis. Furthermore, no clear fragmented bands, which are the signs of apoptosis mechanism, were detected.

4.3.3. Annexin V-PI Staining

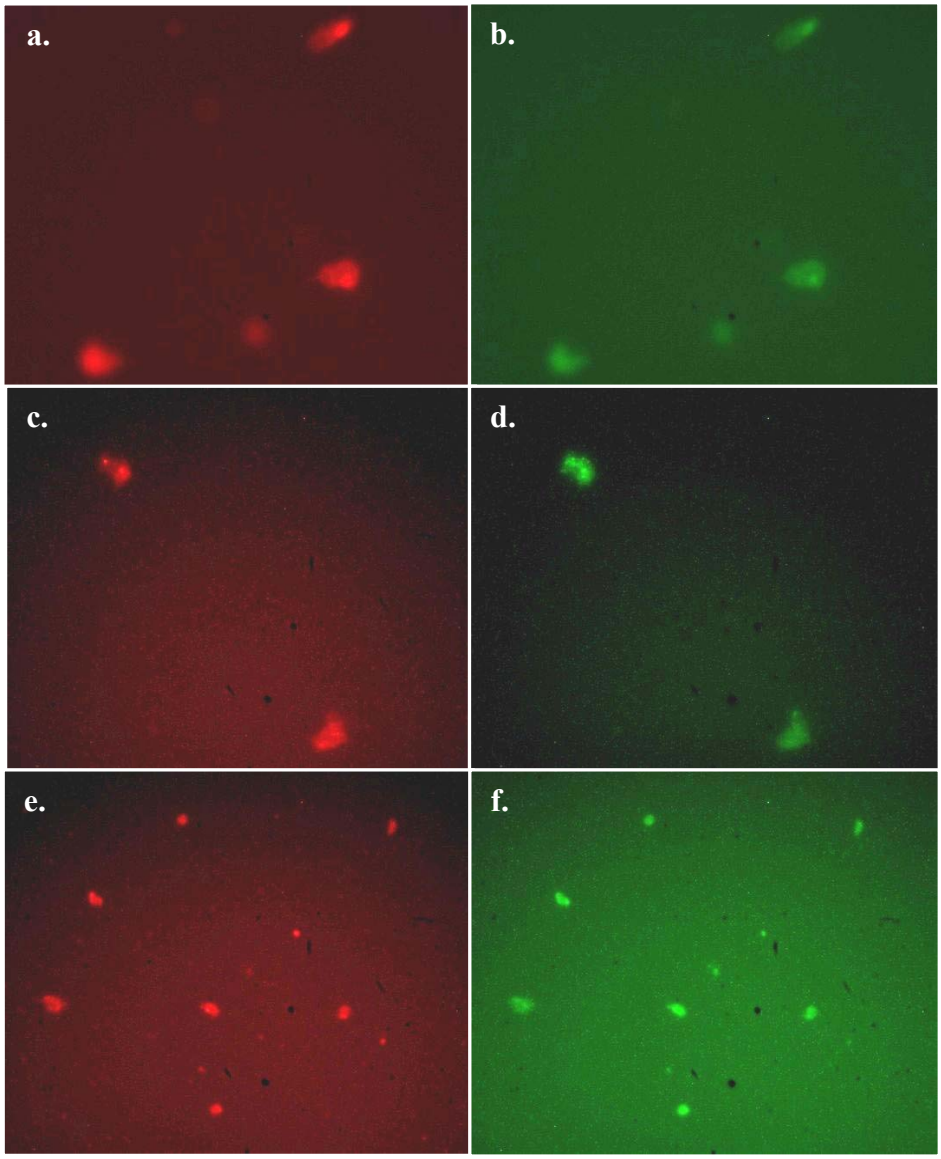

Figure 4.40. Images of HDF cells under fluorescent microscope with 20X magnification. a. PI staining, and b. Annexin staining after 24 hours of exposure with 5 µg/ml $AgNO_3$, c. PI staining, and d. Annexin staining after 24 hours of exposure with 2.5 µg/ml $AgNO_3$, e. PI staining, and f. Annexin staining after 24 hours of exposure with 1 µg/ml $AgNO_3$, g. PI staining, and h. Annexin staining after 24 hours of exposure with 5 µg/ml AgNP-M, i. PI staining, and j. Annexin staining after 24 hours of exposure with 2.5 µg/ml AgNP-M

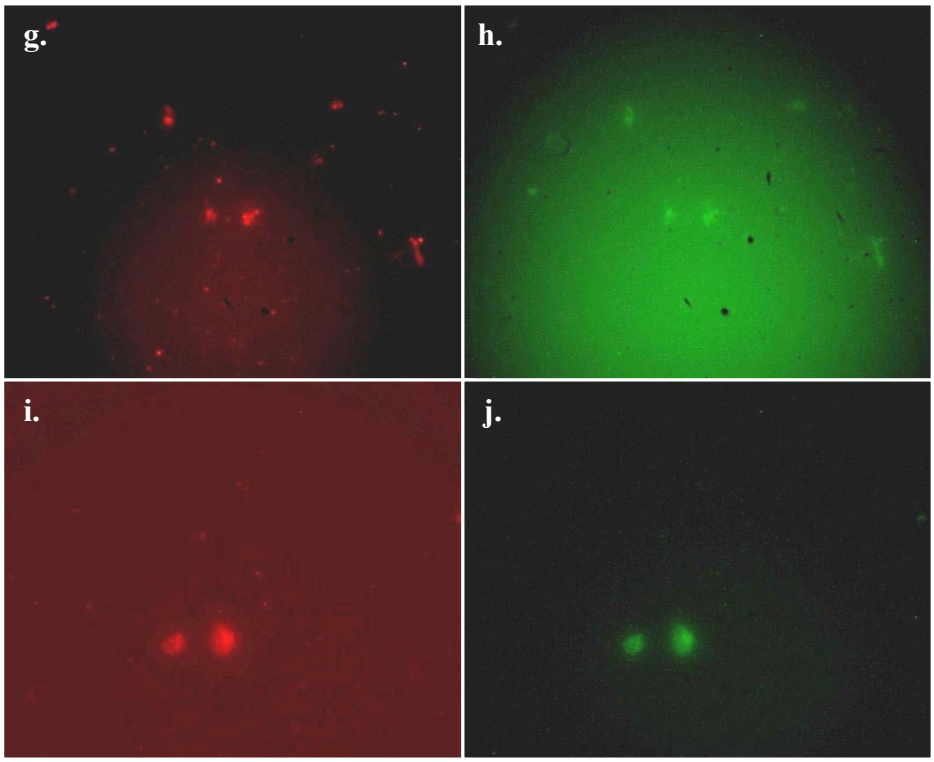

Figure 4.40. Images of HDF cells under fluorescent microscope with 20X magnification. a. PI staining, and b. Annexin staining after 24 hours of exposure with 5 µg/ml $AgNO_3$, c. PI staining, and d. Annexin staining after 24 hours of exposure with 2.5 µg/ml $AgNO_3$, e. PI staining, and f. Annexin staining after 24 hours of exposure with 1 µg/ml $AgNO_3$, g. PI staining, and h. Annexin staining after 24 hours of exposure with 5 µg/ml AgNP-M, i. PI staining, and j. Annexin staining after 24 hours of exposure with 2.5 µg/ml AgNP-M (continue)

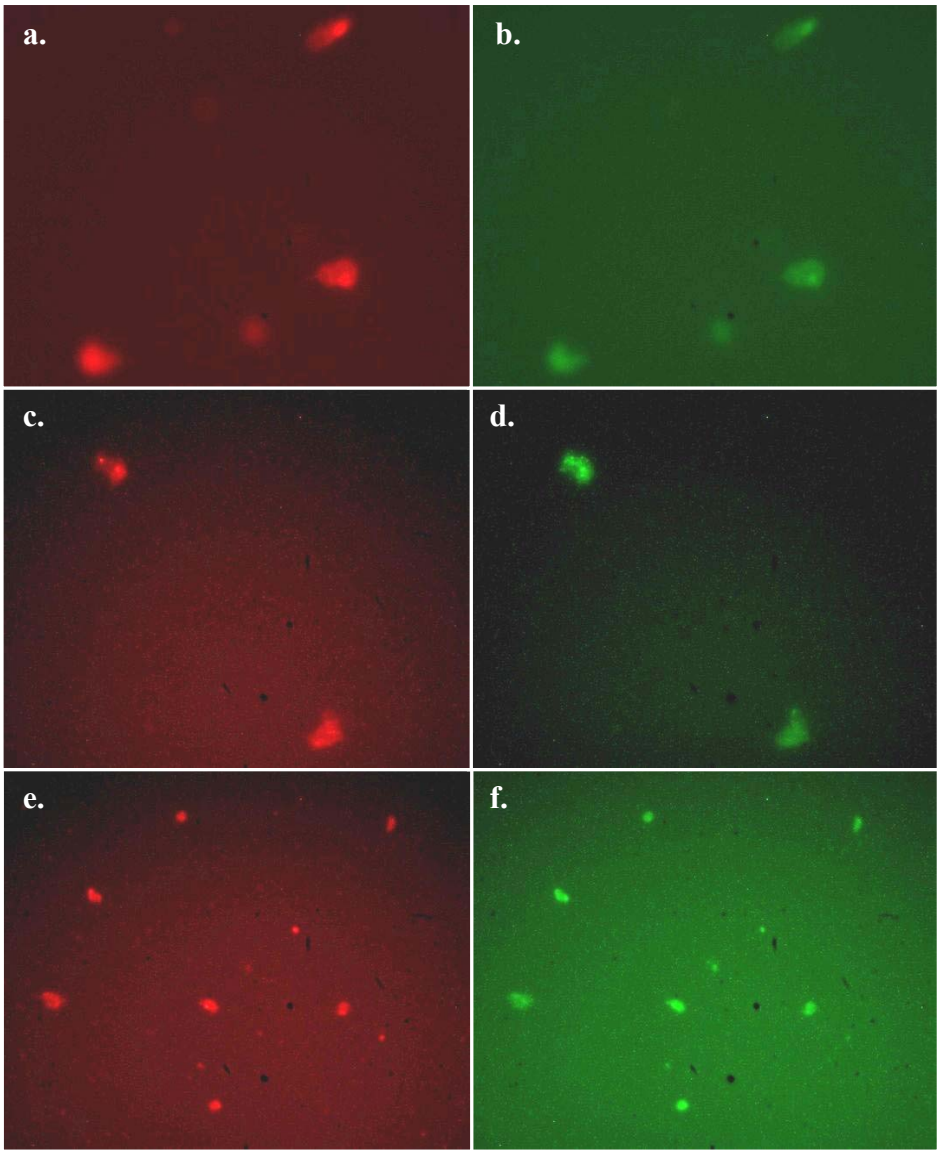

Figure 4.41. Images of L929 cells under fluorescent microscope with 20X magnification. a. PI staining, and b. Annexin staining after 24 hours of exposure with 5 µg/ml $AgNO_3$, c. PI staining, and d. Annexin staining after 24 hours of exposure with 2.5 µg/ml $AgNO_3$, e. PI staining, and f. Annexin staining after 24 hours of exposure with 1 µg/ml $AgNO_3$, g. PI staining, and h. Annexin staining after 24 hours of exposure with 5 µg/ml AgNP-M, i. PI staining, and j. Annexin staining after 24 hours of exposure with 2.5 µg/ml AgNP-M

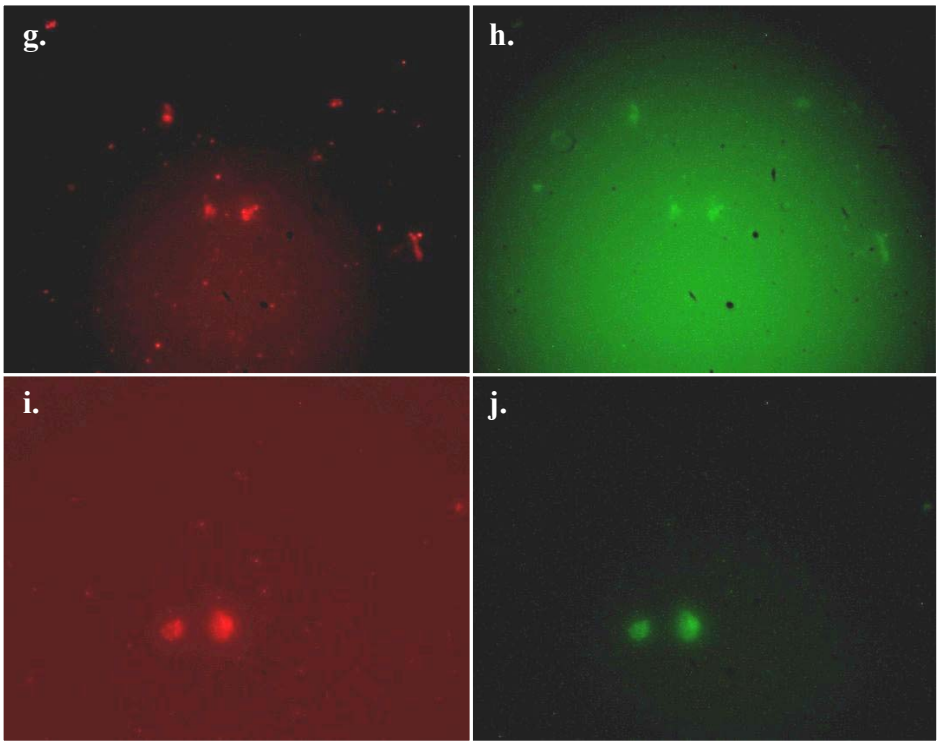

Figure 4.41. Images of L929 cells under fluorescent microscope with 20X magnification. a. PI staining, and b. Annexin staining after 24 hours of exposure with 5 µg/ml $AgNO_3$, c. PI staining, and d. Annexin staining after 24 hours of exposure with 2.5 µg/ml $AgNO_3$, e. PI staining, and f. Annexin staining after 24 hours of exposure with 1 µg/ml $AgNO_3$, g. PI staining, and h. Annexin staining after 24 hours of exposure with 5 µg/ml AgNP-M, i. PI staining, and j. Annexin staining after 24 hours of exposure with 2.5 µg/ml AgNP-M (continue)

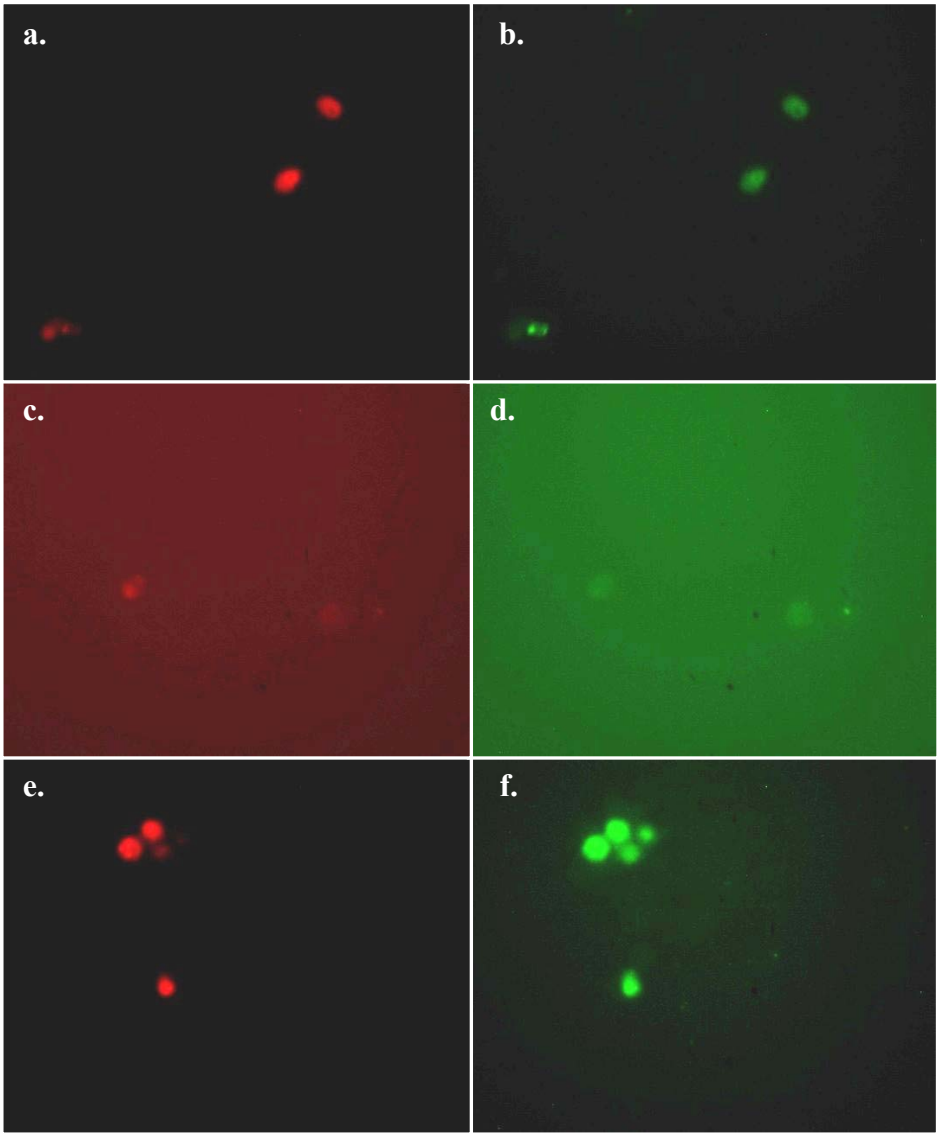

Figure 4.42. Images of RAW 264.7 cells under fluorescent microscope with 20X magnification. a. PI staining, and b. Annexin staining after 24 hours of exposure with 5 µg/ml $AgNO_3$, c. PI staining, and d. Annexin staining after 24 hours of exposure with 2.5 µg/ml $AgNO_3$, e. PI staining, and f. Annexin staining after 24 hours of exposure with 1 µg/ml $AgNO_3$, g. PI staining, and h. Annexin staining after 24 hours of exposure with 5 µg/ml AgNP-M, i. PI staining, and j. Annexin staining after 24 hours of exposure with 2.5 µg/ml AgNP-M

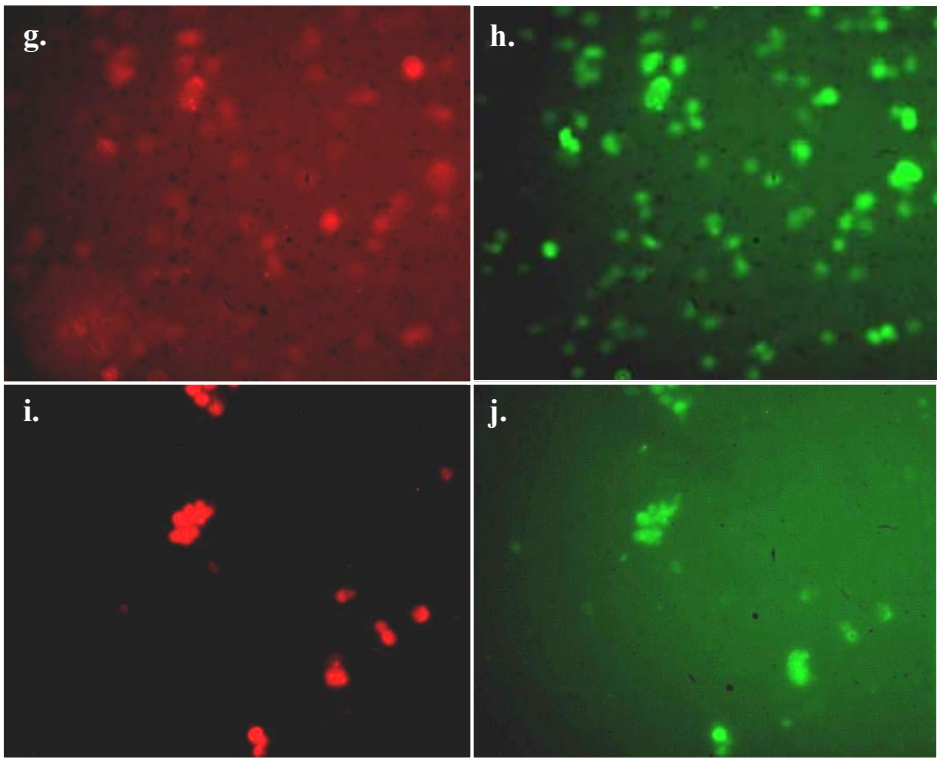

Figure 4.42. Images of RAW 264.7 cells under fluorescent microscope with 20X magnification. a. PI staining, and b. Annexin staining after 24 hours of exposure with 5 µg/ml $AgNO_3$, c. PI staining, and d. Annexin staining after 24 hours of exposure with 2.5 µg/ml $AgNO_3$, e. PI staining, and f. Annexin staining after 24 hours of exposure with 1 µg/ml $AgNO_3$, g. PI staining, and h. Annexin staining after 24 hours of exposure with 5 µg/ml AgNP-M, i. PI staining, and j. Annexin staining after 24 hours of exposure with 2.5 µg/ml AgNP-M (continue)

Annexin V and PI (Propidium iodide) staining was carried out to see the effects of Ag^+ and AgNPs whether they have apoptotic or necrotic effect on the cells.

Apoptosis and necrosis are two different forms of cell death [96]. Apoptosis is a controlled type of cell death. It depends on a genetic mechanism with many morphological changes; cell shrinkage, dense chromatin, and DNA fragments [97]. However, necrosis is known as nonapoptotic cell death [98]. In necrotic cell death, cell swells, plasma membrane losses its integrity, and cell losses its intracellular contents. It is an irreversible process and it can only start after the cells die [99].

In living cells, phosphatidylserine (PS), which is a kind of phospholipid, exists in the inner (cytosolic) part of the cell membrane. This condition changes in apoptotic cells. Due to dispersed integrity of plasma membrane, PS is exposed to the outer surface of the cell membrane [100]. Annexin V, which is an anticoagulant protein, specifically identifies and binds PS in the presence of Ca^{2+} [101, 102]. Thereby, apoptotic cells can be detected by using Annexin V. For detection, FITC, a fluorescein, was conjugated to Annexin V and it gave fluorescent at 520 nm giving green color. In addition to FITC conjugated Annexin V, propidium iodide (PI) which is a fluorescent molecule, was utilized to detect death cells. PI was used as a DNA stain to differentiate healthy living cells, apoptotic cells, and necrotic cells by observing nucleus [103]. It is impermeable for cell membranes so living cells do not allow PI to pass through. Due to their disposed cell membrane structure, only dead cells take this stain, so it separates the death cells from the living cells. When PI locates in DNA, it shows luminescence at 620 nm giving red color. Annexin V-PI staining was carried out as manufacturer's instruction (FITC Annexin V/Dead Cell Apoptosis Kit with FITC annexin V and PI) for all three cell types; HDF, L929, and RAW 264.7. Figure 4.40-Figure 4.42 showed images of the cells by using fluorescent microscope after the staining.

In this part, only toxic concentrations were chosen to test. Three concentrations for $AgNO_3$; 5 µg/ml, 2.5 µg/ml, 1 µg/ml and two concentrations for AgNP-M; 5 µg/ml, 2.5 µg/ml were used to treat cells for 24 hours. After DNA fragmentation, this part provided a better understanding about how toxic concentrations cause cell death. Due to the fact that, many cells were lost during the procedure and fluorescence activity of dyes reduced fast, images could not be obtained in a high quality. Nevertheless, detected cells formed an opinion about the cell death. After 24 hours of exposure, almost all cells were stained with both FITC conjugated annexin V (green) and PI (red). This situation indicated necrotic stage of the cell death. Moreover, some cells, that were stained only green, showed apoptotic phase. In general, it can be said that after 24 hours of exposure, toxic concentrations caused necrotic death for the majority of the cells. These results also resembled the results in DNA fragmentation part. Not- fragmented, smear bands were a sign of necrotic cell death.

5. CONCLUSION AND RECOMMENDATIONS

5.1. CONCLUSION

Silver is being used for a long time on the wound healing. Although there are many studies concerning this matter in literature, there is controversy over the silver use in wound healing. In this study, we aimed to investigate the affects of silver ions and AgNPs synthesized using different reducing agents to generate different surface properties. The presence of a relationship between cytotoxicity and genotoxicity of silver ions and AgNPs is investigated. The three cell types, HDF, L929, and RAW 246.7, are used as model cell lines.

Cytotoxicity studies showed that $AgNO_3$ (the source of Ag^+) was toxic for all cell types at concentrations higher than 0,5 μg/ml. At lower concentrations of Ag^+ (0,05 μg/ml and 0,005 μg/ml) not only any toxic effect but also a slight proliferative effect was observed as in $NaNO_3$ (the source of Na^+) and $Na_3C_6H_5O_7$ (the source of $C_6H_5O_7^{3-}$). Therefore, it is difficult to conclude that the Ag^+ induces proliferation individually at its lower concentrations without any molecular study. Besides, the AgNPs reduced with citrate (for AgNP-C) showed no toxic effect compared to Ag^+. Cytotoxicity results showed that AgNP-C did not have any observable toxic effect on the cells, although AgNP-M, AgNP-L, AgNP-G were toxic for the concentrations higher than 1 μg/ml. To understand this difference, dissolution part must be considered. In the dissolution study, the AgNP-M and AgNP-C showed different dissolution profiles that help to explain the cytotoxicity results. During the 3-day period, the Ag^+ concentration released from AgNP-C and AgNP-M, which was chosen as a representative of carbohydrate-reduced AgNPs, was measured. Although AgNP-C released very small to no Ag^+, the concentration of Ag+ was high for AgNP-M immediately after the synthesis due to the incomplete reduction of Ag^+ to AgNPs. However, after first washing step, the release of the Ag^+ was diminished significantly.

Different reducing agents used for synthesis results AgNPs with altered surface chemistry properties. This affects the interaction between AgNPs and the cells, although size of

AgNPs was in the same range. Therefore, observing different effects is expected for AgNPs, which were synthesized with different reducing agents. However, characterization studies showed that carbohydrates are not strong reducing agents as much as citrate. While they are green agents for synthesis, there are limitations because of the problems about scalability and controlling the particle morphologies. Although maltose was observed to yield a better synthesis than lactose and glucose, high concentration of free Ag^+ immediately after synthesis showed that maltose could also not reduce AgNPs efficiently.

At the very low concentrations of AgNPs and Ag^+, proliferative effect on the cells was observed. However, these effects did not show continuity and consistency with respect to the concentrations and the source of silver. Additional studies on the proliferation are necessary. In addition, the exposure duration did not have a dramatic effect on the silver performance of neither Ag^+ nor AgNPs. Both Ag^+ and AgNPs showed their effects up to 24 h, thus longer exposure time did not change the outcome significantly. Only a slight decrease was detected on the values in time, due to the diminishing effect.

Genotoxicity studies were performed after the cytotoxic effects of both AgNPs and Ag^+ were determined. According to DNA fragmentation and immunostaining with annexin V and PI, silver caused mostly necrotic cell death for its toxic concentrations and these concentrations change depending on the silver source ($AgNO_3$, carbohydrate-reduced AgNPs).

Although we did not use a dialysis step to relate the free Ag^+ ions and its toxicity, it is necessary to perform dialysis procedure to the synthesized colloidal suspension to observe the effect of AgNPs alone. Additional studies are necessary to see the effects of AgNPs, which are synthesized with different reductants and procedures.

This study suggests that there is a relationship between the toxicity of Ag^+ and wound healing. It should be noted that the possible positive effects of AgNPs on wound healing could be due to the slow dissolution of AgNPs.

5.2. RECOMMENDATIONS

Our study suggested that Ag^+ is more toxic than AgNPs that were synthesized with different reducing agents. In addition, the dissolution study indicates that the sodium citrate is more effective reducing agent than carbohydrates for the synthesis of AgNPs. Among carbohydrates, glucose and lactose could not reduce Ag^+ to nanoparticle form efficiently. Maltose was observed to be a better reductant similar to citrate reduction from the characterization results. However, when the dissolution of the AgNPs was analyzed, the incomplete reduction of Ag^+ into AgNP-M suggested that maltose was also not an effective reductant as much as citrate. The dissolution study also showed that an additional dialysis was necessary to observe the AgNPs alone, when the toxicity is considered.

In the following steps of the study, toxicity tests were performed to see the effects of Ag^+ and AgNPs on the cell viability. Opposite to the analysis of toxic effects, cell proliferation can also be investigated by performing cell proliferation assays such as migration assay. Thus, variable and unclear proliferative effects in the cell viability results for low concentrations of Ag^+ and AgNPs can be clarified. In addition to these, beside fibroblasts and macrophages, use of additional cells such as neutrophils and mast cells can be tested to enhance the results.

Finally, it must be said that all results were obtained from *in vitro* studies during this experiment. *In vivo* studies are also needed to be investigated for a better understanding of the effects of silver on the wound healing. Additionally, exact mechanism of the silver on the wounds is still unknown. Additional studies must be carried out to find out the molecular mechanism of the effect of silver.

REFERENCES

1. Teare J. and C. Barrett, "Using quality of lift, assessment in wound care", *Nurse Standard*, Vol. 17, No. 6, pp. 59-60, 64, 67-68, 2002.

2. Yamada K. M. and R. A. F. Clark, "Provisional matrix", in: R. A. F. Clark, *The molecular and cellular biology of wound repair,* pp. 51-94, London, Plenum Press, 1996.

3. Nguyen, D. T., D. P. Orgill and G. F. Murphy, "The pathophysiologic basis for wound healing and cutaneous regeneration", *Biomaterials for Treating Skin Loss*, pp. 25-57, CRC Press (US) & Woodhead Publishing (UK), Boca Raton-Cambridge, 2009.

4. Grinnell, F., R. E. Billingham and L. Burgess, "Distribution of fibronectin during wound healing in vivo", *Journal of Investigative Dermatology,* Vol. 76, No. 3, pp. 181-189, 1981.

5. Koveker, G. B., “Growth factors in clinical practice”, *International Journal of Clinical Practice*, Vol. 54, No. 9, pp. 590-593, 2000.

6. Clark, R. A., J. M. Lanigan, P. DellaPelle, E. R. Manseau, H. F. Dvorak and R. B. Colvin, "Fibronectin and fibrin provide a provisional matrix for epidermal cell migration during wound reepithelialization", *Journal of Investigative Dermatology*, Vol. 79, No. 5, pp. 264-269, 1982.

7. Hopkinson-Woolley, J., D. Hughes, S. Gordon and P. Martin, "Macrophage recruitment during limb development and wound healing in the embryonic and foetal mouse", *Journal of Cell Science,* Vol. 107, pp. 1159-1167, 1994.

8. Liebovich, S. J. and R. Ross, "The role of the macrophage in wound repair", *The American Journal of Pathology,* Vol. 78, No.1, pp. 71-100, 1975.

9. Chang, H. Y., J. B. Sneddon, A. A. Alizadeh, R. Sood, R. B. West, K. Montgomery, J. T. Chi, M. van de Rijn, D. Botstein and P. O. Brown, "Gene Expression Signature of Fibroblast Serum Response Predicts Human Cancer Progression: Similarities between Tumors and Wounds", *Public Library of Science*, Vol. 2, No. 2, 2004.

10. Midwood, K. S., L. V. Williams and J. E. Schwarzbauer, "Tissue repair and the dynamics of the extracellular matrix", *The International Journal of Biochemistry & Cell Biology*, Vol. 36, No. 6, pp. 1031–1037, 2004.

11. Garg, H. G., *Scarless Wound Healing*, CRC Press, New York, 2000.

12. Winter, G. D., "Formation of the scab and the rate of epithelialization of superficial wounds in the skin of the young domestic pig", *Nature*, Vol. 193, pp. 293-294, 1962.

13. Boyce, D. E., W. D. Jones, F. Ruge, K. G. Harding and K. Moore, "The role of lymphocytes in human dermal wound healing", *British Journal of Dermatology*, Vol. 14, No.1, pp. 59-65, 2000.

14. Clark, R. A. F., "Biology of dermal wound repair", *Dermatologic Clinics*, Vol. 11, pp. 647-666, 1993.

15. Cooper, D. M., E. Z. Yu, P. Hennessey, F. Ko and M. C. Robson, "Determination of endogenous cytokines in chronic wounds", *Annals of Surgery*, Vol. 219, pp. 688-692, 1994.

16. Lorenz, H. P. and M. T. Longaker, "Wounds: Biology, Pathology, and Management", in M. Li, J. A. Norton, R. R. Bollinger, A. E. Chang, S. F. Lowry, S. J. Mulvihill, H. I. Pass and R. W. Thompson, *Essential Practice of Surgery,* pp. 77-88, Springer-Verlag Publishing, New York, 2003.

17. Dealey, C., *The care of wounds: A guide for nurses,* Wiley- Blackwell Publishing, Oxford, 1999.

18. Gillitzer, R. and M. Goebeler, "Chemokines in cutaneous wound healing", *Journal of Leukocyte Biology*, Vol. 69, pp. 513–521, 2001.

19. Trautmann, A., A. Toksoy, E. Engelhardt, E. B. Brocker and R. Gillitzer R, "Mast cell involvement in normal human skin wound healing: expression of monocyte chemoattractant protein-1 is correlated with recruitment of mast cells which synthesize interleukin-4 in vivo", *The Journal of Pathology,* Vol. 90, pp. 100-106, 2000.

20. Büchau, A. S., "EGFR (Trans)activation Mediates IL-8 and Distinct Human Antimicrobial Peptide and Protein Production following Skin Injury", *Journal of Investigative Dermatology*, Vol. 130, pp. 929-932, 2010.

21. Richard, J. W., et al., "Acticoat versus silverlon: the truth", *Journal of Burns and Surgical Wound Care*, Vol. 1, pp. 11-20, 2002.

22. Klasen, H. J., "Historical review of the use of silver in the treatment of burns. I. Early uses", *Burns*, Vol. 26, No. 2, pp. 117-130, 2000.

23. Castellano, J. J., et al., "Comparative evaluation of silver-containing antimicrobial dressings and drugs", *International Wound Journal*, Vol. 4, No. 2, pp. 114-122, 2007.

24. Landsdown, A. B. G., "Silver I: its antibacterial properties and mechanism of action", *Journal of Wound Care*, Vol. 11, pp. 125-138, 2002.

25. Hugo, W. B. and A. D. Russell, "Types of antimicrobial agents", in: W. B. Hugo, A. D. Russell and G. A. J. Ayliff, *Principles and practice of disinfection, preservation and sterilization*, pp. 8-106, Blackwell Scientific Publications, Oxford, 1982.

26. Demling, R. H. and L. DeSanti, "Effects of silver on wound management", *Wounds*, Vol. 13, pp. 4, 2001.

27. Chopra, I., "The increasing use of silver-based products as antimicrobial agents: a useful development or a cause for concern?", *Journal of Antimicrobial Chemotherapy*, Vol. 59, pp. 587-590, 2007.

28. Moyer, C. A., L. Brentano, D. L. Gravens, H. W. Margraf and W. W. Monafo, "Treatment of large human burns with 0.5% silver nitrate solution", A*rchives of Surgery*, Vol. 90, pp. 812-867, 1965.

29. Bellinger, C. G. and H. Conway, "Effects of silver nitrate and sulfamylon on epithelial regeneration", *Plastic and Reconstructive Surgery,* Vol. 45, pp. 582-585, 1970.

30. Fox, C. L. and S. M. Modak, "Mechanism of silver sulfadiazine action on burn wound infections", *Antimicrobial Agents and Chemotherapy*, Vol. 5, No. 6, pp. 582-588, 1974.

31. Gemmell, C. G., D. I. Edwards and A. P. Frainse, "Guidelines for the prophylaxis and treatment of methicillin-resistant Staphylococcus aureus (MRSA) infections in the UK", *Journal of Antimicrobial Chemotherapy*, Vol. 57, pp. 589–608, 2006.

32. Wright, J. B., K. Lam and R. E. Burrell, "Wound management in an era of increasing bacterial antibiotic resistance: a role for topical silver treatment", *American Journal of Infection Control*, Vol. 26, No. 6, pp. 572-577, 1998.

33. Kirsner, R. S., H. Orstead and J. B. Wright, "Matrix metalloproteinases in normal and impaired wound healing: a potential role for nanocrystalline silver", *Wounds*, Vol. 13, No. 3 (Suppl. C), pp. 5-12, 2001.

34. Chu, C. S., A. T. McManus, A. D. Mason and B. A. Jr. Pruitt, "Topical silver treatment after escharectomy of infected full thickness burn wounds in rats", *The Journal of Trauma,* Vol. 58, No. 5, pp. 1040-1046, 2005.

35. Paddock, H. N., G. S. Schultz, K. J. Perrin, et al, "Clinical assessment of silver-

coated antimicrobial dressing on MMPs and cytokine levels in non-healing wounds", *Annual Meeting of the Wound Healing Society*, Baltimore, 2002.

36. Lansdown, A. B. G., "The role of silver", *European Tissue Repair Society Bulletin,* http://www.infomat.net/1/focus/foci/elastoplast/silverhealing_research.asp [retrieved 14 June 2011].

37. Morones, J. R., J. L. Elechiguerra, A. Camacho and J. T. Ramirez, "The bactericidal effect of silver nanoparticles", *Nanotechnology*, Vol. 16, pp. 2346-2353, 2005.

38. Kim, J. S., et al., "Antimicrobial effects of silver nanoparticles", *Nanomedicine: Nanotechnology, Biology and Medicine*, Vol. 3, pp. 95-101, 2007.

39. Flemming, C. A., F. G. Ferris, T. J. Beveridge and G. W. Bailey, "Remobilization of toxic heavy metals absorbed to wall-clay composites", *Applied and Environmental Microbiology*, Vol. 56, pp. 3191-3203, 1990.

40. Russell, A. D. and W. B. Hugo, "Antimicrobial activity and action of silver", *Progress in Medicinal Chemistry*, Vol. 31, pp. 351-370, 1994.

41. Landsdown, A. B. G., "Silver I: its antibacterial properties and mechanism of action", *Journal of Wound Care*, Vol. 11, pp. 125-138, 2002.

42. Rosenkranz, H. S. and H. S. Carr, "Silver sulfadazine: effect on growth and metabolism of bacteria", *Antimicrobial Agents and Chemotherapy*, Vol. 5, pp. 199–201, 1972.

43. Bragg, P. D. and D. J. Rainnie, "The effect of silver ion on the respiratory chain of Escherichia coli", *Canadian Journal of Microbiology*, Vol. 20, pp. 883-889, 1974.

44. Schreurs, W. J. A. and H. Rosenberg, "Effect of silver ions on transport and retention of phosphate by Escherichia coli", *Journal of Bacteriology*, Vol. 152, No. 1, pp. 7-13, 1982.

45. Yamanaka, M., K. Hara and J. Kudo, "Bactericidal Actions of a Silver Ion Solution on Escherichia coli, Studied by Energy-Filtering Transmission Electron Microscopy and Proteomic Analysis", *Applied and Environmental Microbiology,* Vol. 71, No. 11, pp. 7589-7593, 2005.

46. Haefili, C., C. Franklin and K. Hardy, "Plasmid-determined silver resistance in Pseudomonas stutzeri isolated from a silver mine", *Journal of Bacteriology*, Vol. 158, pp. 389-392, 1984.

47. Liau, S. Y., D. C. Read, W. J. Pugh, J. R. Furr and A. D. Russell, "Interaction of silver nitrate with readily identifiable groups: relationship to the antibacterial action of silver ions", *Letters in Applied Microbiology*, Vol. 25, pp. 279-283, 1997.

48. Feng, Q. L., J. Wu, G. Q. Chen, F. Z. Cui, T. N. Kim and J. O. Kim, "A mechanistic study of the antibacterial effect of silver ions on Escherichia coli and Staphylococcus aureus", *Journal of Biomedical Materials Research*, Vol. 52, No. 4, pp. 662-668, 2000.

49. Cervantes, C. and S. Silver, "Metal resistance in pseudomonas: genes and mechanisms", in T. Nakazawa, K. Furukawa, D. Haas and S. Silver, *Molecular biology of Pseudomonads*, pp. 398, American Society for Microbiology Press, Washington, DC, 1996.

50. Modak, S. M. and C. R. Jr. Fox, "Binding of silver sulfadiazine to the cellular components of pseudomonas aeruginosa", *Biochemical Pharmacology,* Vol. 22, pp. 2391-2404, 1973.

51. Dunn, K. and V. Edwards-Jones, "The role of Acticoat TM with nanocrystalline silver in the management of burns", *Burns*, Vol. 30 (Suppl 1), pp. 1-9, 2004.

52. Li, X. Z., H. Nikaido and K. E. Williams, "Silver-resistant mutants of Escherichia coli display active efflux of Ag+ and are deficient in porins", *Journal of Bacteriology*, Vol. 179, pp. 6127-6132, 1997.

53. Gupta, A., M. Maynes and S. Silver, "Effects of halides on plasmidmediated silver resistance in Escherichia coli", *Applied and Environmental Microbiology*, Vol. 64, pp. 5042-5045, 1998.

54. Hendry, A. T. and I. O. Stewart, "Silver-resistant Enterobacteriaceae from hospital patients", *Canadian Journal of Microbiology*, Vol. 25, pp. 915-921, 1979.

55. Kapoor, N., S. Chibber and D. V. Vadehra, "Susceptibility of multidrug-resistant isolates of Klebsiella pneumoniae to silver nitrate", *Folia Microbiologica,* Vol. 34, pp. 94-98, 1989.

56. Atiyeh, B. S., M. Costagliola, S. N. Hayek and S. A. Dibo, "Effect of silver on burn wound infection control and healing: review of the literature", *Burns*, Vol. 33, No. 2, pp. 139-148, 2007.

57. Mcdonnell, G. and D. Russell, "Antiseptics and disinfectants: activity, action, and resistance", *Clinical Microbiology Reviews,* Vol. 12, No. 1, pp. 147-179, 1999.

58. Maple, P. A. C., J. M. T. Hamilton-Miller and W. Brranfltt, "Comparison of the in-vitro activities of the topical antimicrobials azelaic and, nitroforazone, silver sulphadiazine and mupirocin against methcillin-resistant Staphylococcus aureus", *Journal of Antimicrobial Chemotherapy*, Vol. 29, pp. 661-668, 1992.

59. Matsumura, Y., K. Yoshikata, S. I. Kunisaki and T. Tsuchido, "Mode of bactericidal action of silver zeolite and its comparison with that of silver nitrate", *Applied and Environmental Microbiology*, Vol. 69, No. 7, pp. 4278-4281, 2003.

60. Sondi, I. and B. Salopek-Sondi, "Silver nanoparticles as antimicrobial agent: a case study on E. coli as a model for gram-negative bacteria", *Journal of Colloid and Interface Science*, Vol. 275, pp. 177-182, 2007.

61. Song, H. Y., K. K. Ko, L. H. Oh and B. T. Lee, "Fabrication of silver nanoparticles

and their antimicrobial mechanisms", *European Cells & Materials Journal*, Vol. 11, pp. 11-58, 2006.

62. Pal, S., Y. K. Tak and J. M. Song, "Does the antibacterial activity of silver nanoparticles depend on the shape of the nanoparticle? A study of the gram-negative bacterium Escherichia coli", *Applied and Environmental Microbiology*, Vol. 27, No. 6, pp. 1712-1720, 2007.

63. Raimondi, F., G. G. Scherer, R. Kotz and A. Wokaun, "Nanoparticles in energy technology: examples from electochemistry and catalysis", *Angewandte Chemie International Edition.*, Vol. 44, pp. 2190-2209.

64. Trop, M., M. Novak, S. Rodl, B. Hellbom, W. Kroell and W. Goessler, "Silver-coated dressing acticoat caused raised liver enzymes and argyria-like symptoms in burn patient", *The Journal of Trauma*, Vol. 60, No. 3, pp. 648-652, 2006.

65. Poon, V. K. and A. Burd, "In vitro cytotoxity of silver: implication for clinical wound care", *Burns*, Vol. 30, pp. 140-147, 2004.

66. Robson, M. C., "Wound infection: A failure of wound healing caused by an imbalance of bacteria", *Surgical Clinics of North America*, Vol. 77, pp. 637-650, 1997.

67. Wright, J. B., D. L. Hansen and R. E. Burrell, "The Comparative efficacy of two antimicrobial barrier dressings: in vitro examination of two controlled release of silver dressings", *Wounds*, Vol. 10, No. 6, pp. 179-188, 1998.

68. Madsen, S. M., H. Westh, L. Danielsen and V. T. Rosdahl, "Bacterial colonization and healing of venous leg ulcers", *APMIS*, Vol. 104, pp. 895-899, 1996.

69. Warriner, R. and R. Burrell, "Infection and the chronic wound: a focus on silver", *Advances in Skin & Wound Care*, Vol. 18, No. 8, pp. 2-12, 2005.

70. Wright, J. B., K. Lam, A. G. Buret, M. E. Olson and R. E. Burrell, "Early healing events in a porcine model of contaminated wounds: effects of nanocrystalline silver on matrix metalloproteinases, cell apoptosis, and healing", *Wound Repair Regeneration*, Vol. 10, pp. 141, 2002.

71. Lansdown, A. B. G., "Silver 2: its antibacterial properties and mechanism of action", *Journal of Wound Care,* Vol. 11, pp. 173, 2002.

72. Demling, R. H. and L. DeSanti, "The rate of re-epithelialization across meshed skin grafts is increased with exposure to silver", *Burns*, Vol. 28, pp. 264, 2002.

73. Stern, H. S., "Silver sulphadiazine and the healing of partial thickness burns: a prospective clinical trial", *British Journal of Plastic Surgery*, Vol. 42, pp. 581-585, 1989.

74. Sawhney, C. P., R. K. Sharma, K. R. Rao and R. Kaushish, "Long-term experience with 1 percent topical silver sulphadiazine cream in the management of burn wounds ", *Burns*, Vol. 15, pp. 403-406, 1989.

75. Dickinson, S. J., "Topical therapy of burns in children with silver sulphadiazine", *New York State Journal of Medicine*, Vol. 73, pp. 2045-2049, 1973.

76. Hollinger, M. A., "Toxicological aspects of topical silver pharmaceuticals", *Critical Reviews in Toxicology,* Vol. 26, pp. 255-260, 1996.

77. Ziegler, K., et al., "Reduced cellular toxicity of a new silver-containing antimicrobial dressing and clinical performance in nonhealing wounds", *Skin Pharmacology and Physiology*, Vol. 19, No. 3, pp. 140-146, 2006.

78. Baldi, C., C. Minoia, A. Di Nuici, E. Capodaglio and L. Manzo, "Effects of silver in isolated rat hepatocytes", *Toxicology Letters*, Vol. 41, pp. 261-268, 1988.

79. Liedberg, H. and T. Lundeberg, "Assessment of silver-coated urinary catheter toxicity by cell culture", *Urological Research*, Vol. 17, pp. 359-360, 1989.

80. Alt, V., et al., "An in vitro assessment of the antibacterial properties and cytotoxicity of nanoparticulate silver bone cement", *Biomaterials*, Vol. 25, No. 18, pp. 4383-4391, 2004.

81. Zhang, F. Q., W. J. She and Y. F. Fu, "Comparison of the cytotoxicity in vitro among six types of nano-silver base inorganic antibacterial agents", *Zhonghua Kou Qiang Yi Xue Za Zhi*, Vol. 40, No. 6, pp. 504-507, 2005.

82. Hussain, S. M., K. L. Hess, J. M. Gearhart, K. T. Geiss and J. J. Schlager, "In vitro toxicity of nanoparticles in BRL 3A rat liver cells", *Toxicology in Vitro*, Vol. 19, No. 7, pp. 975-983, 2005.

83. Abe, Y., M. Ueshige, M. Takeuchi, M. Ishii and Y. Akagawa, "Cytotoxicity of antimicrobial tissue conditioners containing silver-zeolite", *The International Journal of Prosthodontics*, Vol. 16, No. 2, pp. 141-144, 2003.

84. Tsipouras, N., R. Colin and P. Brady, "Passage of silver ions through membrane-mimetic materials, and its relevance to treatment of burn wounds with silver sulfadiazine cream", *Clinical Chemistry*, Vol. 43, pp. 290–301, 1997.

85. Harrison, H. N., "Pharmacology of sulfadiazine silver-its attachment to burned human and rat skin and studies of gastrointestinal absorption and extension", *Archives of Surgery*, Vol. 114, pp. 281-285, 1979.

86. Sano, S., R. Fujimori, M. Takashima and Y. Itokawa, "Absorption, excretion and tissue distribution of silver sulfadiazine", *Burns*, Vol. 8, pp. 278-285, 1981.

87. Boosalis, M. G., J. T. McCall, D. H. Ahrenholz, L. D. Solem and C. J. McClain, "Serum and urinary silver levels in thermal injury patients", *Surgery*, Vol. 101, pp. 40-43, 1987.

88. Wang, X. W., N. Z. Wang and O. Z. Zhang, "Tissue deposition of silver following topical use of silver sulfadiazine in extensive burns", *Burns*, Vol. 11, pp. 197–201, 1985.

89. Wan, A. T., R. A. Conyers, C. J. Coombs and J. P. Masterton, "Determination of silver in blood, urine, and tissues of volunteers and burn patients", *Clinical Chemistry*, Vol. 37, pp. 1683–1687, 1991.

90. Rowland-Payne, C. M. R., et al, "Argyria from excessive use of topical silver sulphadiazine", *Lancet*, Vol. 340, pp. 126, 1992.

91. Lee, P. C. and D. Meisel, *The Journal of Physical Chemistry*, Vol. 86, pp. 3391, 1982.

92. Filippo, E., A. Serra, A. Buccolieri, D. Manno, "Green synthesis of silver nanoparticles with sucrose and maltose: Morphological and structural characterization", *Journal of Non-Crystalline Solids*, Vol. 356, pp. 344–350, 2010.

93. CytoGLO™ Annexin V-FITC Apoptosis Kit User Guide, IMGENEX Corporation, http://www.imgenex.com/get_details.php?catalog_no=10085K [retrieved 1 July 2011].

94. Amicon® Ultra-15, Centrifugal Filter Devices' User Guide 2009, Millipore Corporation, http://www.millipore.com/userguides.nsf/a73664f9f981af8c852569b9005b4eee/9d8f412cd9c7838385257646005babdb/$FILE/PR02842.pdf [retrieved 1 July 2011].

95. Cory, A. H., T. C. Owen, J. A. Barltrop and J. G. Cory, "Use of an aqueous soluble tetrazolium/formazan assay for cell growth assays in culture", *Cancer communications*, Vol. 3, No. 7, pp. 207–212, 1991.

96. Martin, L. J., "Neuronal cell death in nervous system development, disease, and injury", *International Journal of Molecular Medicine*, Vol. 7, pp. 455-478, 2001.

97. Kerr, J. F., A. H. Wyllie and A. R. Currie, "Apoptosis: a basic biologica phenomenon with wide-ranging implications in tissue kinetics", *British Journal of Cancer*, Vol. 26, pp. 239-257, 1972.

98. Wyllie, A. H., J. F. R. Kerr and A. R. Currie, "Cell death: the significance of apoptosis", *International Review of Cytology,* Vol. 68, pp. 251-306, 1980.

99. Popper, H., "Hepatocellular degeneration and death", in I. M. Arias, W. B. Jakoby, H. Popper, D. Schachter and D. A. Shafritz, *The Liver Biology and Pathobiology*, pp. 1087-1103, Raven Press, New York, 1988.

100. Verhoven, B., R. A. Schlegel and P. Williamson, "Mechanisms of phosphatidylserine exposure, a phagocyte recognition signal, on apoptotic T lymphocytes", *The Journal of experimental medicine*, Vol. 182, No. 5, pp. 1597–1601, 1995.

101. Tait, J. F., D. Gibson and K. Fujikawa, "Phospholipid binding properties of human placental anticoagulant protein-I, a member of the lipocortin family", *The Journal of Biological Chemistry*, Vol. 264, pp. 7944–7949, 1989.

102. Andree, H. A., C. P. Reutelingsperger, R. Hauptmann, H. C. Hemker, W. T. Hermens and G. M. Willems, "Binding of vascular anticoagulant alpha (VAC alpha) to planar phospholipid bilayers", *The Journal of Biological Chemistry,* Vol. 265, pp. 4923–4928, 1990.

103. Lecoeur, H., "Nuclear apoptosis detection by flow cytometry: influence of endogenous endonucleases", *Experimental Cell Research,* Vol. 277, No. 1, pp. 1-14, 2002.

104. Liu, L. and R. H. Hurt, *Environmental Science & Technology,* Vol. 44, pp. 2169-2175, 2010.

105. Ho, C. M., S. K. W. Yau, C. N. Lok, M. H. So and C. M. Che, *Chemistry - An Asian Journal,* Vol. 5, pp. 285-293, 2010.

106. Zook, J. M., S. E. Long, D. Cleveland, C. A. Geronimo and R. I. MacCuspie, *Analytical and Bioanalytical Chemistry*, Vol. 401, pp. 1993-2002, 2011.